ISTANBUL TECHNICAL UNIVERSITY ★ GRADUATE SCHOOL OF SCIENCE ENGINEERING AND TECHNOLOGY

CONTROLLED RELEASE SYSTEM INCLUDING NANOPARTICLES THAT CAN BE USED FOR HYPOTHYROIDISM TREATMENT

Ph.D. THESIS

Ceren KUTLU KAYA

Nano Science and Nano Engineering Department

Nano Science and Nano Engineering Programme

JULY 2020

ISTANBUL TECHNICAL UNIVERSITY ★ GRADUATE SCHOOL OF SCIENCE ENGINEERING AND TECHNOLOGY

CONTROLLED RELEASE SYSTEM INCLUDING NANOPARTICLES THAT CAN BE USED FOR HYPOTHYROIDISM TREATMENT

Ph.D. THESIS

Ceren KUTLU KAYA
(513122004)

Nano Science and Nano Engineering Department

Nano Science and Nano Engineering Programme

Thesis Advisor: Prof. Dr. Fatma Neşe KÖK

JULY 2020

ISTANBUL TEKNİK ÜNİVERSİTESİ ★ FEN BİLİMLERİ ENSTİTÜSÜ

HİPOTİROİDİ TEDAVİSİNDE KULLANILABİLECEK NANOPARTİKÜL İÇERİKLİ KONTROLLÜ SALIM SİSTEMİ

DOKTORA TEZİ

Ceren KUTLU KAYA
(513122004)

Nano Bilim ve Nano Mühendislik Anabilim Dalı

Nano Bilim ve Nano Mühendislik Programı

Tez Danışmanı: Prof. Dr. Fatma Neşe KÖK

TEMMUZ 2020

Ceren Kutlu Kaya, a Ph.D. student of İTU Graduate School of Science Engineering and Technology student ID 513122004, successfully defended the thesis/dissertation entitled "CONTROLLED RELEASE SYSTEM INCLUDING NANOPARTICLES THAT CAN BE USED FOR HYPOTHYROIDISM TREATMENT", which she prepared after fulfilling the requirements specified in the associated legislations, before the jury whose signatures are below.

Thesis Advisor :	**Prof. Dr. Fatma Neşe KÖK** İstanbul Technical University	.....
Jury Members :	**Prof. Dr. Zeynep Petek ÇAKAR** Istanbul Technical University	.....
	Prof. Dr. Sedef TUNCA GEDİK Gebze Technical University	.....
	Prof. Dr. Fatma Seniha GÜNER Istanbul Technical University	.....
	Assoc. Prof. Dr. Halime KENAR Acıbadem University	.....

Date of Submission : 12 June 2020
Date of Defense : 14 July 2020

To all tenacious,

FOREWORD

I would like to express my gratitude to Prof. Fatma Neşe KÖK for her continuous suppport during my long journey as a PhD student. I believe that I will follow her footsteps in the way of having humanitarian values and principles both socially and academically.

I gratefully acknowledge Prof. Sezai SARAÇ from Istanbul Technical University, Polymer Science and Technology Programme and Selin GÜMRÜKÇÜ, graduate student in Chemistry Division.

I would like to thank to Prof. Zeynep Petek ÇAKAR and Prof. Sedef TUNCA GEDİK, the esteemed members of thesis monitoring commitee for their valuable contributions to make possible to finalize the thesis.

I appreciate to Istanbul Technical University Scientific Research Office,for supporting my PhD studies in the context of General Research Projects with TGA-2018-41084 grant number.

Special thanks goes to my dear friend, Ayşe Buse ÖZDABAK SERT for supporting me in everyway and making me feel lucky during I was working in another location. I can never forget the names of Burcu DOYMUŞ, Gizem KEREM, Elifcan ZENGİN, Canan ÇİL, Şebnem SEHERLER, Yeliz ERŞAN, Hatice EKER and Arife KUŞBAZ who are provide me full support and never let me feel myself alone.

Of course to 'the friends' that I always want to be close to them; Derya, Müşra, Dilem, Selin, Anıl, Işıl, Sedef, Onur, Uraz, Aylin, and Nuray thanks for being in my life.

To my beatiful mommy and beloved brother the ones encourage me with their endless loves. Thank you to other family members; only people with huge families can understand my feelings. I would like to express my most profund gratitude and thanks to my dear husband Yusuf Ziya KAYA for all the times we spend together and overcome the difficulties hand-to-hand.

This thesis would not be exist without help of all the names mentioned above.

July 2020

Ceren KUTLU KAYA
(Bioengineer)

TABLE OF CONTENTS

Page

ABBREVIATIONS

AITD : Autoimmune Thyroid Disease
Anti- Tg : Thyroglobulin Antibody
Anti- TPO : Thyroid Peroxidase Antibody
CEP : Cepharanthine
DAPI : 40,6-diamidino-2-phenylindole Dihydrochloride
DCM : Dichloromethane
DIT : Diiodothyrozines
DMEM : Dulbecco's Modified Eagle's Medium
DMF : Dimethylformamide
EE : Encapsulation Efficiency
EtOH : Ethanol
FBS : Fetal Bovine Serum
FDA : Food and Drug Administration
fT4 : Free Thyroxine
FTIR : Fourier Transform Infrared
GPx : Glutathione Peroxidases
H_2O_2 : Hydrogen Peroxide
M : Molar
MIT : Monoiodothyrosines
Nm : Nanometer
NMR : Nuclear Magnetic Resonance
NPs : Nanoparticles
PDI : Polydispersity Index
PEG : Poly (ethylene glycol)
PEG20-PEVA: PEVA (100 % w/w) and PEVA-PEG (20% w/w of PEVA) monomethyl ether
PEVA : Poly (ethylene-co-vinyl acetate)
PU : Polyurethane
Se : Selenium
SEM : Scanning Electron Microscopy
T4 : Thyroxine
T3 : Triiodothyronine
THF : Tetrahydrofuran
Tg : Thyroglobulin
TPO : Thyroid Peroxidase
TSH : Thyroid Stimulating Hormone
TRH : Thyrotropin-releasing hormone

µm **:** Micrometer

LIST OF TABLES

Page

LIST OF FIGURES

Page

CONTROLLED RELEASE SYSTEM INCLUDING NANOPARTICLES THAT CAN BE USED FOR HYPOTHYROIDISM TREATMENT

SUMMARY

Thyroxine (T4) and Triiodothyronine (T3) hormones secreted by the thyroid gland are required for many vital functions such as regulation of metabolic rate, heart rate, body temperature, breathing, and development of central and peripheral nervous systems, control of body weight, growth and brain development. Hypothyroid disease, which develops due to the low functioning of the thyroid gland, is a clinical condition that should be treated for lifelong to substitute the function of the thyroid hormones that can not be secreted at the required levels. The immune system of hypothyroid patients produces anti-TPO and anti-Tg antibodies against thyroid peroxidase (TPO) and thyroglobulin (Tg) found in thyroid cells. These antibodies not only destroy TPO and Tg, but also damage thyroid cells over time. As the thyroid gland cells are damaged and diminished, the gland begins to lose its feature further due to the reduced number of cells that produce hormones.

While some of the T3 needed is produced in parenchymal cells in healthy people, the rest is produced by the deiodination of T4 and Selenium (Se) plays a very important role in performing the functions of deiodinase enzymes. Cepharanthine (CEP), another active agent used in this thesis, is a natural plant extract and can prevent T cell activation by blocking the binding of Tg peptides to the corresponding sequence (HLA-DRβ1-Arg74).

In the light of this information, a double-effect release system was created in order to regulate hormones and prevent autoimmune response formation in hypothyroid disease within the scope of this thesis. Characterization studies of the system was performed, release profiles of CEP and Se, which are the active agents, were followed, and at the last step, cytotoxicity tests of each component of the system were carried out in-vitro cell experiments.

In the first part of the thesis, nanoparticles (NP) consisting of poly (ethylene-co-vinyl acetate) (PEVA) and poly (ethylene glycol) (PEG) monomethyether were produced by using emulsion diffusion - solvent evaporation method. Nanoparticle synthesis process was optimized by changing the amount of PEG monomethyether (15, 20, 25 and 30%, w/w) added to PEVA and sonication time. It was determined that PEVA based NPs containing 20% PEG monomethyether by weight of PEVA (PEG20-PEVA) and sonicated for 5 minutes have the most appropriate particle size (166.1 nm) and the most monodisperse (PDI: 0.464) size distribution. The chemical characterization of the produced PEG20-PEVA NPs was performed with Raman spectroscopy, and the physical characterization studies were carried out by zetasizer and Scanning Electron Microscopy (SEM). CEP, with 10%, 20 and 30% by weight of PEVA, was loaded into

the NPs and encapsulation efficiency and the amount of encapsulated active agent was determined. Although the amount of encapsulated CEP increased as the initial CEP concentration increased, there was a significant decrease in encapsulation efficiency so it was decided to load 10% of CEP by weight of PEVA to the NPs. It was measured that the average size of the CEP loaded particles was 190.5 nm and the PDI value was 0.54.

At the beginning of release studies, the effect of particles' drying method on CEP release profile was analyzed. In the study carried out for 14 days, it was determined that the NPs dried in oven released ~7.7% of encapsulated CEP, while the NPs dried in freeze dryer released ~11.3% of CEP. This difference is probably due to the reduction of surface areas of the particles which were agglomerated while drying in the oven. For this reason, long-term release studies in the following stages were carried out using NPs which were freeze-dried and it was observed that PEG20-PEVA NPs released ~35% of encapsulated CEP in 100 days.

In the second part of the thesis, block copolymer containing Se was produced in two successive steps. At first, di-(1-hydroxylundecyl)selenide and then PEG-PUSe-PEG block copolymer were synthesized. Characterization of these materials was performed by Nuclear Magnetic Resonance (NMR) and Fourier Transform Infrared (FTIR) spectroscopy. Scale-up could not be achieved during the polymer synthesis, so PEG-PUSe-PEG block copolymer was synthesized in low quantities (~0.45 g/ batch). The synthesized block copolymer was mixed with polyurethane (PU) which is a commercial polymer and matrix production was carried out by using physical mixing - particulate leaching technique. The porosities of the matrices produced by using PU: PEG-PUSe-PEG block copolymers in the ratio of 2: 1 and 1: 1 by weight were both measured as 60% using the liquid exchange method. The pore structures of the matrices were analysed with SEM images and it was seen that matrices had wide pore area distribution with more than half of pore areas are less than 40 μm^2.

The NPs containing CEP produced in the first stage of the thesis were integrated into the matrices with the help of a micropipette and SEM images showed that the NPs were distributed homogeneously in the matrix. In the parallel study, the release of CEP from both free NPs and NPs loaded into the matrix was followed for 66 days, and it was found that CEP release from NPs are ~23% and ~21.5%, respectively. No hindering effect of matrices to CEP release was observed due to the large pore size.

The release of Se which is the second active agent used in the thesis, was followed in ultrapure water and water including 0.1% H_2O_2 (v/v) and samples taken for 7 days were analysed by Inductively Coupled Plasma-Mass Spectrometry (ICP-MS). At the end of this period, it was determined that 2:1 and 1:1 (w/w) PU: PEG-PUSe-PEG block copolymers released 0.88 and 11.96 µg Se in ultra pure water, respectively; and 2525.90 µg and 2097.76 µg Se in water containing 0.1% H_2O_2, respectively. Significant increase in Se release in H_2O_2 presence was probably caused by the oxidation sensitivity of selenide block copolymers. The responsiveness of Se release to oxidative stress may be an advantage in hypothyroid disease, which has been reported to cause oxidative stress.

In the last part of the thesis, three different cytotoxicity tests were done. Firstly, NPs with and without CEP were directly incubated with NIH 3T3 cells. Secondly, matrix effluents of 100% PU, 2:1 and 1:1 PU: PEG-PUSe-PEG block copolymers (w/w) were interacted with cells in cell media (indirect interaction), and finally matrices were

seeded with cells (direct interaction). In MTS analysis performed to measure cell viability, it was determined that the cells which interact with the materials showed similar viability with the control groups, in other words, none of the materials had cytotoxic effects on fibroblast cells. The images taken by light microscope, fluorescence microscope and SEM showed that, the cells interacted with the materials, spread on matrices and inside of pores, at the same time, they could interact each other and no difference in the cell morphology was observed compared to the control group.

The chemical and physical characterization, imaging, release and cell culture studies carried out within the scope of the thesis have shown that the double-acting system produced by biocompatible materials has the potential to be used as local long-term delivery system for effective treatment of hypothyroidism by reducing the autoimmune response and regulating related hormones.

.

HİPOTİROİDİ TEDAVİSİNDE KULLANILABİLECEK NANOPARTİKÜL İÇERİKLİ KONTROLLÜ SALIM SİSTEMİ

ÖZET

Tiroid bezi tarafından salgılanan Tiroksin (T4) ve Triiyodotironin (T3) hormonları, metabolizma hızının düzenlenmesi, kalp atış hızının ayarlanması, nefes alma, merkezi ve periferik sinir sistemlerinin gelişimi, vücut ısısının ayarlanması, vücut ağırlığının kontrolü, büyüme ve beyin gelişimi gibi birçok hayati fonksiyonun gerçekleşmesi için gerekli olan tiroid hormonlarıdır. Tiroid bezinin az çalışmasına bağlı olarak gelişen hipotiroidi hastalığı, bu hormonların gerekli düzeyde salgılanmamasına yol açan ve hayat boyu tedavi edilmesi gereken klinik bir durumdur. Hipotiroid hastalarının bağışıklık sistemi, tiroid hücrelerindeki tiroid peroksidaz (TPO) ve tiroglobuline (Tg) karşı, anti-TPO ve anti-Tg antikorlarını üretir. Bu antikorlar sadece vücut tarafından üretilen TPO ve Tg'yi yok etmekle kalmaz, zaman içerisinde tiroid hücrelerine de zarar vermeye başlarlar. Tiroit bezi hücreleri zarar görüp azaldıkça, bez özelliğini kaybetmeye başlar ve hacmi küçülerek hormon üretecek hücre sayısı azalır.

Sağlıklı bireylerde ihtiyaç duyulan T3'ün bir bölümü parankim hücrelerinde üretilirken, geri kalanı T4'ün deiyodinizasyonu ile oluşur ve deiyodinaz enzimlerin işlevlerini yerine getirebilmesi için Selenyum (Se) çok önemli bir rol oynamaktadır. Bu çalışmada kullanılan diğer bir aktif madde olan Cepharanthine (CEP) ise doğal bir bitki ekstraktıdır ve Tg peptidlerinin ilgili sekansa (HLA-DRβ1-Arg74) bağlanmasını engelleyerek, T hücre aktivasyonunun önüne geçebilmektedir.

Bu bilgiler ışığında tez kapsamında, hipotiroid hastalığındaki hem otoimmun cevap oluşumunun önüne geçilmesi hem de hormonların düzenlenmesi amacıyla çift etkili bir salım sistemi oluşturularak karakterizasyonu yapılmış, etken maddeler olan CEP ve Se'nin salım profilleri çıkarılmış, son olarak *in-vitro* koşullarda sistemin her bileşeninin sitotoksisite testleri gerçekleştirilmiştir.

Tezin ilk bölümünde, emülsiyon difüzyon-çözücü buharlaştırma yöntemi ile poli(etilen-ko-vinil asetat) (PEVA) ve poli(etilen glikol) (PEG) monometileter'den oluşan nanopartiküller (NP) üretilmiştir. Nanopartikül üretimi PEVA'ya eklenen PEG monometileter (%15, 20, 25 ve 30) miktarı ve sonikasyon süresi değiştirilerek optimize edilmiştir. Ağırlıkça %20 PEG monometileter içeren ve 5 dk boyunca sonikatörde homojenize edilen PEVA bazlı NP'lerin (PEG20-PEVA) en uygun partikül büyüklüğü (166,1 nm) ve en monodispers (PDI: 0,464) dağılıma sahip olduğu tespit edilmiştir. Üretilen PEG20-PEVA NP'lerin kimyasal karakterizasyonu Raman spektroskopisi, fiziksel karakterizasyonu ise zetasizer ve Taramalı Elektron Mikroskobu (SEM) ile gerçekleştirilmiştir. Enkapsülasyon verimi ve enkapsüle edilen etken madde miktarları göz önünde bulundurularak NP'lere, ağırlıkça PEVA'nın %10, 20 ve 30'u kadar CEP yüklenmiş ve başlangıç CEP konsantrasyonu arttıkça enkapsüle edilen CEP miktarı da artmasına rağmen enkapsülasyon veriminin düşmesi nedeniyle, partiküllere ağırlıkça PEVA'nın %10'u kadar CEP yüklenmesine karar verilmiştir. CEP yüklü NP'lerin ortalama büyüklüklerinin 190,47 nm, PDI değerinin de 0,54 olduğu tespit edilmiştir.

NP'lerden CEP salımının incelendiği çalışmalarda, partikülleri kurutma yönteminin salım profiline etkisi analiz edilmiş ve 14 gün boyunca sürdürülen çalışmada etüvde kurutulan NP'lerin enkapsüle ettikleri CEP'in ~ %7,7'sini saldığı tespit edilirken, dondurarak kurutma cihazında kurutulan NP'lerin içerdikleri CEP'in ~ %11,3'ünü saldıkları ölçülmüştür. Söz konusu fark, etüvde kurutulan partiküllerin aglomere olmaları nedeniyle yüzey alanlarının küçülmesinden kaynaklanmaktadır. Bu nedenle ilerleyen aşamalardaki uzun süreli salım çalışmaları dondurularak kurutulan NP'ler kullanılarak gerçekleştirilmiş ve PEG20-PEVA NP'lerin 100 günde enkapsüle ettikleri CEP'in ~ %35'ini saldıkları gözlenmiştir.

Tezin ikinci aşamasında Se içeren blok kopolimer, önce di-(1-hidroksilundesil) selenid ve ardından PEG-PUSe-PEG blok kopolimerinin sentezi olacak şekilde iki aşamada üretilmiştir. Her iki aşamada da sentezlenen malzemelerin karakterizasyonları Nükleer Manyetik Rezonans (NMR) ve Fourier Dönüşümlü Kızılötesi (FTIR) spektroskopisi ile yapılmıştır. Üretim aşamasında ölçek büyütmenin gerçekleştirilememesi ve buna bağlı olarak polimerin az miktarlarda sentezlenebilmesi nedeniyle, sentezlenen blok kopolimer, ticari bir polimer olan poliüretan (PU) ile karıştırılmış ve matris üretimi fiziksel karıştırma-parçacık uzaklaştırma tekniği kullanılarak gerçekleştirilmiştir. Ağırlıkça 2:1 ve 1:1 oranında PU:PEG-PUSe-PEG blok kopolimerleri kullanılarak üretilen matrislerin gözeneklilikleri sıvı değişimi metodu kullanarak ölçülmüş ve her iki matris tipinin de %60 gözenekliliğe sahip olduğu görülmüştür. Matrislerin gözenek yapıları ise SEM görüntüleri ile incelenmiş, geniş bir gözenek alanı dağılıma sahip olan matrislerin gözenek alanlarının yarısından fazlasının 40 μm^2'den küçük olduğu hesaplanmıştır.

Tezin ilk aşamada üretilen CEP içeren NP'ler matrislere mikropipet yardımıyla emdirilmiş ve çekilen SEM görüntülerinde NP'lerin matris içerisinde homojen bir şekilde dağıldıkları görülmüştür. Paralel yürütülen çalışmada, hem serbest NP'lerden hem de matrise yüklenen NP'lerden CEP salımı 66 gün boyunca incelenmiş ve partiküllerin sırasıyla, enkapsüle ettikleri CEP'in ~ %23'ünü ve ~ %21,5'ini saldıkları tespit edilmiştir. Matrislerin geniş gözenek büyüklüğüne sahip olmaları nedeniyle CEP salımını ihmal edilebilir bir oranda geciktirdiği gözlemlenmiştir.

Tez kapsamında kullanılan ikinci etken madde olan Se salımı, ultra saf su ve %0,1 H_2O_2 eklenmiş su içinde incelenmiş ve 7 gün boyunca alınan örnekler İndüktif Eşleşmiş Plazma - Kütle Spektrometresi (ICP-MS) ile ölçülmüştür. Süre sonunda ağırlıkça 2:1 ve 1:1 oranında PU: PEG-PUSe-PEG blok kopolimerlerinden üretilen matrislerde ultra saf suda sırasıyla, 0,88 ve 11,96 µg Se salınırken; %0,1 H_2O_2 içeren suda sırasıyla 2525,90 µg ve 2097,76 µg Se salındığı tespit edilmiştir. H_2O_2 (v/v) içeren ortamda Se salımın büyük oranda artmasının selenid blok kopolimerlerinin oksidasyon duyarlılığı sayesinde olduğu sonucuna varılmış ve salınan Se miktarının oksidatif strese cevaben ayarlanabilmesinin, oksidatif stres oluşumuna yol açtığı raporlanmış hipotiroidi hastalığında bir avantaj olabileceği düşünülmüştür.

Çalışmanın son aşamasında CEP içeren ve içermeyen NP'ler doğrudan; %100 PU, 2:1 ve 1:1 oranında PU: PEG-PUSe-PEG blok kopolimerlerinden üretilen matrisler ise hem eluentleri alınarak dolaylı olarak hem de üstlerine hücreler ekilerek doğrudan NIH 3T3 hücreleri ile etkileştirilmiştir. Hücre canlılığını ölçmek için yapılan MTS analizlerinde, malzemelerle etkileşen hücrelerin kontrol grupları ile benzer canlılık gösterdikleri tespit edilmiş, yani proje çıktısı olan hiçbir malzemenin fibroblast hücreleri üzerinde sitotoksik etkisi olmadığı belirlenmiştir. Işık mikroskobu, floresans mikroskop ve SEM'de çekilen görüntülerde ise hücrelerin malzemelerle etkileşime girdikleri, malzeme yüzeyinde ve gözeneklerinde yayıldıkları, aynı zamanda birbirlerine tutunabildikleri ve hücre morfolojilerinde kontrol grubuna kıyasla herhangi bir fark olmadığı görülmüştür.

Tez kapsamında gerçekleştirilen kimyasal ve fiziksel karakterizasyon, görüntüleme, salım ve hücre kültürü çalışmaları, biyouyumlu malzemelerden üretilen çift etkili sistemin, hem otoimmün cevabı azaltıp, hem de ilgili hormonları düzenleyerek hipotiroidizmin uzun süreli ve etkin tedavisi için lokal bir uygulama olarak kullanılabilme potansiyeli olduğunu göstermiştir.

1. INTRODUCTION

Thyroid diseases are the most common endocrine system disease and one of the common disease groups both in the world and in our country (Türkiye Endokrinoloji ve Metabolizma Derneği, 2013). Thyroid dysfunction is divided into 3 main groups as hypothyroidism, hyperthyroidism and thyroid nodules / cancer. When clinical epidemiology of thyroid dysfunctions is analysed, it is seen that functional thyroid diseases are several times more common in iodine deficient regions of the world, like some settlements in Africa and Latin America. And it is seen in 10% of pregnant women, worlwide. The statistics showed that, congenital hypothyroidism affects 1 in every 4000 newborns, and has high prevelence in women (1-10 of every 1000 women and 1-4 of every 1000 men in developed countries). Depending on age and biochemical structure, subclinical hypothyroidism symptoms are observed in 4-20% of adults (Gregory and Sadrzadeh, 2017).

Hypothyroid disease, which is also the focus of this thesis, is a clinical condition that progresses with a slowdown in metabolism due to the lack of thyroid hormones. Treatment should continue throughout life for symptomatic relief as the disease can not be treated in many patients. This situation causes a decrease in the quality of life of people affected by the disease. In order to address this problem, a multifunctional controlled release system has been developed within the scope of this doctoral thesis to compansate thyroid hormone deficiency for individuals with hypothyroid disease.

1.1 Purpose of Thesis

Thyroid hormones secreted by the thyroid glands are necessary to control vital body functions such as heartbeat, breathing, central and peripheral nervous system development, body temperature regulation, reproduction and regulation of energy metabolism (Eaton, 2019; Fujita, 1975; Url-1). The thyroid gland, stimulated by thyroid-stimulating hormone (TSH), releases triiodothyronine (T3) and thyroxine (T4) hormones (Ersoy, 2014). Insufficient amount of T3 and T4 hormones in the blood

causes hypothyroidism disorder (Calonne et al, 2019). Thyroid peroxidase (TPO) and thyroglobulin (Tg) play a vital role in the mechanism of hypothyroidism which is an autoimmune disorder (Tomer and Huber, 2009). Tg is the largest and most common autoantigen in the thyroid gland and acts as the precursor of T4 and T3 hormones after reacting with iodine. TPO, on the other hand, is the most important enzyme involved in thyroid hormone synthesis (McLachlan and Rapoport, 2007).

Cepharanthine (CEP), which is a natural alkaloid, prevents T cell activation which is necessary for generating autoimmune response and by this way Tg peptide formation is blocked (Li et al, 2016). The other agent used in the thesis, Selenium (Se), is an extremely important element for immune system functions. Taking supplemantal Se in addition to the daily diets caused to decrease in the concentration of thyroid peroxidase antibody (anti-TPO) and TSH receptor antibody in the blood of hypothyroid patients (Gartner et al, 2003).

The aim of this thesis is to develop a multi-functioned system for the treatment of hypothyroidism disorder that negatively affects the lives of a significant number of people. For this purpose, two different active agents, namely CEP and Se, was chosen to prevent T-cell activation and to decrease the anti-TPO concentration, respectively. First, CEP was loaded to nanoparticles made by poly (ethylene-co-vinyl acetate) (PEVA) and poly (ethylene glycol) (PEG) monomethyl ether with emulsion solvent evaporation method. Then, Se containing block copolymer, PEG-PUSe-PEG, was synthesized and this copolymer was combined with commercial polyurethane (PU) at different ratios by particulate leaching technique for matrix fabrication. The whole system was combined as shown in Figure 1.1. Characterization studies of all synthesized and produced materials were performed and the effects of both optimized materials and active agents on cells were examined in-vitro conditions. In sum, a multifunctional long-term release system was designed by using biocompatible polymers to decrease the anti-TPO concentration and to prevent T-cell activation, respectively, for the treatment of hypothyroidism.

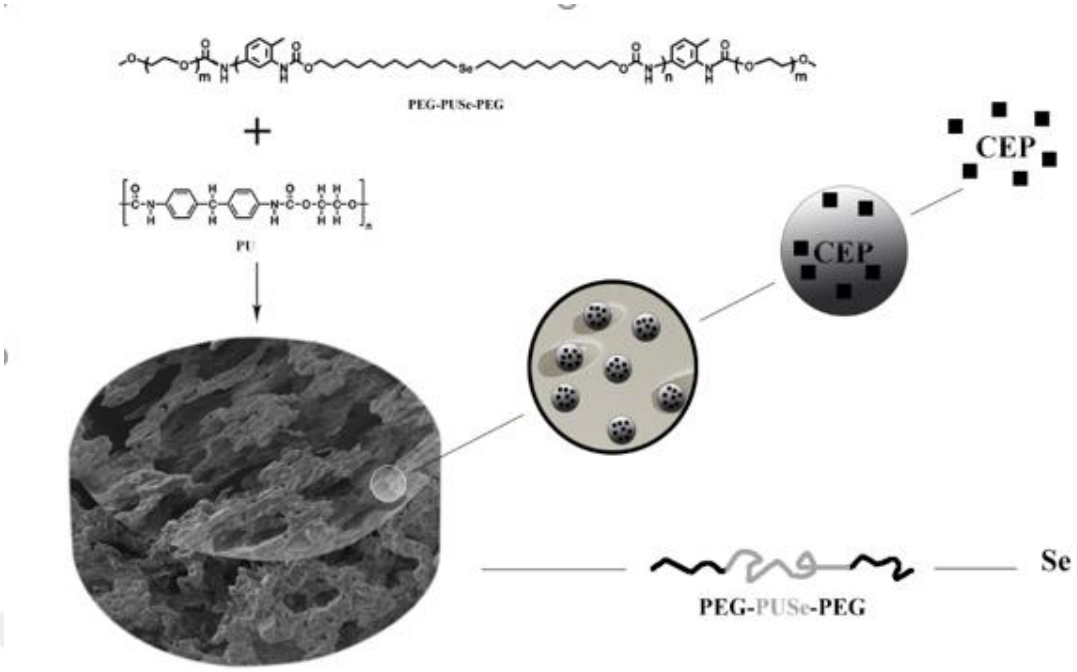

Figure 1.1 : Schematic representation of the whole system.

1.2 General Information About Hypothyroidism

Hypothyroidism is more common dysfunction in women, characterized by an insufficient amount of thyroid hormone secretion from the thyroid gland or rarely thyroid hormone inefficiency, resulting in slowed metabolic rate (Özyardımcı Ersoy, 2014). Thyroid-stimulating hormone (TSH) screening tests are routinely performed in babies as congenital hypothyroidism in newborns can cause permanent mental retardation. Thus, in the early stage, hypothyroidism can be diagnosed and treatment are started after birth to prevent permanent brain damage, mental retardation and somatic developmental retardation (Cooper and Ladenson, 2011).

Iodine nutrition is the most important parameter to determine the risk of thyroid disease and the other factors such as ageing, genetic susceptibility, the advent of novel therapeutics, including immune checkpoint inhibitors, smoking status, ethnicity, and endocrine disruptors also influence its epidemiology (Taylor et al, 2018).

The causes of hypothyroidism are grouped under 3 sub-titles:

1. Primary autoimmune hypothyroidism; it develops due to the shrinking or permanent loss of thyroid gland tissues.

2. Goiter hypothyroidism; it develops as a result of the growth of the thyroid gland due to the decrease in the synthesis of thyroid hormones.

3. Central hypothyroidism; it is a type of hypothyroidism that develops due to a problem in the synthesis or secretion processes of the thyrotropin-releasing hormone (TRH) secreted by the hypothalamus or TSH secreted by pituitary gland or a problem in the TSH molecule. Due to the problem, thyroid gland could not be situmulated enough and central hypothyroidism is observed (Yılmaz, 2009; Persani and Bonomi, 2017).

Hypothyroidism is not a disease in which the cause of the disease can be completely eliminated. However, it is possible to remove its symptoms in adult individuals with different treatment methods developed specifically for the patient. In treatments, synthetic thyroxine (T4) preparations, the dosage of which is determined according to the needs of the patient, are used, thus, TSH hormone can be optimised in between ideal range for the patient. In the 2-week period following the development of the optimum treatment, the symptoms of the patient begin to disappear, but in most cases the patient should be kept under lifelong control and should continue the therapy (Kramer et al, 2009).

1.2.1 Thyroid gland

The thyroid gland, located on the front of the neck, consists of two lobes and connects with the isthmus to the midline just below the cricoid cartilage (Figure 1.2) (Akçakaya et al, 2012). Thyroid hormones are produced in the thyroid gland by using iodine taken with food. Many functions are controlled by thyroid hormones, such as regulating the metabolic rate, adjusting the heart rate, breathing, development of the central and peripheral nervous systems, adjusting the body temperature, control of body weight, growth and brain development in children (Fujita, 1975).

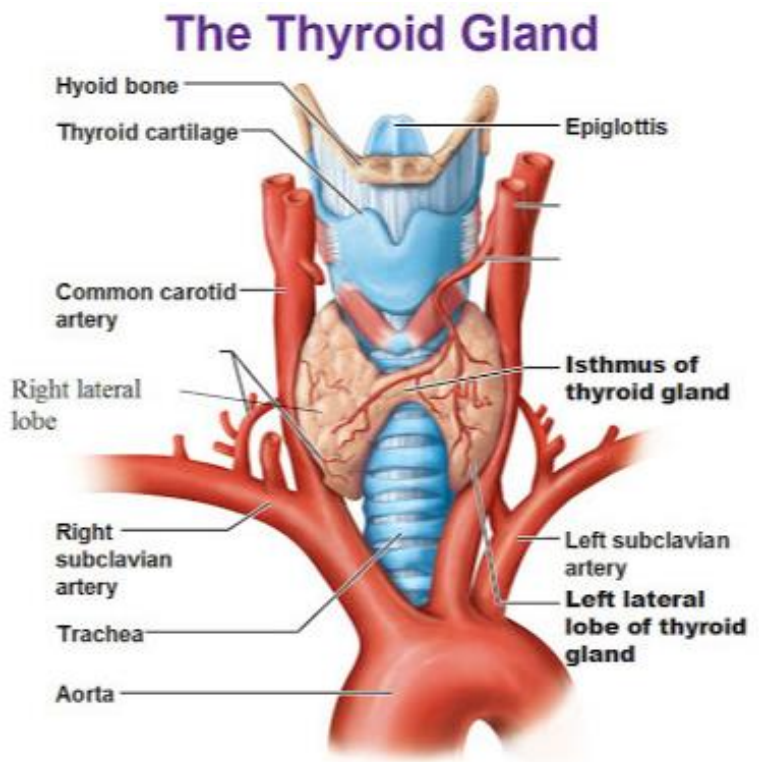

Figure 1.2 : Gross anatomy of the thyroid gland, anterior view (Url-2).

Hyperthyroid and hypothyroid diseases caused by functional disorder of the thyroid gland are among benign thyroid diseases. They are resulted from high or low hormone production in thyroid gland, respectively. Hashimoto's thyroiditis which is an autoimmune disease, is the most important cause of hypothyroidism. In Hashimoto thyroiditis, autoantibodies, thyroid peroxidase antibody (anti-TPO) and thyroglobulin antibody (anti-Tg), are formed against thyroid peroxidase (TPO) and thyroglobulin (Tg), respectively. These antibodies not only destroy TPO and Tg produced by the body, but also begin to damage thyroid cells over time. As the thyroid gland cells are damaged and diminished, gland begins to lose its characteristic, its volume decreases, the number of cells that produce hormones decreases, and eventually the deficiency of thyroid hormones appears (Url-1).

1.2.2 Thyroid hormones

Thyroid hormones produced by the parenchymal cells in the thyroid gland are thyroxine (T4) and triiodothyronine (T3). The release of these hormones is regulated by thyroid-stimulating hormone (TSH-Thyrotropin) secreted from the anterior pituitary. TSH secretion is controlled by thyrotropin-releasing hormone (TRH) secreted from the hypothalamus. TRH causes TSH release and TSH causes T3 and T4

release. T3 and T4 keep TSH and TRH releases under control with negative feedback. In particular, there is a negative logarithmic linear relationship between serum free T4 (fT4) and TSH (Demirci and Deliaşı, 2014). Increased TSH and decreased fT4 levels are the most used markers in hypothyroidism diagnosis (Chaker et al, 2017). T3 and T4 hormones, which are necessary for the differentiation of all mammals, including humans, also play a role in regulating metabolic functions by regulating the cellular oxidation rate in all tissues. The thyroid gland acts as a storage for hormones as well as the production of thyroid hormones.

Thyroglobulin (Tg), is a glycoprotein and the first reactant of thyroid hormone synthesis. During synthesis; oxidized iodine reacts with Tg, forming monoiodothyrosines (MIT), and when MIT reacts with another iodine, diiodothyrozines (DIT) is synthesized (organification). Two DITs combine to form T4, a molecule MIT and a molecule DIT combine to form T3 (coupling) and Se is required for DIT functions (Gregory, 2012). All these processes are oxidative and catalyzed by the peroxidase enzyme (Figure 1.3) (Tavukçu, 2005).

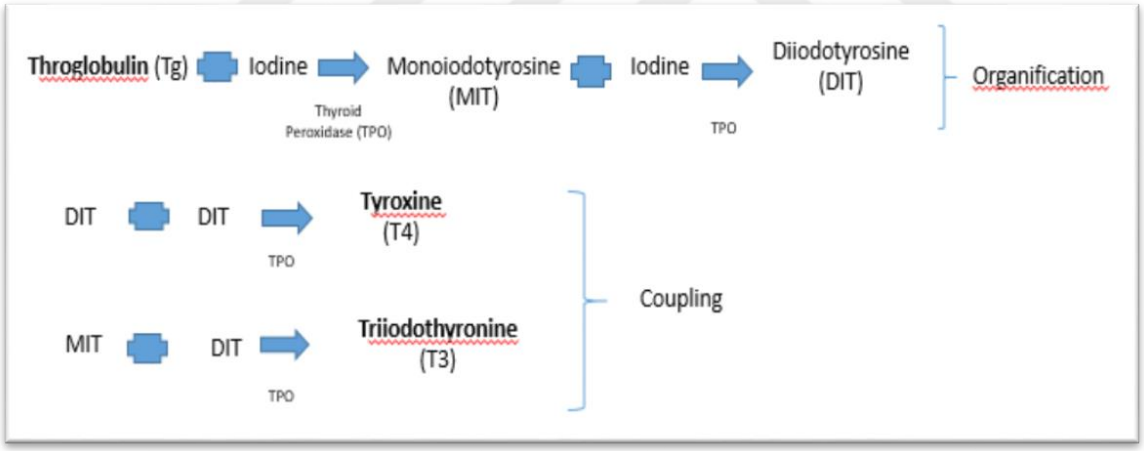

Figure 1.3 : Synthesis of T3 and T4.

1.3 Polymers Used in Biomedical Applications

Polymers are widely used in biomedical science because of their biocompatibility, and good mechanical properties; and also they are, in general, chemically and biologically inert. Surface characteristics, including topography, chemistry, energy, charge, or wettability are other properties which cooperatively influence the biological performance of materials. They regulate the biological response at the implant/tissue

interface (e.g., influencing the cell adhesion, cell orientation, cell motility, etc.) (Riveiro et al, 2018).

Various kinds of polymers or polymer based devices are used in biomedical applications such as cardiovascular and neurosurgical implants, valves, grafts, hydrocephalus shunts, pacemakers etc. which are essential for human life to sustain the biological process in the body (Ivanova et al, 2014). Additionally, biodegradable and/or biocompatible polymers are increasingly used as fibers, clips, contact lenses, bone plates, tissue scaffolds, drug release systems, filling materials, and wound dressing materials (Mozafari and Chauan, 2019; Takacs and Vlachopoulos, 2008). Especially in drug delivery systems, they have an indispensable role and act as solubilizers, stabilizers, taste-masking, release-modifiers, bioavailability enhancers, carriers for drug payload (D'souza and Shegokar, 2016).

Polymers used in biomedical applications can be grouped as natural and synthetic polymers. Collagen, chitin, chitosan, silk, gelatin, fibrinogen, hyaluronic acid, keratin and alginate are the examples of natural polymers whereas polyethylene, poly(ethylene-vinyl acetate), polyether ketone, polylactic acid-based composites, poly(lactic-co-glycolic acid), polycaprolactone, poly(ethylene glycol), poly(hydroxybutyrate), poly(methyl methacrylate), poly(amid) and poly(acrylonitrile butadiene styrene) are the examples of synthetic polymers (Kashirina et al, 2019; Feroz et al, 2020). Biocompatible polymers, which can be both natural and man-made (synthetic), can be used to treat and replace any organ, tissue or function in the body as they are compatible with tissues and physiological fluids. Because of their biocompatibility feature, they can improve the body functions without causing any allergies or side effects. These properties together with the advantages in their fabrication makes them suitable candidates for pharmaceutical and therapeutic applications

Biocompatible polymers were used in both drug release and matrix synthesis stages of the thesis. Detailed information about polymers used in nanoparticles and matrix production are given in Sections 1.3.1, 1.3.2 and 1.3.3, respectively .

1.3.1 Poly(ethylene-co-vinyl acetate)

As a rubbery copolymer, poly (ethylene-co-vinyl acetate) (PEVA) has a wide usage area from hard to soft domains like electronics, packaging, adhesives, solar energy, agriculture and sport materials (Vahabia et al, 2017). PEVA formed by block copolymerization of a large number of vinyl acetate with ethylene is a low cost, transparent material with high elasticity, high hardness, high chemical resistance, easy processability (Onlaora et al, 2019). It cannot be degraded biologically within the body, but it is inert and does not cause any allergic reaction after implanting to the body. Materials produced by PEVA are used in drug delivery studies at therapeutic levels over extended periods of time and they can provide a constant drug release rate per unit of time (Jaleh et al, 2014).

PEVA has also been used in biomedical applications by mixing with hydroxyapatite, polycarbonate, polyester, carbon nanotube, etc. materials (Vahabia et al, 2017). In addition, it is the main material of drug release systems used in the digestive system and vagina channel (Mariotti and Vannozz, 2019). Ocusert® and Progesterat®, which are Food and Drug Administration (FDA) approved and commercially available devices based on PEVA, are being used for ocular and intra-vaginal use, respectively (Bhusal et al, 2017).

In this study, PEVA was used in nanoparticle synthesis by mixing with other polymers in different ratios and active agent was released from these nanaoparticles.

1.3.2 Poly(ethylene glycol)

Poly(ethylene glycol) (PEG) is a biodegredable, biocompatible, FDA approved polymer, and has high structure flexibility, amphiphilicity. Since it is devoid of any steric hindrances, and has high hydration capacity, it is widely used to prevent non-specific protein adsorption to the surface. PEGlation is a common method used in drug and protein delivery studies because PEG-coated materials are capable to escape from host's immune defense system (Webster et al, 2007). The chemical reactivity of free hydroxyl groups at the chain ends can be used for attachment of bioactive molecules (Harris and Chess, 2003; Sundararajan et al, 2018). PEG can be dissolved in both organic solvents and aqueous solutions which makes its processing and modification easy. It can be fabricated by polycondensation of ethylene glycol in the presence of

acidic or basic catalysts, yielding to low molecular weight product. In order to produce high molecular weight PEG, ethylene oxide should be used as precursor during polymerisation (Ivanova et al, 2014).

From 1950s, PEGs have been used as seperation and purification agents, embedding matrices, anti-freeze material, medical devices lubricant, food additive, stabilizer, carrier for dermotological use and biological molecules, parenterals, pills&tablets, and suppository (D'souza and Shegokar, 2016; Roberts et al, 2012).

When there is alcohol dehydrogenase in media, PEG is metabolized by oxidation of its alcohol group to form carboxylic acid, diacids, and metabolites of hydroxyl acid. PEG has two different release mechanisms for physically entrapped drugs; erosion-controlled and diffusion controlled mechanisms. Sometimes both mechanisms can be used for drug release. Water can go through the polymer structure and dissolve the drug by diffusion (D'souza and Shegokar, 2016). In the thesis, PEG was mixed with poly (ethylene-co-vinyl acetate) (PEVA) in the fabrication of nanoparticles to take advantage of its biodegradability feature.

1.3.3 Polyurethane

Polyurethanes (PUs) are plastic type polymers that can be incorporated into different materials including paints, liquid coatings, elastomers, insulators, elastic fibres, foams, integral skins, etc (Akindoyo et al, 2016). It was first developed during World War II and it has large usage area such as building and construction applications, biomedical applications, automotive, textiles and in several other industries because of its good mechanical properties (Rafiee and Keshavarz, 2015).

PUs is produced by the reaction of alcohol (–OH) and isocyanate (NCO) and besides the major repeating urethane unit, it can also contain ethers, esters, urea and some aromatic compounds. Thanks to this variety, different PUs having different properties, such as rigidity, flexiblity, thermoplasticity, etc can be synthesized and used in the production of binders, coatings, sealants, and various medical devices (Figure 1.4) (Akindoyo et al, 2016).

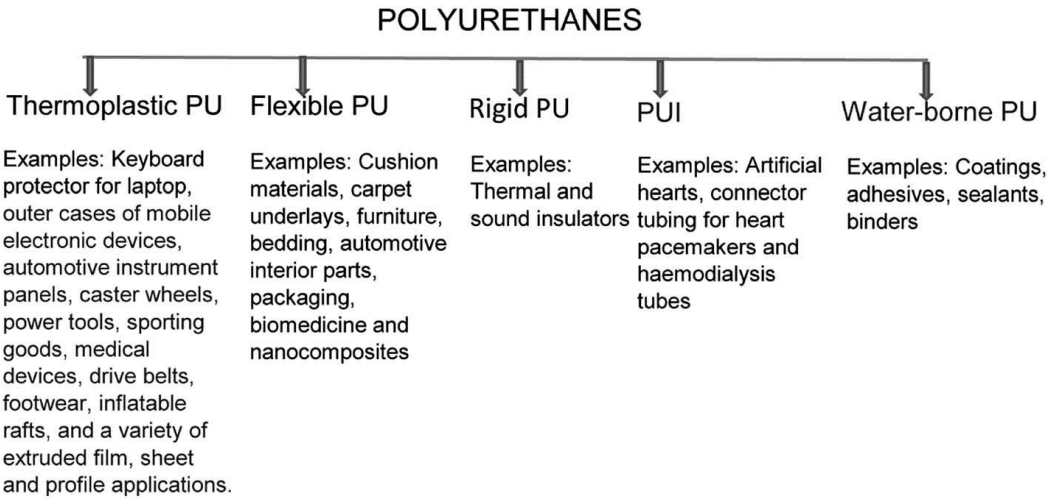

Figure 1.4 : Important PU types and their common applications (Akindoyo et al, 2016).

General purpose tubing, catheters, hospital beddings, surgical drapes, wound dressing materials and different injection-moulded equipments are the medical applications where PUs are used due to their availability, good mechanical and physical characteristics, and -albeit limited- hemocompatibility and biocompatibility properties (Zhou et al, 2014). To improve their limited biocompatibility, cytocompatibility and hemocompatibility and to increase PUs in vivo performance, other components can be added and various fabrication techniques can be performed (Kashirina et al, 2019).

1.4 Polymeric Nanoparticles and Their Applications

Particles sized between 10 to 1000 nm (1 μm) are called nanoparticles (McNamara and Tofail, 2017). They have wide application area in biomedical field such as biosensors, targeted and controlled drug delivery, bioimaging, hyperthermia and photoablation therapy, thanks to the advantage of increased surface to volume ratio compared to the larger particles, easy penetration through cell membranes properties, low off-target effects, better drug kinetics and lysosomal escape after endocytosis (Afsharzadeh et al, 2018). Nanoparticles carrying active agents can be defined in 2 main subgroup; matrix-like nanoparticles (nanospheres and polymer micelles) and reservoir-type nanoparticles (nanocapsules and polymersomes) (Figure 1.5) (Mora-Huertas et al, 2010).

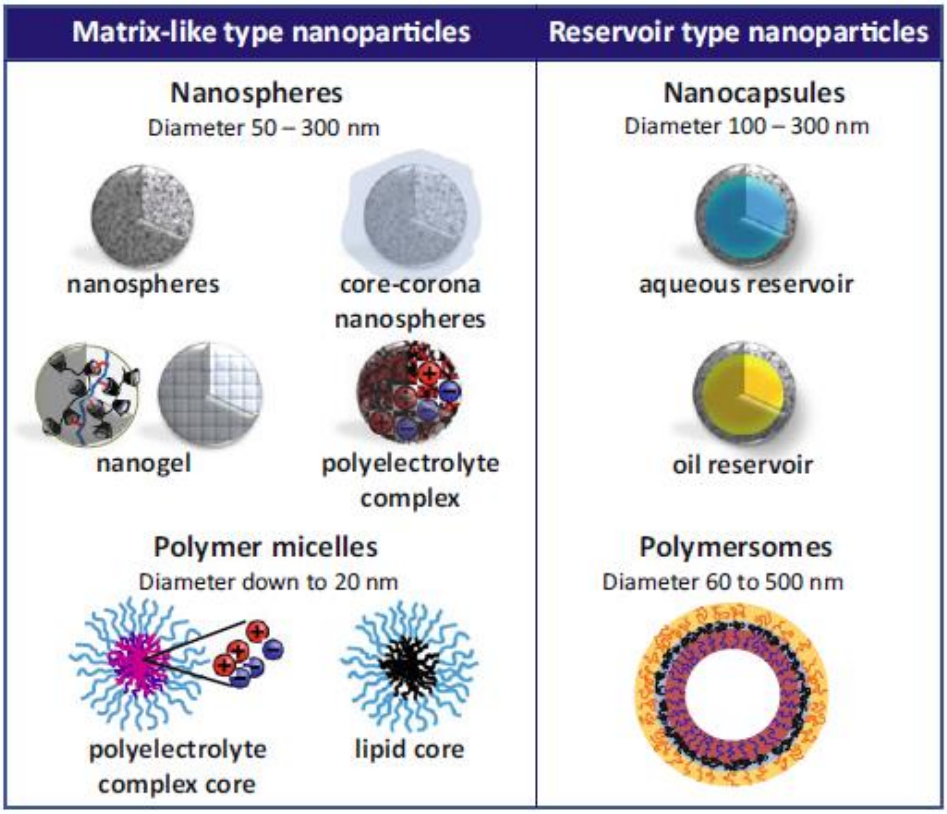

Figure 1.5 : Structures of different types of polymer nanoparticles (Vauthier and Ponchel, 2016).

Polymeric nanoparticles used in biomedical applications have 6 critical challenges; polymer characterization at the beginning (purity, molecular weight and distrubution, and polydispersity), size, surface properties, drug loading capacity and release profile, stability, and batch-to-batch reproducibility (Vauthier and Ponchel, 2016). Despite the challenges, nanoparticles can be produced using different polymers, and can be modified to improve efficacy so they are the key players for drug release studies, especially good candidates to carry and deliver poorly water-soluble drugs to the target locations (Tao et al, 2019). In addition, as any other drug carrier system, they increase the stability of any volatile pharmaceutical agents and offer complete drug protection, so they are excellent carrier for controlled and sustained delivery of different drugs. Stealth and surface modified nanoparticles can be used in active and passive drug delivery applications (Bhatia, 2016). Nanoparticles have potential to carry and deliver multiple therapeutics at the same time or alternately. When more than one chemical agent is used in the same nanoparticle, the complexity of the polymeric nanoparticle systems increases. It requires more careful formulation, and both controlled release and physico-chemical and structural characteristics should be evaluated and optimised (Amreddy et al, 2017).

1.4.1 Synthesis methods

Nanoparticles have many advantages to be used especially as controlled release systems but the main challenge is to develop a suitable method for nanoparticle preparation (Tao et al, 2019). Different methods can be used to produce nanoparticles as nanospheres or nanocapsules. All types of nanoparticles which will be used in biomedical applications need to meet the requirements in terms of degradability and safety.

Both top-down and bottom-up approaches are present for nanoparticle fabrication. The methods which are started with large solid structures and continues with mechanical breaking down process to handle smaller particles are called “top-down”. Shear, attrition, friction, pressure,or any combination of these stress types provide particle size reduction in top-down fabrication techniques such as nanoprecipitation, media milling, high-pressure homogenization. Other approach is “bottom-up” which is generally used to prepare nanoparticles smaller than 100 nm. Nanoprecipitation, evaporation, salting-out, supercritical fluid technique, liquid jet precipitation, sonocrystallization and multi-inlet vortex mixing and emulsification are the most known methods in bottom-up approach and they all require expensive equipments (Ahire et al, 2018).

Polymeric nanoparticles can be prepared in different methods such as;

- Solvent evaporation method,
- Spontaneous emulsification or solvent diffusion method,
- Double emulsion and evaporation method,
- Salting out method,
- Emulsions-diffusion method,
- Solvent displacement/precipitation method,
- Coacervation or ionic gelation method,
- Polymerization method,
- Supercritical fluid technology (Bhatia, 2016).

The emulsification-solvent evaporation method which is used in this study to produce poly (ethylene-co-vinyl acetate) (PEVA) & poly (ethylene glycol) (PEG) monomethyl

ether nanoparticles is the most common method to obtain submicron nanocarriers from preformed polymers. This technique was reported by Vanderhoff in 1970s and improved in the course of time. Because of its flexibility, it is modified based on the raw material and final product. For example; toxic solvents used in conventional fabrication method can be replaced with less toxic ones. Integration of new technologies on homogenization equipments increase the efficiency and reproducibility of the technique (Vauthier and Ponchel, 2016).

The parameters effecting the characteristics of nanoparticles are speed of agitation, flow regime, area of container for evaporation, temperature, pressure, ratio of the dispersed-to-continuous phase, and dispersed phase composition (Conti et al, 1995). Process variables are explained in figure 1.6.

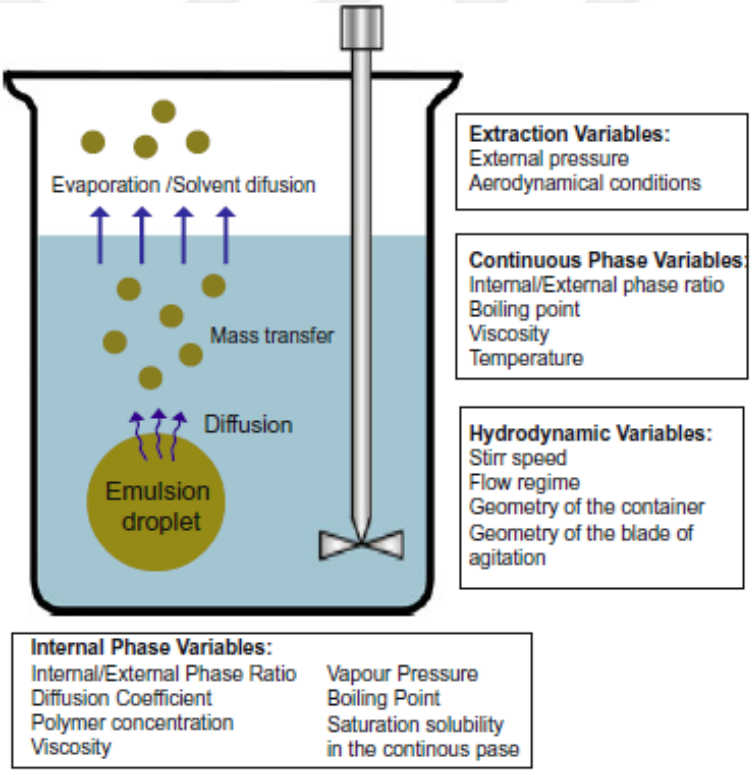

Figure 1.6 : Schematic representation of variables in solvent evaporation process (Vauthier and Ponchel, 2016).

1.5 Controlled Release Systems

There is a growing interest focused on drug delivery systems loaded with active pharmaceutical ingredients in medicine. These ingredients are delivered using various different systems including liposomes, micelles, polymeric nanoparticles, nanocrystals, mesoporous silica nanoparticles, and nanoemulsions (Zhoua et al, 2018).

Using nanoparticles in controlled release systems has many advantages. Having high surface area to volume ratio improves the dissolution rate and solubility of drugs and promotes specific interaction of nanoparticles (and also drugs) with cells or tissues, increases absorption and enhances bioavailability. Formulating as nanoparticles increases drugs' chemical stability and makes the control of release profiles possible in gastrointestinal tract, and to further promote the efficiency by ensuring long circulation and targeted delivery, nanoparticle surfaces can be modified (Tao et al, 2019).

The aim of controlled release systems is to increase the bioavailability of the drug by increasing its concentration in the target site and to release at appropriate rate. To achieve that goal, drug should be stable in nanoparticle, the encapsulation yield and retention of the drug should be optimum, and release rate should be controlled (ideally with minimum burst release) (Vauthier and Ponchel, 2016).

Drug release mechanisms can be classified in 3 different subgroup;

1) standard diffusion controlled release mechanism,

2) release by the degradation of the nanoparticles made by biodegradable polymers,

3) release depending on stimulation (Figure 1.7).

The common problem associated with delivery systems is the burst release which is observed at the begining and caused by the presence of drug on nanoparticle surface. In diffusion-controlled systems, drug release depends on effective diffusion coefficient throughout the polymer matrix and its porosity and tortuosity (Jäger et al. 2009). Drug release rate from biodegredable nanoparticles, on the other hand, depends on the bulk erosion rate (Chan et al. 2009). In stimuli-triggered release, different stimulus such as light, pH, temperature, enzymes, ultrasounds, magnetic force, reductive, or oxidative stress can trigger drug release from nanoparticles (Mura et al, 2013).

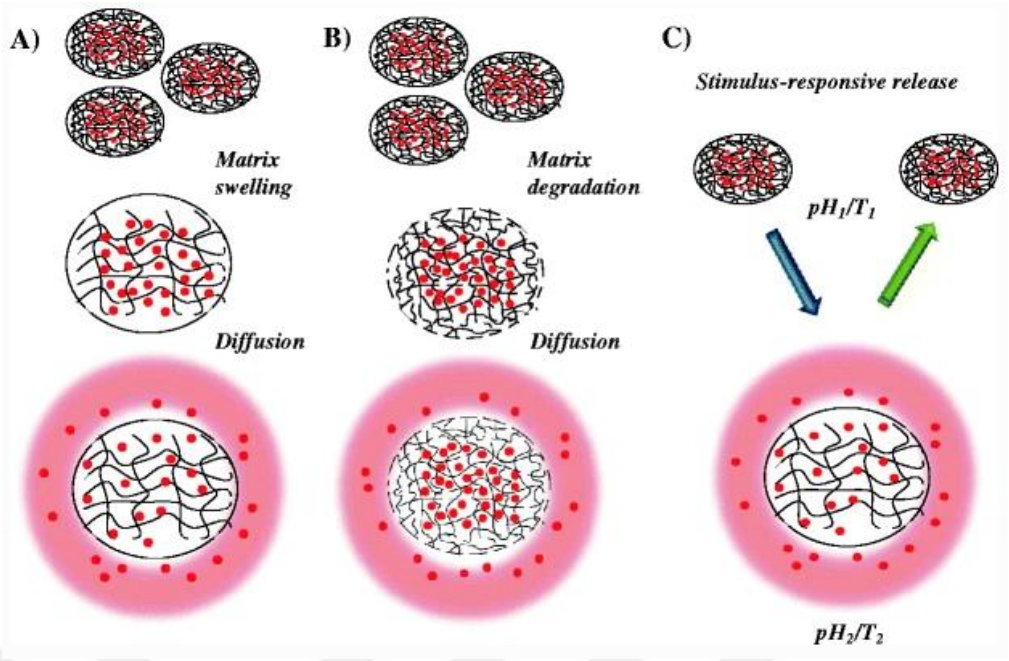

Figure 1.7 : Schematic representation of different drug release mechanisms (Balmayor et al, 2011).

In order to evaluate the efficiency of drug release from nanoparticles different techniques can be used at different steps:

- In vitro methods: Dissolution Dialysis

- In cellulo methods: Cellular uptake and biological effect detection

- Ex vivo methods: Release across biological membranes

- In vivo methods: Pharmacokinetics in healthy animals and therapeutic effect in diseased animals.

Dissolution dialysis is easily implemented and low cost method which can be adapted to different drugs. This method is used in this thesis, and the release profile depends on nature, pH, and temperature of medium and sink conditions (Ribeiro et al, 2014; Lee at al, 2002).

1.5.1 Selenium

Selenium (Se) is an essential nutrient for humans and provides various health benefits even though its essential nutritional role continues to be a matter of debate. Humans can get Se with crop, animal products, fish, and seafood, and sometimes in supplements (Vinceti et al, 2017). Organically bound Se (e.g. selenomethionine, selenocysteine) and inorganic forms (e.g. selenate, selenite) are the subgroups of Se

species (Weekley, 2013). According to the USA Institute of Medicine, upper intake level of Se is 400 µg/day for adults (Benardot, 2011). In recent researches, the ability of Se to prevent cancer cell growth was observed so using Se compounds is recommended for cancer prevention and therapy (Vinceti et al, 2018).

Studies have shown that Se deficiency reduces the synthesis of thyroid hormone. Because it reduces the functions of selenoproteins which are essential for deiodinase enzymes operations and these enzymes are responsible for the conversion of triiodothyronine (T3) and thyroxine (T4). This decrease in thyroid hormone production causes stimulation of the hypothalamic-pituitary axis and increased thyroid-stimulating hormone (TSH) production due to the lack of negative feedback control. TSH situmulates DIOs to convert T3 and T4, and also to produce hydrogen peroxide. Hydrogen peroxides cannot be eliminated by insufficiently active glutathione peroxidases (GPx) and accumulate in thyroid tissue. This accumulation causes destruction of thyroid epithelial cells (tyrosides). At the same time, when the production of TSH increases, the secretion of T3 and T4 increases, as well as the level of thyroid peroxidase antibody (anti-TPO). Gartner et al. found a significant decrease in serum anti-TPO levels with daily intake of 200 µg (2.53 micromol) sodium selenite for 3 months (36.4% decrease in Se group versus 12% decrease in placebo group), and there was no change observed in average fT3, fT4 and TSH levels (Gartner et al, 2002).

In the following study of the same group, there was 56% decrease in anti-TPO concentration by taking sodium selenite at the same dose for another 6 months, 57% increase upon discontinuation of treatment, and antibody concentrations did not change significantly in the placebo group. Additionally, when placebo group that took placebo for 3 months, started to take sodium selenite for 6 months, anti-TPO concentration decreased by 52% (Gartner et al, 2003).

1.5.2 Cepharanthine

Cepharanthine (CEP) (6 ′, 12′-dimethoxy-2,2′-dimethyl-6,7- [methylenebis (oxy)] oxacantan), used to inhibit T cell activation in the immune system, is a natural alkaloid which extracted from the roots of *Stephania Cepharantha Hayata*. (Figure 1.8). CEP has pharmacological effects on improvement of the body immunity (Chu et al, 2018). Besides, it has anti-cancer effects originated from inhibition of cell proliferation and

angiogenesis, induction of autophagy and cell death, anti-inflammatory effects (Gao et al, 2017).

Li et al, showed that HLA-DR3 gene and specific HLA-DR pocket sequences which are strongly identified with autoimmune thyroid disease (AITD), Graves'disease and Hashimoto's thyroiditis (Li et al, 2020). The presence of arginine at position DR β1-74, which is the key aminoacid position in the AITD-associated pocket signature, is associated with strong susceptibility to AITD while the glutamine at this position is protective. They found 4 different thyroglobulin (Tg) peptides (Tg.1951, Tg.2098, Tg.1571, Tg.726) which can bind to DR β1- Arg74 HLA-DR stringly and selectively (Menconi et al, 2010).

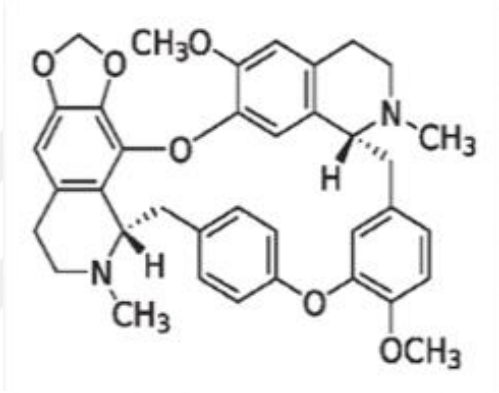

Figure 1.8 : Chemical structure of CEP.

In the light of this information, Li et al., hypothesized that blocking peptides bound to DRβ1-Arg74 would also inhibit T cell activation, which is necessary for maintaining an autoimmune response in thyroiditis patients, and for this purpose they investigated molecules that would inhibit Tg peptide formation and therefore T cell activation. As a result of their research, they found that CEP prevents binding Tg peptides to HLA-DRβ1-Arg74. Thus, the formation of Tg, which is the key antigen of autoimmune thyroiditis and thought to cause both Hashimato and Graves Disease, was prevented and parallel to this, the formation of thyroglobulin antibody (anti-Tg) produced in response to Tg was prevented. Moreover, CEP can block the activation of T-cells by Tg peptides because CEP has hydrophobic residues which directly interact with DRβ1-Arg74. This interaction had been found to effectively inhibit Tg peptide presentation to T-cells in autoimmune thyroiditis (Li et al, 2016).

1.6 Hypothesis

Hypothyroidism is an autoimmune disease associated with underactive thyroid gland. The characteristic symptoms of the disease are the high level of thyroid peroxidase (anti-TPO) and thyroglobulin (anti-Tg) antibodies in blood. Anti-TPO is produced against thyroid peroxidase (TPO), and anti-Tg is produced against thyroglobulin (Tg) secreted by thyroid cells to bloodstream. Cepharanthine (CEP), which is a natural alkaloid, can block T cell activation and Selenium (Se), which is an essential nutrient, can decrease anti-TPO concentration.

It was hypothesized that if a dual effect system is created to release CEP and Se, it will have potential to effectively threat hypothyroidism by addressing both auto-immune response and hormone regulation.

For this purpose, matrix-like-type nanoparticles were synthesized by poly (ethylene-co-vinyl acetate) (PEVA) with different poly (ethylene glycol) (PEG) mono methyl ether concentrations (0, 15, 20, 25, 30 %w/w of PEVA) by emulsion solvent evaporation method, and CEP was loaded to these nanoparticles. Then, PEG-PUSe-PEG block copolymer were synthesized and it was mixed with different PU concentrations (0, 33, 50% w/w block copolymer) to fabricate porous matrices by particulate leaching technique. Long term release of CEP was examined in PBS at 37°C both separately and after their incorporation on matrices. Se release from 1:1 and 2:1 matrices was followed for 7 days in both distilled water and water including H_2O_2 (0.1% v/v). Cytotoxic effects of nanoparticles and matrices were investigated on NIH 3T3 fibroblasts.

2. MATERIALS AND METHODS

2.1 Materials

Poly(ethylene-co-vinyl acetate) (PEVA; 12 wt% vinyl acetate), 11-bromo- 1-undecanol (≥99.0%), Selenium (Se; ≥99.5%), Cepharanthine (CEP; >95%), toluene-2,4-diisocyanate (TDI; ≥95%), and anhydrous sodium sulfate (Na2SO4; ≥99.99%) were supplied from Sigma-Aldrich. Poly(ethylene glycol) (PEG) monomethyl ether (MW: 1,900), and thermoplastic polyurethane (PU) was purchased from Polysciences, and Inc and Flokser Co. respectively. Sodium borohydride (≥96%), ethanol (EtOH; 96%), carbon tetrachloride (CCl4; ≥99.5%), dichloromethane (DCM; ≥ 99.8%), and anhydrous tetrahydrofuran (THF; ≥99%) were bought from Merck Millipore.

For cell culture studies, fetal bovine serum (FBS), and trypsin/EDTA solution, Dulbecco's Modified Eagle's Medium (DMEM), penicillin– streptomycin were obtained from Sigma-Aldrich and Pan Biotech, respectively. CellTiter 96® AQueous One Solution Cell Proliferation Assay (MTS; Dojindo Molecular Technologies, Inc.) was used for the evaluation of cell viability. Cells were dyed with 40,6-diamidino-2-phenylindole dihydrochloride (DAPI; 100 nM; ≥97%) (Santa Cruz Biotechnology, Inc), and phalloidin CruzFluor™ 488 conjugate for fluorescence microscopy analysis. Before taking SEM micrographs, cells were fixed with glutaraldehyde solution (Sigma-Aldrich; ≥98%) and cacodylic acid sodium salt trihydrate (Sigma; >98%).

2.2 Methods

2.2.1 Nanoparticle synthesis

Nanoparticles (NPs) were prepared using poly(ethylene-co-vinyl acetate) (PEVA) and poly(ethylene glycol) (PEG) monomethyl ether using emulsion–diffusion–evaporation method (Varshosaz et al, 2014). In order to synthesize blank NPs as a negative control, 36 mg PEVA was solved in 3 mL carbon tetrachloride (CCl_4) at 60^{o}C, and PEG

monomethyl ether at different ratios (0%, 15%, 20%, 25% and 30% w/w of PEVA) were dissolved in 1.3 mL in dichloromethane (DCM) at room temperature. DCM solution was added into CCl_4 and two solutions were mixed for 1 hr, then added dropwise into 25 mL distilled water including Tween 20 (0.5% w/v) at 45ºC. After mixing 30 min, the mixture was sonicated by an Sonoplus, Bandelin ultrasonic homogenizer with micro tip probe (MS 72) on "pulse on" and "pulse off" modes at different durations to obtain particles in desired size range. Then, the mixture was agitated with a magnetic stirrer under fume hood to evaporate the organic solvent completely. After organic solvent removal, NPs were washed 3 times with EtOH (96%) with centrifuge at 5,000 rpm for 10 min.

2.2.2 Characterization of NPs

The effect of different PEG monomethyl ether ratios and sonication times on particle size and distribution was determined by Zetasizer (Nano series, Malvern). Before starting to measure the particle sizes with Zetasizer, the solutions including NPs were diluted with EtOH (96%) (1: 10,000 v/v) and sonicated 4 minutes by an ultrasonic homogenizer to prevent agglomeration of NPs (Bhattacharjee, 2016).

The chemical structures of the synthesized particles made by PEVA (100 % w/w) and both PEVA and PEG (20% w/w of PEVA) monomethyl ether were investigated by using Raman spectroscopy (JY HR 800, Horiba). The NPs in EtOH (96%) were dried by freeze dryer (Alpha 1-2 LD Plus, Chris) for 24 hours at -35°C. All samples spectra were obtained at 500 – 4000 cm^{-1} wavelength.

Scanning electron microscopy (SEM, Quanta 650, Fei Company) was used to examine the morphology of both blank and CEP loaded NPs. Before capturing images, NPs were diluted with EtOH (96%) (1:100, v/v), then vortexed and sonicated to avoid the agglomeration and finally dried at room temperature. Then NPs were coated with a thin layer of gold-platinum under vacuum and analysed with an Everhart-Thornley Detector (ETD) in SEM under high vacuum mode.

2.2.3 CEP loading efficiency

After the particle synthesis procedure, and PEVA and PEG monomethyl ether ratios (w/w) were optimised, CEP was loaded to the particles at different ratios (10, 20 and 30% w/w of PEVA) during sythesis phase. In order to calculate CEP loading

efficiency, the particles including CEP were washed three times with EtOH (96%) by consecutive centrifugation steps at 5000 rpm, for 10 min and the supernatants were collected. Then the supernatant was anaysed at 283 nm in UV–Vis spectrophotometer (UV-1601, Shimadzu) to determine CEP concentration. Encapsulation efficiency (EE%) of CEP loaded to NPs was calculated according to the equation 2.1 mentioned below:

$$\text{EE } \% = \frac{\text{Total Drug} - \text{Free Drug}}{\text{Total Drug}} \times 100 \quad (2.1)$$

2.2.4 Synthesis of PEG-PUSe-PEG block copolymer

To prepare monoselenide containing amphiphilic block copolymers (PEG-PUSe-PEG) two successive steps approach was used. The first step is involving the condensation of dihydroxylalkyl selenide and diisocyanate, followed by a termination of PEG monomethyl ether (Ma et al, 2010). At the begining, di-(1-hydroxylundecyl) selenide was synthesized by dissolving 0.15 g sodium borohydride in water and 0.16 g Selenium (Se) powder was dissolved with the generation of H_2(g) and a colorless solution was obtained within 5 min. After the flask was degassed with $N_{2(g)}$, it was sealed with a rubber plug. In another flask, 1.0 g 11-bromoundecanol was dissolved in anhydrous THF and it was injected into the first flask under fume hood. The reaction was performed at 50ºC for 12 h in oil bath. The di-(1-hydroxylundecyl) selenide solution was diluted with CH_2Cl_2, dried with anhydrous Na_2SO_4, and purified by column chromatography with a 4 : 1 mixture of CH_2Cl_2 and ethyl acetate as eluent.
At the second step of block copolymer sythesis, 0.52 g di-(1-hydroxylundecyl) selenide was dissolved in anhydrous THF and a rubber plug was placed to the reaction flask for sealing, and the flask was degassed with $N_{2(g)}$. A solution of 0.19 mL toluene-2,4-diisocyanate (TDI) in anhydrous THF was injected into the flask under $N_{2(g)}$ flow and the flask was put into an oil bath to be stirred for 12 h at 50ºC. Then 0.16 g PEG monomethyl ether dissolved in anhydrous THF was added dropwise into the flask and the reaction was performed for another 12 h. When the reaction completed, the solvent was removed under fume hood and the solid residue was washed with the mixture of deionized water and acetone and PEG-PUSe-PEG block copolymer was dried under fume hood.

2.2.5 Preparation of blank and NP loaded blend matrices

Before matrix fabrication, nine different solvents (EtOH (96%), 1,1,1,3,3,3-hexafluoro-2-propanol, dichloromethane, anhydrous THF, hexane, acetic acid, acetone, 2,2,2- trifluoroethanol, and dimethylformamide (DMF)) were tried to find the suitable solvent to solve PEG-PUSe-PEG block copolymer.

2.2.5.1 Preliminary studies

In order to obtain a sponge-like matrix structure by using PEG-PUSe-PEG block copolymer, 10 mg/mL copolymer was dissolved in DMF and the solution was poured into distilled water (dH_2O) mixing at 1500 rpm to remove the organic phase, at room temperature. After 2 hours, the copolymer solution was put into deep freeze at -80 ^oC overnight and then freeze-dried for 24 hours at -35°C. A regular and porous structure could not be observed so polymer concentration was increased to 100 mg/mL and then to 170 mg/mL and the same freezing and drying procedure mentioned above was followed.

In another method, to fabricate a matrix using PEG-PUSe-PEG block copolymer, 10 mg/mL copolymer was dissolved in DMF and sonicated by an ultrasonic homogenizer (Sonoplus, Bandelin) on 20 sec "pulse on" and 10 sec "pulse off" modes for 5 minutes and then the solution was transferred to deionized water. The color of the mixture changed and it was placed into the dialysis membrane and waited for 72 hours in dH_2O to be dialyzed (Ma et al, 2010) but the desired sponge like structure was not obtained.

2.2.5.2 Matrix preparation

After these preliminary experiments, optimum porous matrices were fabricated by particulate leaching technique from PEG-PUSe-PEG block copolymer and PU (Tetteh, 2016). Three different matrix combination including (1) 100 % PU, (2) 66% PU and 34% PEG-PUSe-PEG block copolymer and (3) 50% PU and 50% PEG-PUSe-PEG block copolymer were prepared. Briefly for each matrix type, 20 wt % polymer composite was dissolved in THF and DMF (1:1 (v/v)) containing bottles. Then 15 g NaCl/bottle was transferred to the polymer solutions and vigilantly stirred with a thin spatula in order to obtain homogeneous dispersion. These mixtures were dropped into glass disks (60 mm diameter) and 2g NaCl per disk were dusted onto the surface of

the polymer to prevent thick non-porous layer formation on cast surface. The casts were dried to solidify under fume hood and washed with 2000 mL of deionized water on a rotating spinner for 3 days to leach all salt particles. After salt had been removed completely, the porous matrices were dried under fume hood.

For further studies, NPs were impregnated into synthesized matrices by using micropipette and left for drying at room temperature.

2.2.6 Characterization of PEG-PUSe-PEG block copolymer and matrices

1H-NMR spectra of PEG-PUSe-PEG block copolymer and di-(1-hydroxylundecyl) selenide were obtained by Agilent VNMRS spectrometer. Fourier transform infrared (FT-IR) spectra of block copolymer were determined by FTIR-ATR, Perkin Elmer spectrometer. In order to analyze pore structure and size of matrices, SEM images were captured. Matrix porosity measurements were done by liquid displacement method with n-hexane. The initial volume of n-hexane in a graduated cylinder was recorded as V1 and then matrices were placed into n-hexane and after 5 min, the new volumes were noted as V2. After removing the matrices from cylinders, the left volumes were recorded as V3 and the porosity ratios (ε%) were determined by using the equation 2.2 mentioned below:

$$\varepsilon\% = \frac{V1-V3}{V2-V3} X\ 100 \qquad (2.2)$$

2.2.7 In vitro CEP and Se release studies

In order to understand the release profile of PEVA and PEG (20% w/w of PEVA) monomethyl ether NPs, Ibuprofen was loaded as model drug and its release kinetic was carried out using dialysis bags for 6 days, using UV spectrophotometer for quantitative measurement of drug concentration (Kutlu et al, 2014). For CEP release studies, calibration curves in both EtOH (96%) and PBS (pH 7.4) were drawn and CEP release kinetics from both NPs and matrices including NPs were performed by using these curves. Briefly, PEVA and PEG monomethyl ether NPs were dried either in an oven or freeze dryer and they were placed into cellulose membranes with 1 mL PBS, and then transferred to bottles containing 5 mL PBS. CEP release was followed on a shaking incubator at 37^{o}C. The effect of drying method to CEP release from NPs were analysed.

Matrices containing NPs were placed into cellulose membranes including 5 mL PBS, and these membranes were put into PBS containing bottles (15 mL) (Figure 2.1). The amounts of CEP relased from these systems were measured by using the same procedure described above.

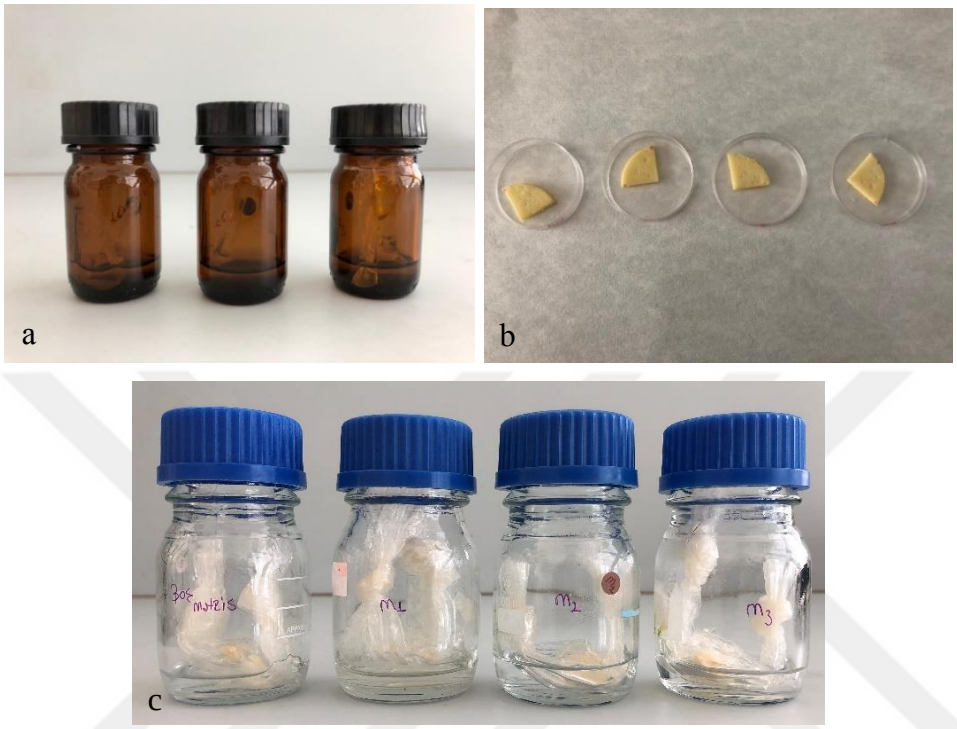

Figure 2.1 : a) CEP loaded NPs in dialysis bags, b) NPs integrated matrices, c) matrices including CEP loaded NPs in dialysis bags.

In order to measure the released amount of Se, ICP-MS in Koç University, Surface Science and Technology Center was used. The matrices have 1cm diameter and 0.5 cm thickness were sterilized in EtOH (70%) overnight and then they were washed with distilled water 3 times and after air-drying in laminar flow hood, matrices were placed into the falcons containing 25 mL ultra pure water and water including H_2O_2 (0.1 % v/v) in parallel (Figure 2.2). Se release studies were also followed on a shaking incubator at 37^{o}C.

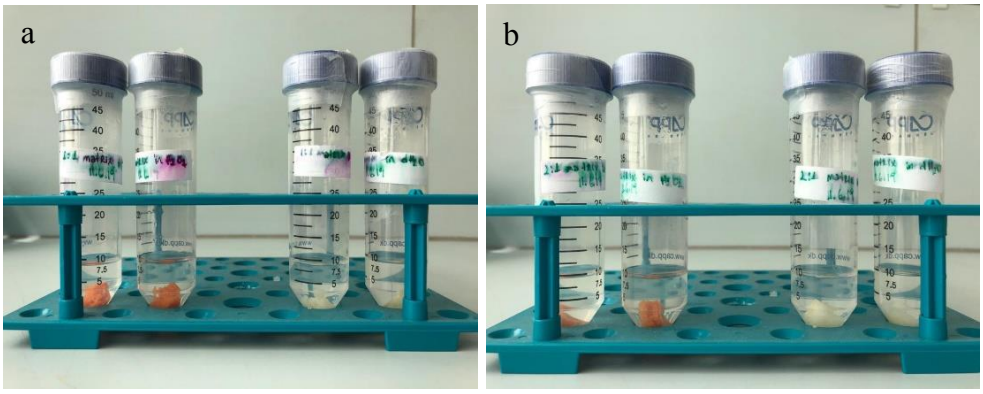

Figure 2.2 : Se release systems from a) matrices made by 50% PU and 50% PEG-PUSe-PEG block copolymer, b) matrices made by 66% PU and 34% PEG-PUSe-PEG block copolymer. Falcons with light yellow and orange matrices contain ultra pure water and water including H_2O_2, respectively.

2.2.8 Cell culture studies

All cell culture studies were performed by NIH 3T3 (mouse fibroblast) cells. Primarily, NIH 3T3 cells were subcultured in flasks using Dulbecco's Modified Eagle's Medium (DMEM) supplemented with 10% (v/v) fetal bovine serum (FBS) and 1% (v/v) penicillin– streptomycin solution and incubated at 37°C in a humidified CO_2 (5%) atmosphere (Series C, Binder). The cells were detached by trypsinization (0.25% trypsin–EDTA), then centrifuged and resuspended in medium before cell seeding.

2.2.9 Observation of cells by fluorescence microscopy

The attachment, spreading, cytoskeleton organization, and cellular morphology of cells were carried out by light microscopy and inverted fluorescence microscope from different spots. Before recording fluorescence microscopy images, cells were fixed with 4% (w/v) formaldehyde for 15 min. After washing 3 times with PBS, 0.5% Triton® X-100 (v/v) in PBS (15 min) was used to increase the permeabilization of cells, and then cells were washed with PBS again. To stain cell nuclei, cells were treated with 40,6-diamidino-2-phenylindole dihydrochloride (DAPI; 100 nM in PBS) for 15 min. Actin filaments were incubated with Phalloidin CruzFluor™ 488 Conjugate (Excitation/Emission wavelength 493/517 nm) for 20 min to be stained. After washing with PBS, images were captured by inverted fluorescence microscope (Axiovert A1, Zeiss) and processed by ImageJ software.

2.2.10 Cell viability assay

MTS assay was used to measure the mitochondrial activities of NIH 3T3 cells on days 1, 4 and 7 days of incubation (Url-3). The experiments were performed in the dark and all plates were covered with aluminium foil. At the specified time intervals, 100 µL MTS solution was added to cell culture plates, then samples were incubated at 37°C for 3 hr in the CO_2 incubator. At the end of incubation, 100 µL of solutions on the samples were transferred to 96-well plate to measure the optical density spectrophotometrically, and Elisa Plate Reader (Benchmark Plus, Bio-Rad) was used at 450 nm with reference to 690 nm.

2.2.11 Cell culture studies with NPs and matrices

Cytotoxicity studies were carried out in three main groups: In the first group, both blank and CEP loaded NPs were directly interacted with NIH 3T3 cells (denoted as direct interaction with NPs). In the second group, matrix eluents were interacted with NIH 3T3 cells (denoted as indirect interaction with matrices). In the third group, matrices were interacted with NIH 3T3 cells directly (denoted as direct interaction with matrices). All studies were conducted in 5% CO_2 atmosphere at 37°C.

2.2.11.1 Toxicity of NPs (direct interaction)

For the first group, 50 µL suspended blank and CEP loaded NPs in EtOH (96%) were placed into the wells of a 24-well plate. Then they were air-dried for 30 min in laminar flow hood and then kept under UV light for 30 min to sterilize. One day later, subconfluent NIH 3T3 cells (P26) were washed with PBS (pH 7.4) and then trypsinized to dissociate adherent cells from the vessel, and resuspended in high glucose DMEM (1×10^4 cells/mL) and seeded on NPs. Cells were allowed to adhere to the plate surface for 2 hr, and then, 1 mL culture medium (DMEM supplemented with 10% (v/v) FBS and 1% (v/v) penicillin– streptomycin solution) was added to each well. Cells were analyzed under a fluorescence microscope as described in Section 2.2.9 and cell viability was evaluated as described in Section 2.2.10.

2.2.11.2 Toxicity of Matrices (indirect interaction)

In indirect interaction with matrices group; 1cm diameter and 0.5 cm thickness samples from 3 types of matrices (100 % PU, 66% PU and 34% PEG-PUSe-PEG block copolymer and 50% PU and 50% PEG-PUSe-PEG block copolymer) were sterilized in EtOH (70%) overnight and then they were washed 3 times with sterilized PBS (pH 7.4) with 3 times and dried in laminar flow hood. According to ISO 10993-1 standard, samples were kept in culture media for 24 and 72 hr to allow any leachable to be released in the medium (ISO 10993-1, 2016). Then eluents from each matrix type at different volumes (50, 100 and 200 µL) were added to adherent cells in the 1st and 3rd days. In order to anaylse cytotoxic effects of matrix eluents to NIH 3T3 cells, MTS assay was carried out as described in Section 2.2.10. Cells were analyzed under flurescence microscopy as described in Section 2.2.9.

2.2.11.3 Toxicity of Matrices (direct interaction)

In direct interaction with matrices group, 1 cm diameter and 0.5 cm thickness matrix samples were sterilized in EtOH (70%) overnight. Then they were placed into disposable petri dishes and waited under UV light for 60 min for further sterilization. In order to remove EtOH (70%) from matrices, samples were washed with sterilized PBS (pH 7.4) and dried in laminar flow hood. In order to observe cell–matrix interactions, cell suspensions (3×10^5 cells/mL) were directly seeded on matrices on TCPS surface and in the 1st and 3rd day, SEM images were captured. Before recording, cells were washed with sodium cacodylate buffer (0,1 M) 3 times and fixed with 2.5% glutaraldehyde solution (v/v) for an hour at +4ºC. Then the samples were coated with a thin layer of gold–platinum under vacuum for SEM analysis.

2.2.12 Statistical analysis

All data are presented as means ±SD for n = 3. Statistical comparisons were carried out by Minitab software. Values of $p < 0.05$ were considered statistically significant.

3. RESULTS AND DISCUSSION

3.1 Nanoparticle Synthesis and Characterization

In this thesis, blank and CEP loaded NPs were prepared by emulsion–diffusion–evaporation method using poly(ethylene-co-vinyl acetate) (PEVA) and poly(ethylene glycol) (PEG) monomethyl ether. During nanoparticle synthesis, different concentrations of PEG (0, 15, 20, 25, and 30% w/w of PEVA) were mixed with PEVA to increase water penetration into NPs and help drug release because of its hydrophilic macromonomer structure (Varshosaz and Moazen, 2014).

3.1.1 Effect of PEG amount on particle size

Particle size analysis results for all samples were given in Table 3.1. As it can be seen from the table, 20% PEG resulted in fairly monodisperse sample (PDI: 0.464) with an acceptable average size (166.1 nm) so it was chosen for further studies. Qian and McClements mentioned that adding an active agent or drug to the solution affects the viscosity and this effect makes stirring more difficult and increases the particle size (Qian and McClements, 2011). In accordance with the literature, it was seen that loading CEP to nanoparticles increased both particle size and PDI values to 190.5 nm and 0.543, respectively.

3.1.2 Effect of sonication time on particle size

It is known that when speed and duration of agitation increases, the particle size generally decreases because of the increase in shear stress (Lee et al., 2002; Conti et al, 1995). In order to test this, different sonication times were tried during synthesis. Increasing sonication time causes the particle size to decrease while PDI increased marginally (Table 3.2). Therefore, 5 minutes, which gave low particle size with acceptable PDI value, was chosen as sonication time during the synthesis of NPs.

Table 3.1 : Effects of PEG amount and drug loading on size distribution and polydispersity index of NPs.

PEG monomethyl ether contents (w/w of PEVA)	Intensity	Particle size (nm)	Average (nm)	Polydispersity Index (PDI)	CEP loaded
0%	43.7	141.8	154.53	0.68	No
	55.7	164.2			
	0.5	190.1			
15%	79.1	105.7	109.19	1.00	No
	20.9	122.4			
20%	25.2	141.8	166.09	0.46	No
	45.7	164.2			
	29.1	190.1			
25%	31.8	141.8	162.67	0.89	No
	46.7	164.2			
	21.6	190.1			
30%	2.4	295.3	434.14	0.41	No
	16.9	342			
	30	396.1			
	30	458.7			
	17.3	531.2			
	3.4	615.1			
20%	26	164.2	190.47	0.54	Yes
	50.4	190.1			
	23.6	220.2			

Table 3.2 : Effects of sonication time on particle size.

Sonication time (min)	Average particle size (nm)	PDI
3	974.1	0.734
4	212.5	0.615
5	154.5	0.684
6	147.6	0.991

3.1.3 FTIR and Raman analysis of NPs

In order to understand the chemical structures of the synthesized NPs made by PEVA (100 % w/w) and PEVA-PEG (20% w/w of PEVA) monomethyl ether (denoted as PEG20-PEVA), FTIR spectra was obtained but the differences after PEG incorporation were not clearly observed, therefore Raman spectroscopy (JY HR 800, Horiba) was used to investigate the structure of NPs. When Raman spectra of 100% PEVA and PEG20-PEVA were compared, an additional peak (844 cm^{-1}) which is specific to the TGT (helical) configuration along the polymer chain and belongs to

mixed character of CH_2-rocking and backbone (C–O and C–C) stretching vibrations was observed for the PEG20-PEVA NPs (Figure 3.1) (Samuel and Umapathy, 2014). These spectra proved that PEG was permanently incorporated on NPs and was not lost during washing and/or lyophilization.

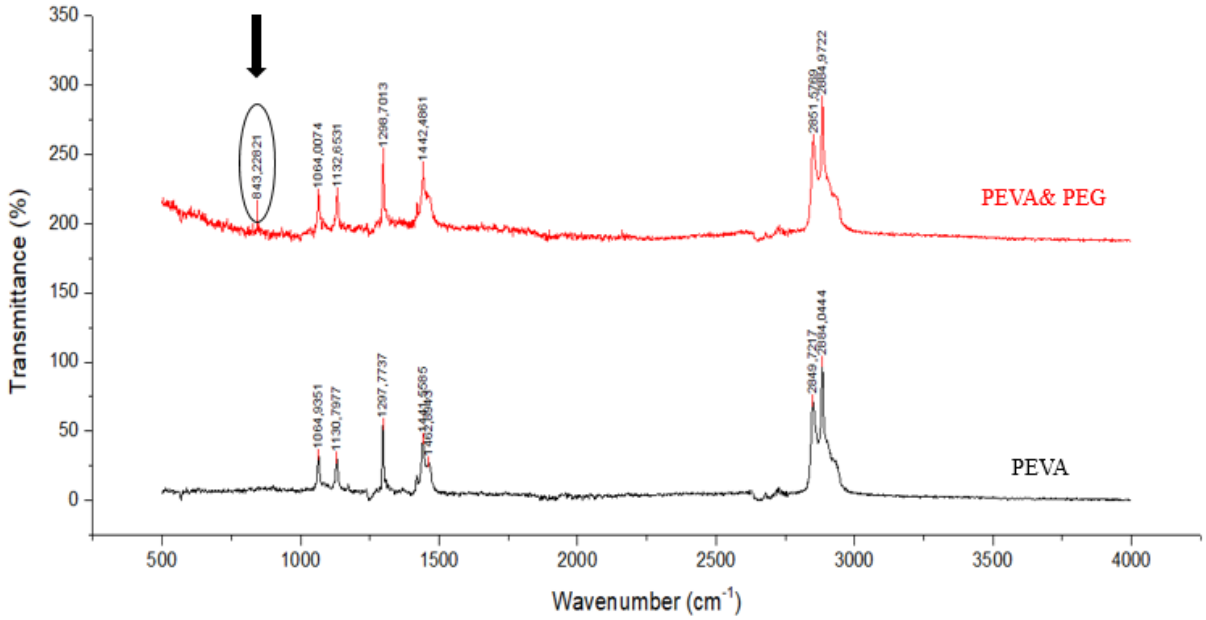

Figure 3.1 : Raman spectra of 100% PEVA and PEG20-PEVA NPs.

3.1.4 Scanning electron microscopy images of NPs

Scanning electron microscopy (SEM, Quanta 650, Fei Company) with an Everhart-Thornley Detector (ETD) was used to observe the morphology of both blank and CEP loaded NPs. Particle diameters comparable with those found with zetasizer were observed. Additionally, agglomeration caused hydrophobic nature of PEVA was seen on SEM images (Figure 3.2).

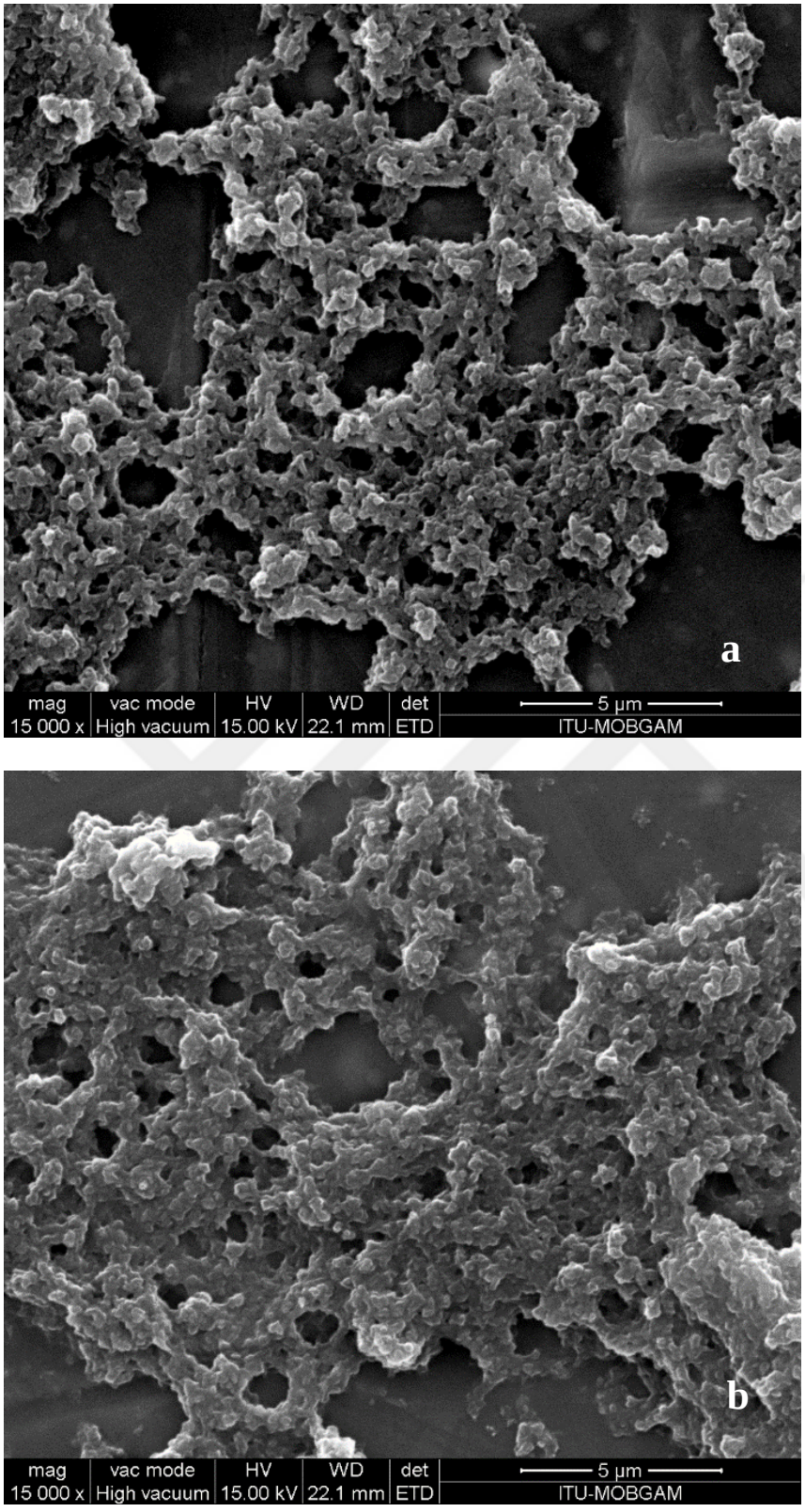

Figure 3.2 : SEM images of PEG20-PEVA NPs (a) blank (b) CEP loaded.

3.2 Loading Efficiency of CEP

After PEG/PEVA ratio and sonication time were optimised, different amounts of CEP were loaded to NPs during synthesis step. According to the literature, entrapment

efficiency of NPs synthesized by emulsion–diffusion–evaporation method mainly depends on emulsification process, phase compositions (concentrations of polymer and drug), and the stability of emulsion globules (Piacentini at al, 2020). In this thesis, encapsulation efficiencies of CEP were calculated as both total amount and percentage (Table 3.3). It was observed that there was no linear relationship between the initial CEP concentration and the entrapment efficiency. As seen in Table 3.3, when the initial concentration of CEP (w/w of PEVA) was increased to 2 and 3 times, neither encapsulation efficiency (%) nor encapsulated CEP amount increased proportionally, even encapsulation efficiency decreased. This results could be originated from the limited solubility of CEP in DCM (Gartner et al, 2002). Although the initial CEP concentration and accordingly the amount of encapsulated CEP is low, 10 % CEP (w/w of PEVA) was chosen as initial drug concentration because of relatively high encapsulation efficiency (%).

Table 3.3 : Comparision of CEP loading efficiencies according to initial concentrations.

CEP amounts (w/w of PEVA)	Encapsulation efficiency (%)	Encapsulated CEP amounts (μg)
10 %	23.3	840.4
20 %	12.2	878.2
30 %	12.1	1165.2

3.3 Selenium Containing Block Copolymer Synthesis and Characterization

PEG-PUSe-PEG block copolymer synthesis was done in two-step procedure involving di-(1-hydroxylundecyl) selenide synthesis and final copolymer synthesis.

3.3.1 Di-(1-hydroxylundecyl) selenide synthesis and characterization

In order to obtain PEG-PUSe-PEG block copolymer, as a first step, di-(1-hydroxylundecyl) selenide was synthesized, purified by column chromatography, and analysed by using FTIR and NMR. In FTIR spectrum, all characteristic peaks of di-(1-hydroxylundecyl) selenide such as amine N–H stretch (3426 cm^{-1}), alkane C-H bonds (2916 cm^{-1}), C=O stretch of carboxylic acid (1711 cm^{-1}), stretching band of N–O (1344 cm^{-1}), and C-O stretching of alcohol compounds (1055–1173 cm^{-1}) were seen (Figure 3.3).

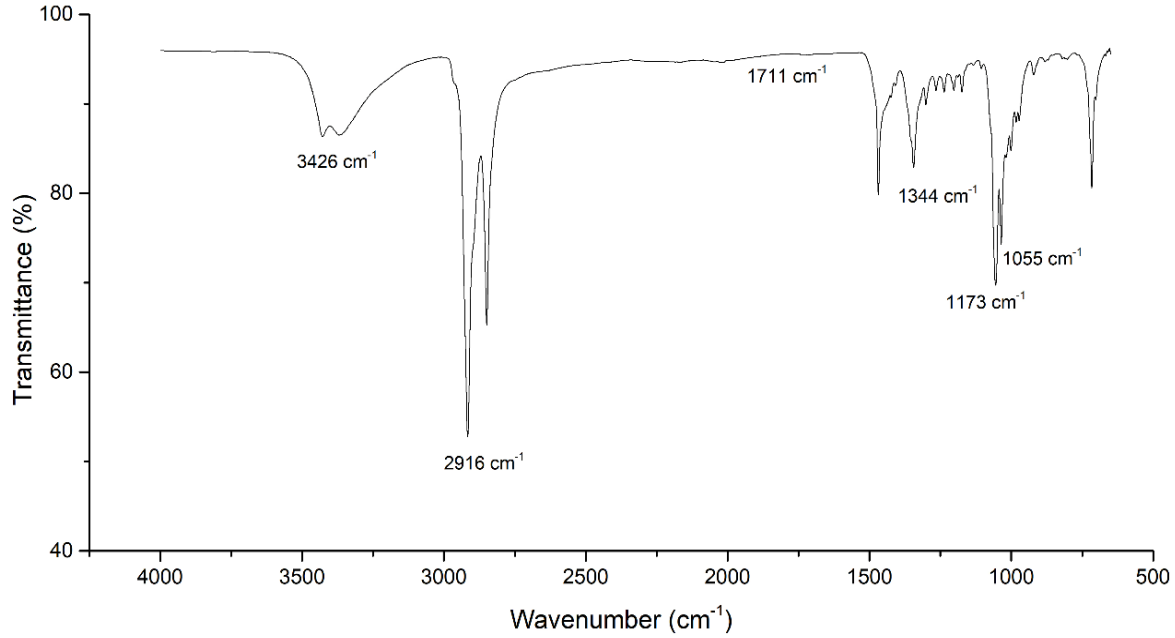

Figure 3.3 : FTIR spectrum of di-(1-hydroxylundecyl) selenide.

According to NMR spectrum of di-(1-hydroxylundecyl) selenide, H-NMR (300 MHz, CDCl3) d (ppm): 3.64 (4H, t, $HOCH_2$), 2.55 (4H, t, $SeCH_2$), 1.71–1.20 (36H, m, $HOCH_2[CH_2]_9CH_2Se$) was observed and the result was compatible with the literature (Figure 3.4) (Kutlu Kaya et al, 2020). After the optimization and confirmation of the synthesis procedure by using the volumes in reference (Ma et al, 2010), scale up experiments were done. The initial amounts and volumes were increased 5, 3 and 2 times, respectively. But in all cases, it was seen that monomer could not be eluted from chromatography column during purificiation step, so both di-(1-hydroxylundecyl) selenide and PEG-PUSe-PEG block copolymer synthesis experiments were performed according to the amounts and volumes in the literature (Ma et al, 2010).

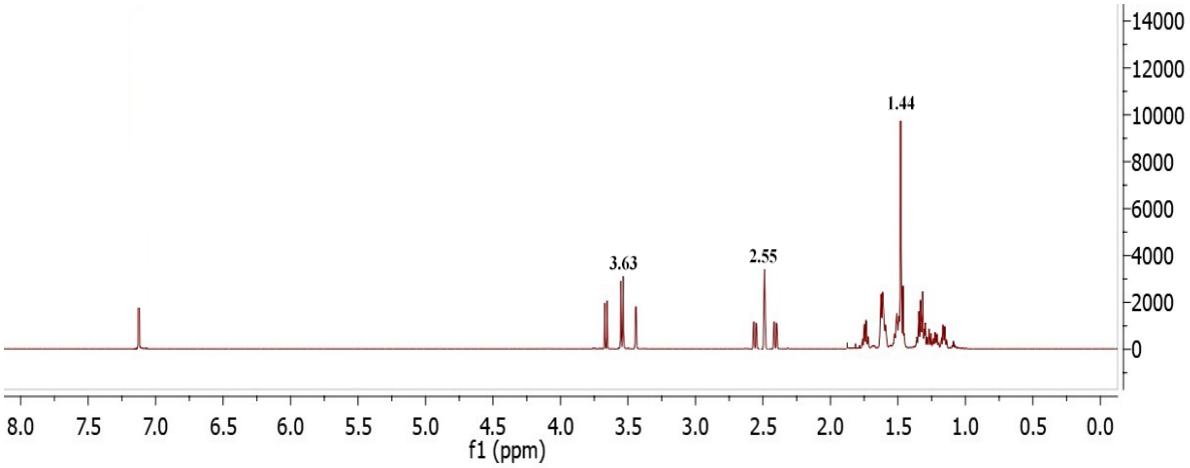

Figure 3.4 : NMR spectrum of di-(1-hydroxylundecyl) selenide.

3.3.2 PEG-PUSe-PEG block copolymer synthesis and characterization

At the second step of process, PEG-PUSe-PEG block copolymer was synthesized, washed, and dried. During polymer synthesis, removal of anhydrous THF was problematic. When THF was not removed from copolymer, a yellow-green and jelly-like material was obtained (Figure 3.5a). To overcome this problem, the amounts of deionized water and acetone used in the washing phase was increased and washing process was repeated 5 times. After drying under fume hood, a light-yellow colored block copolymer as powder form was obtained (Figure 3.5b).

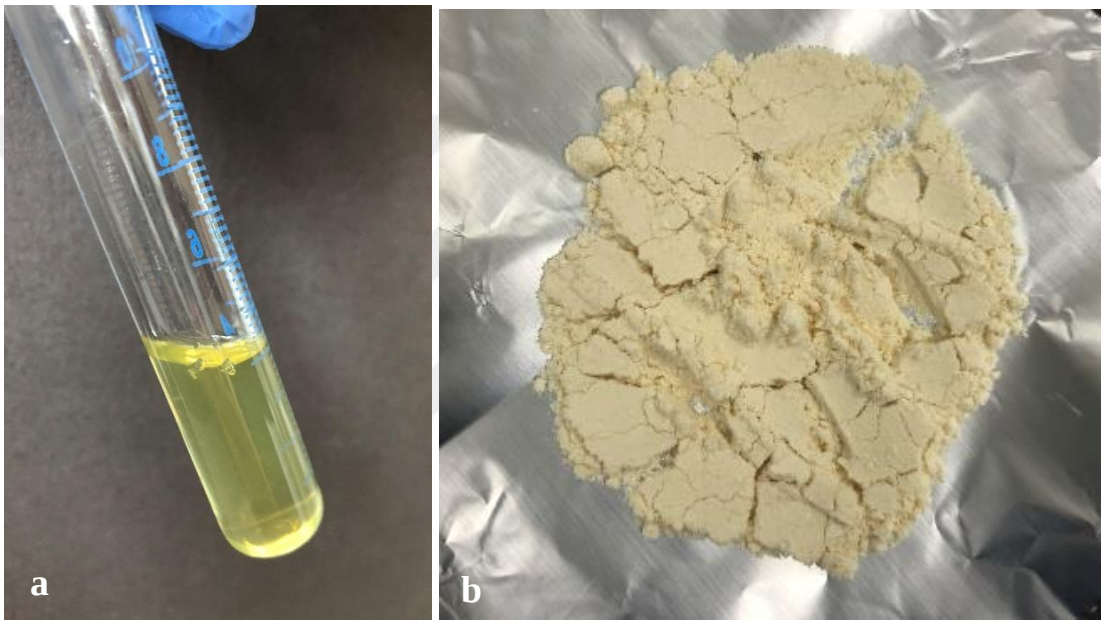

Figure 3.5 : a) Not purified, b) well purified PEG-PUSe-PEG block copolymer.

Chemical properties of synthesized block copolymer was examined by using FTIR and NMR. The peaks of O-H stretch due to the hydrogen bonding (3,373 cm^{-1}), C-H stretching (2,917–2,849 cm^{-1}), C=O stretch (1,708 cm^{-1}) and N–H stretching band (1,520–1,570 cm^{-1}), C-H bending vibrations (1,464–1,343 cm^{-1}), O-H stretch, and C-OH bending (1,094 cm^{-1}) were seen at FTIR spectrum of block copolymer (Figure 3.6). Specific absorption bands of Se could be seen only in far-infrared band (400-200 cm^{-1}), therefore, its specific absorption bands in the region between 400 and 4000 cm^{-1} spectrum was not observed (Shumaila et al, 2011).

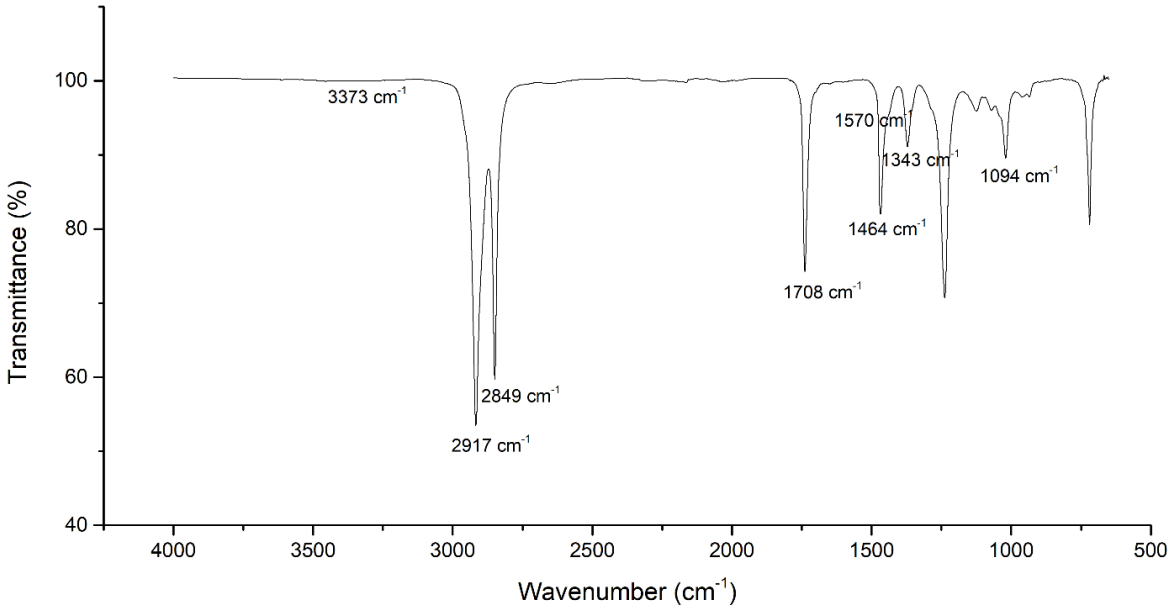

Figure 3.6 : FTIR spectrum of PEG-PUSe-PEG block copolymer.

In NMR spectrum, H-NMR (300 MHz, $CDCl_3$) d (ppm): 7.04 (3H, b, aromatic H), 4.15 (4H, b, $NHCOOCH_2$), 3.66 (8H, b, OCH_2CH_2 of PEG), 2.57 (4H, b, $SeCH_2$), 2.19 (4H, b, $NHCOOCH_2CH_2$), 1.94–1.19 (32H, b, $NHCOOCH_2CH_2(CH_2)_8CH_2Se$ were observed (Figure 3.7). When compared to the reference article written by Ma et al (2010), it was seen that the chemical characterization results of the synthesized block copolymer are compatible with the results in the article.

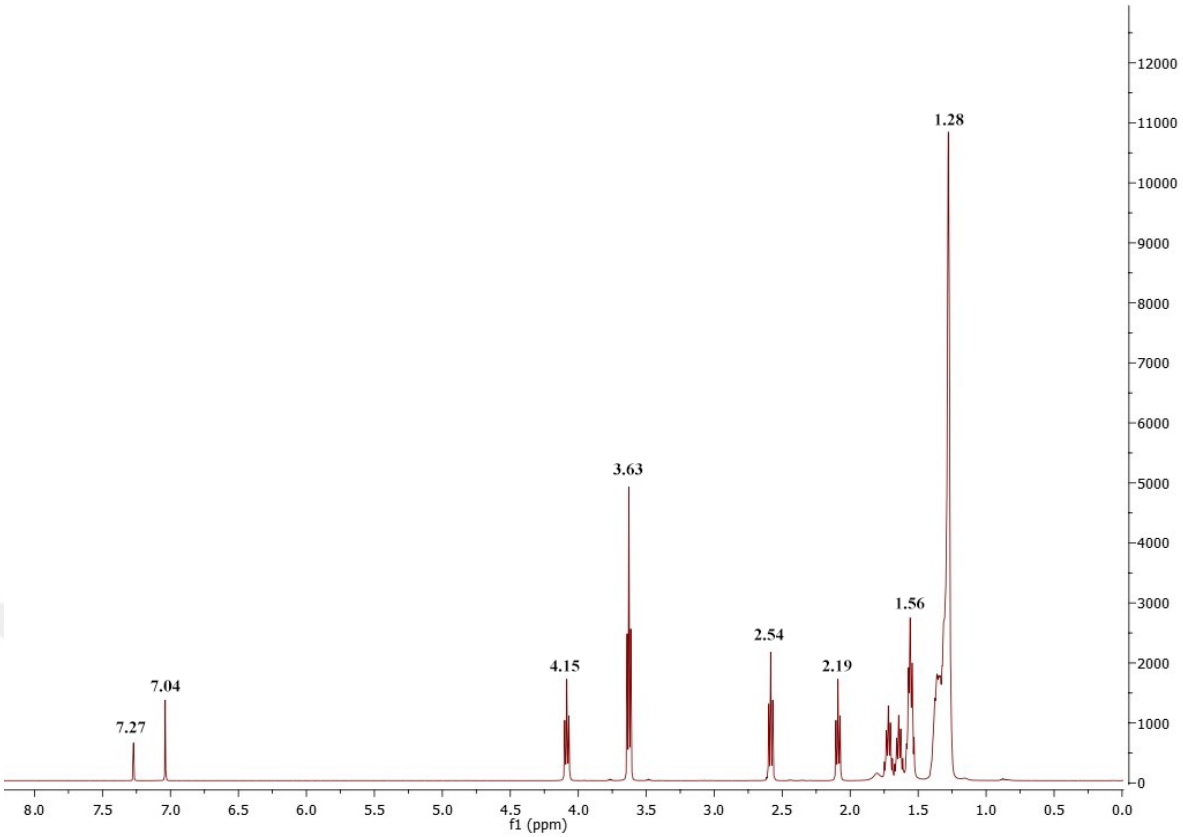

Figure 3.7 : NMR spectrum of PEG-PUSe-PEG block copolymer.

3.4 Preparation of Blank and NP Loaded Blend Matrices

3.4.1 Preliminary studies

In order to fabricate sponge-like matrix structure by using PEG-PUSe-PEG block copolymer, freeze dryer and dialysis membrane were used but the desired structure could not be achieved in the first trials. Instead the solution overflowed from wells and spreaded on plates in freeze-dryer (Figure 3.8) and no agglomeration was observed in cellulose membranes at the end of the processes.

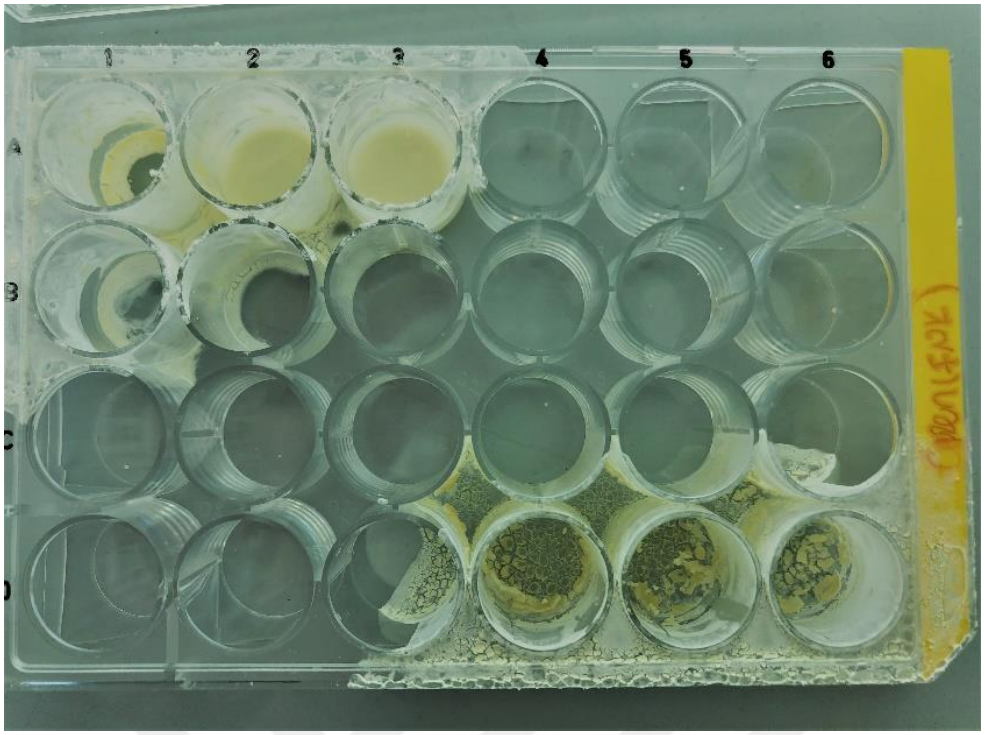

Figure 3.8 : Failed matrix fabrication experiment by using freeze-dryer.

3.4.2 Matrix preparation and characterization

The optimum porous matrices were fabricated by particulate leaching technique from PEG-PUSe-PEG block copolymer and PU (Figure 3.9). According to the results of liquid displacement method with n-hexane, the porosity of the reference matrix (100% PU) was 74% while this value was 60% for both 66% PU and 34% PEG-PUSe-PEG block copolymer (denoted as 2:1) matrices and 50% PU and 50% PEG-PUSe-PEG block copolymer (denoted as 1:1) matrices.

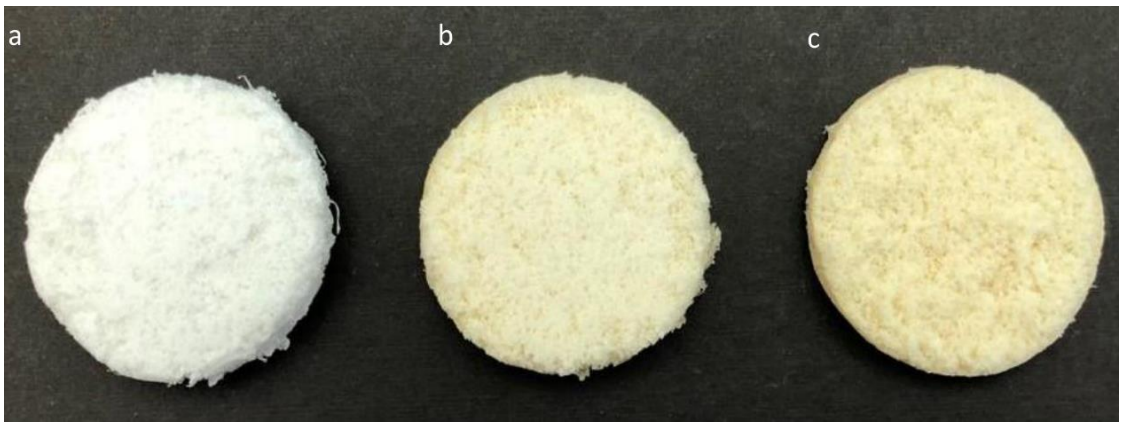

Figure 3.9 : Matrices made of (a) 100% PU, (b) 2:1 PU and PEG-PUSe-PEG block copolymer (w/w) and (c) 1:1 PU and PEG-PUSe-PEG block copolymer (w/w).

Surface and pore structures of both blank and NP loaded matrices were observed by SEM images (Figure 3.10 and 3.11) and the cross-sectional images showed that NPs were distributed homogeneously within the matrix (Figure 3.11a and b).

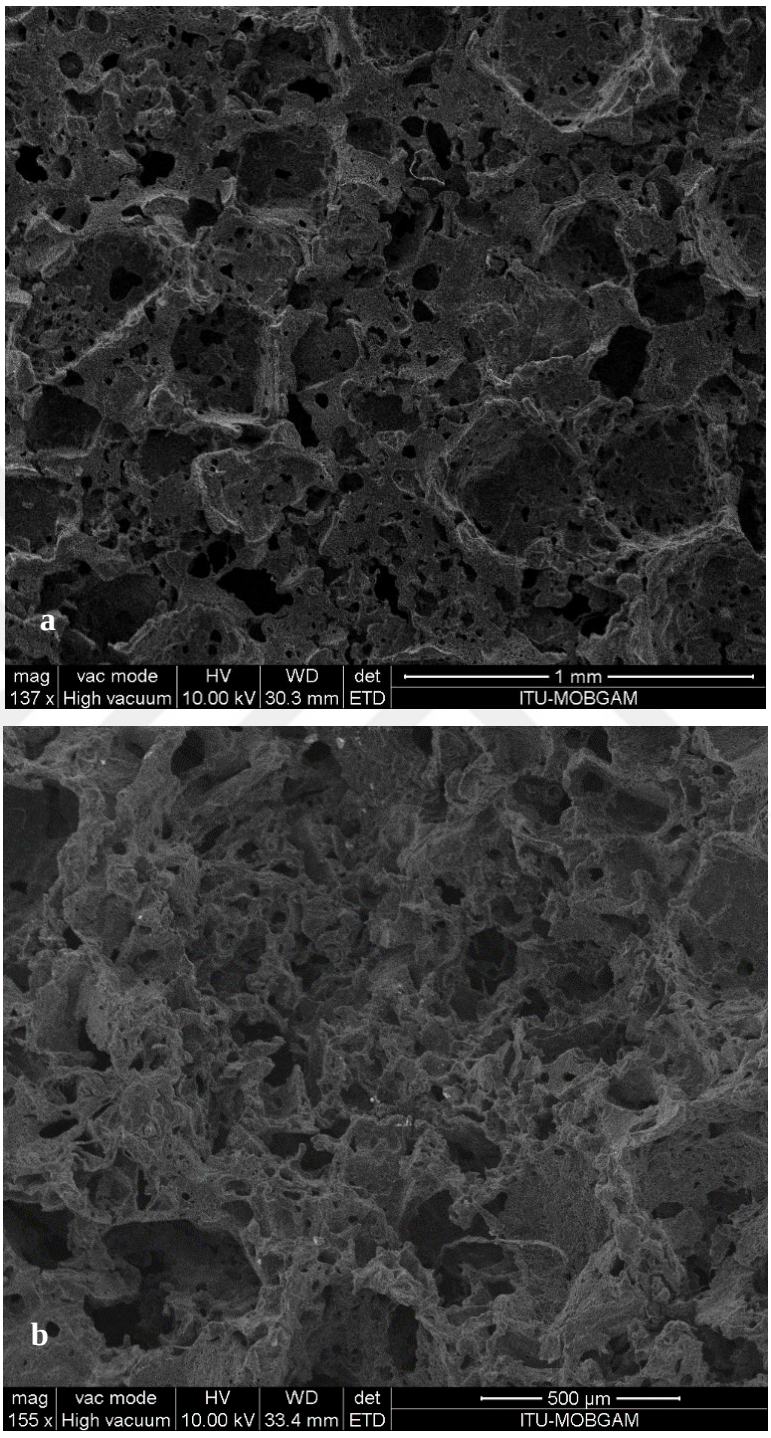

Figure 3.10 : SEM micrograph of (a) surface (b) cross-sectional view of blank matrices made by 2:1 PU/PEG-PUSe-PEG block copolymer.

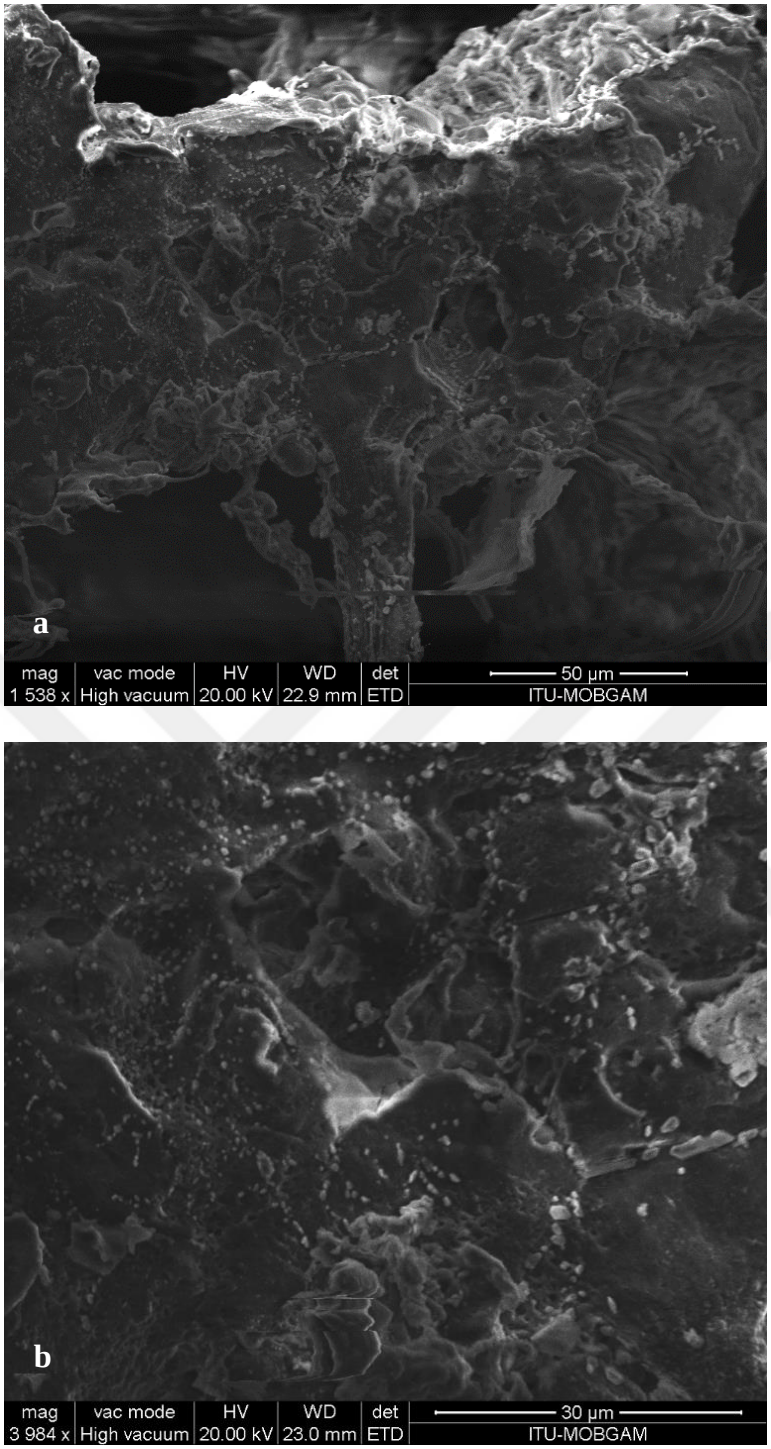

Figure 3.11 : a, b)Cross-sectional SEM micrograph from different parts of NP loaded 2:1 PU/PEG-PUSe-PEG block copolymer (w/w).

Additionally, these images were analyzed by Image J program to calculate pore area distribution. Although the mean area was calculated as 52.2 μm^2, a wide distribution range which changes between 10 μm^2 and 300 μm^2 was measured and it was seemed that more than 50% of the pores were within the 0–40 μm^2 range (Figure 3.12).

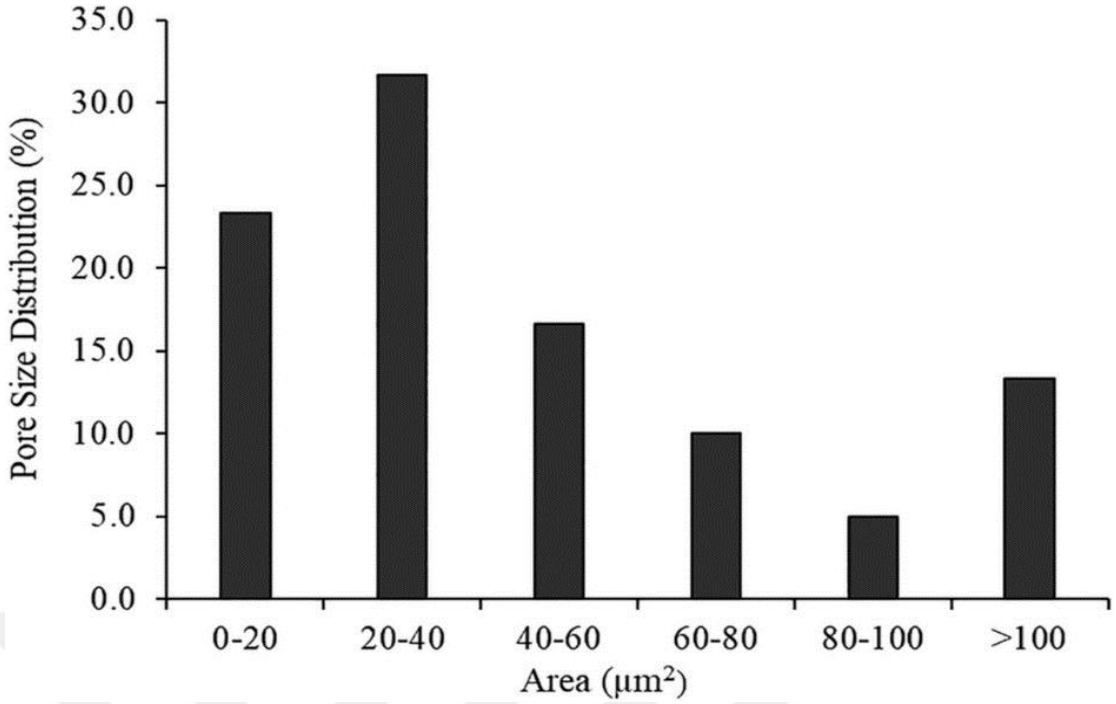

Figure 3.12 : Pore area distribution of PU/PEG-PUSe-PEG matrices.

3.5 In vitro CEP and Se Release Studies

3.5.1 CEP release from NPs

Before analysing CEP release from NPs, calibration curves of CEP in EtOH (96%) and PBS (pH 7.4) were drawn and used for detection of encapsulation efficiency and release amounts, respectively (Figure 3.13 and 3.14).

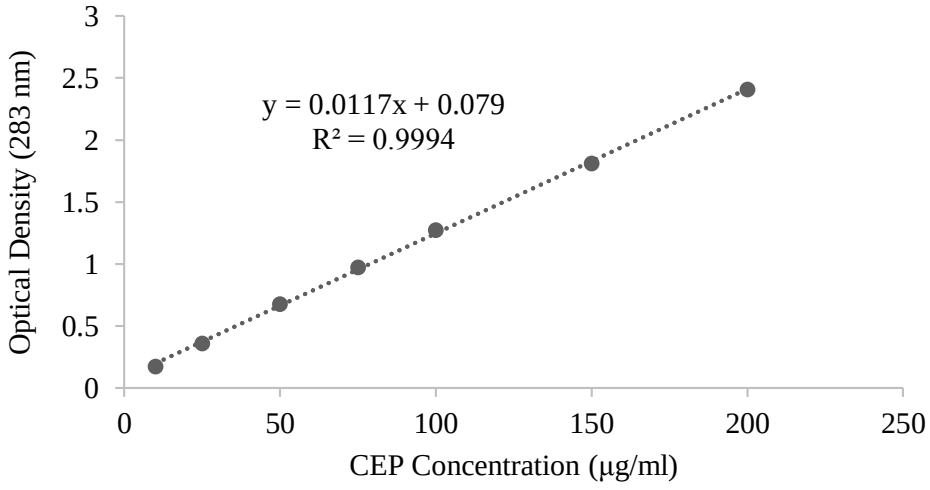

Figure 3.13 : Calibration curve of CEP dissolved in EtOH (96%).

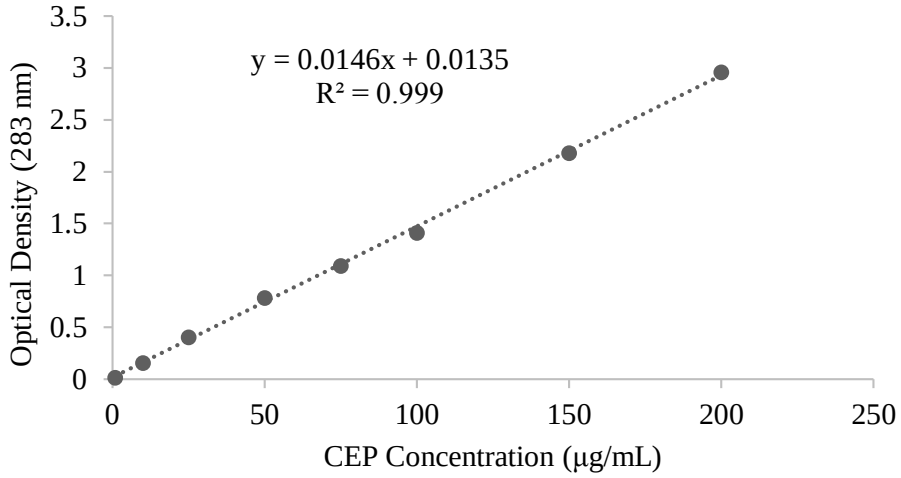

Figure 3.14 : Calibration curve of CEP dissolved in PBS.

In the first release experiment, NPs containing ~ 9% CEP by weight of PEVA were washed using 96% EtOH and the amount of CEP remaining in the washing liquid was measured as ~ 2.9 mg. According to the CEP amount in washing liquid, encapsulation efficiency was calculated as 10.7% by using equation 2.1. The release of CEP from NPs dried in the oven was followed at 100 rpm at 37 ºC for 15 days and at the end of the period ~8% (27,3 µg) of encapsulated CEP was released (Figure 3.15).

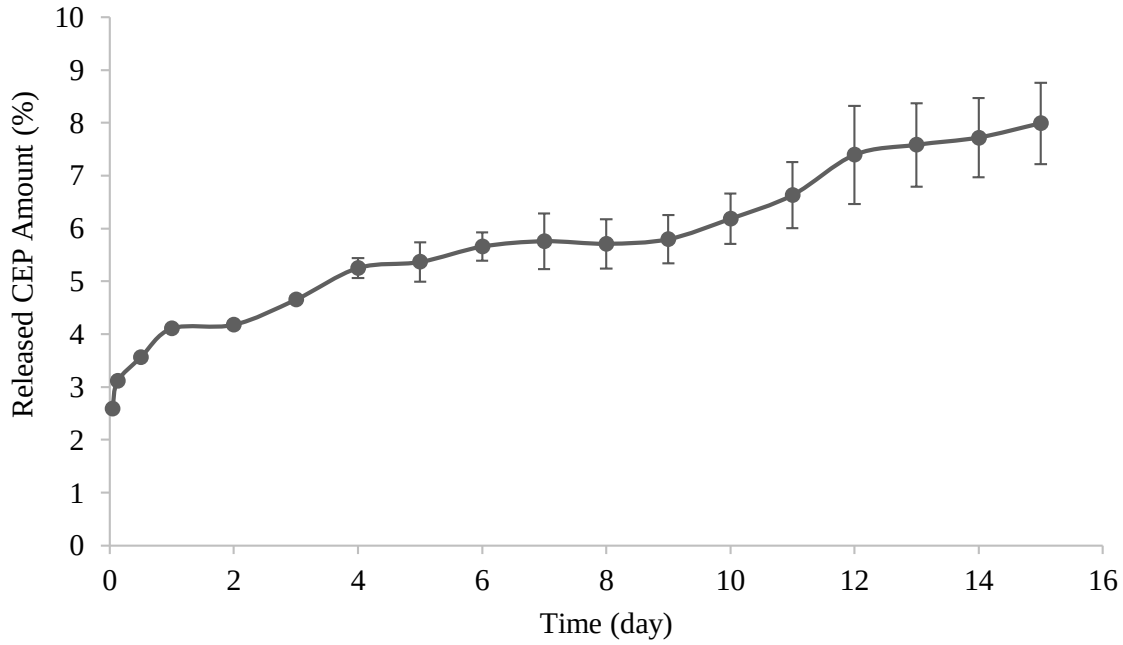

Figure 3.15 : CEP release from oven dried NPs.

Li et al mentioned that 0,001 mM (3,6 µg) CEP significantly blocked the activation of T-cells of hTg immunized mice (Li et al, 2016). There is no research that shows the

CEP amount to block T- cell activation in human but it should be more due to the size difference between mice and human.

In the first experiment, the released CEP amount was not sufficient to be able to attain therapeutical doses. In order to increase both release rate and amount of released CEP, the initial amount of CEP was increased 3 times, yielding nanospheres with ~ 27% CEP (w/w) loading and encapsulation efficiency of ~ 12%. CEP release profile of NPs dried in oven was followed for 36 days and it was observed that 1.5% (8.8 µg) CEP was released (Figure 3.16). Although an increase in encapsulation efficiency was observed when the amount of initial CEP was increased, the desired release rates can not be attained.

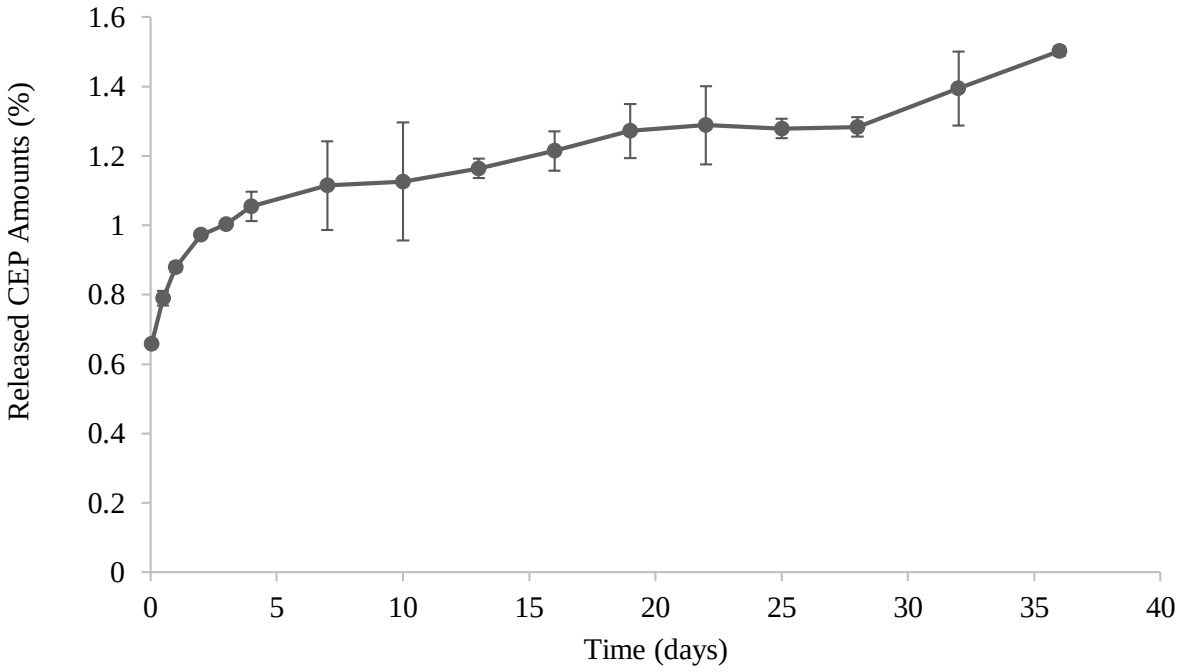

Figure 3.16 : CEP release from oven dried NPs where the initial drug concentration was 3X.

When the reasons behind this slow release behavior was studied, one of the causes was thought to be the agglomeration of NPs dried up in the oven which led to decrease in effective surface area. To be able to decrease agglomeration and increase the NP surface area exposed to release medium, an alternative drying method, lyophilization, was tried. The dried particles were transferred to the cellulose membranes, and released CEP amounts were determined in PBS. In this experiment, 3.2 mg CEP (~ 9% of PEVA w/w) was used and only ~ 5% (172.2 µg) was encapsulated. In order to

understand the effect of drying method, CEP release from both NPs dried in oven and freeze-dryer were compared (Figure 3.17). In 14 days, while freeze dried NPs released ~ 11.3 % of encapsulated CEP, oven dried NPs released ~ 7.7 % of total encapsulated CEP.

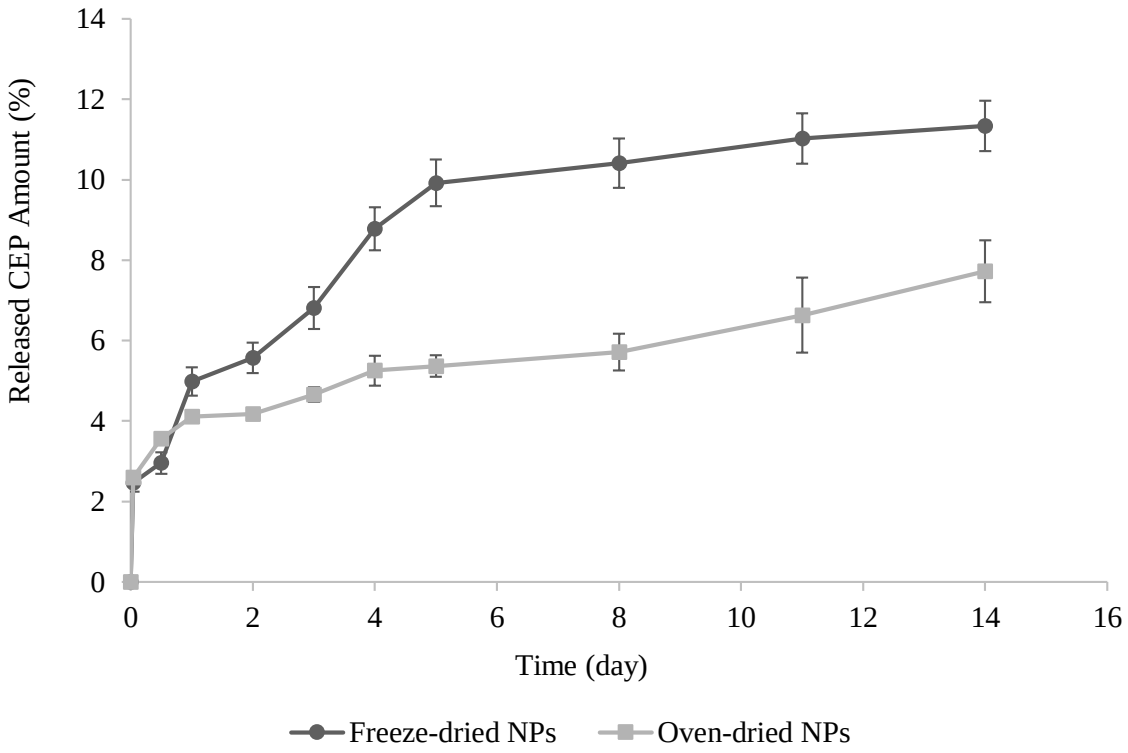

Figure 3.17 : CEP release from freeze-dried and oven-dried NPs in 14 days.

It was observed that drying particles by lyophilization increased the release rate compared the ones dried in oven. While particles were agglomerated in the oven, a powder-like material was obtained with the particles dried in freeze dryer. Because of powder-like structure, S/V ratio of NPs increased and this increase caused higher CEP release rate. Therefore, freeze dried NPs were chosen for further studies. Longterm (100 days) release study (Figure 3.18) showed that ~ 35% of encapsulated CEP was released in 100 days and except for the short burst release observed on the first day, zero-order release profile was seen.

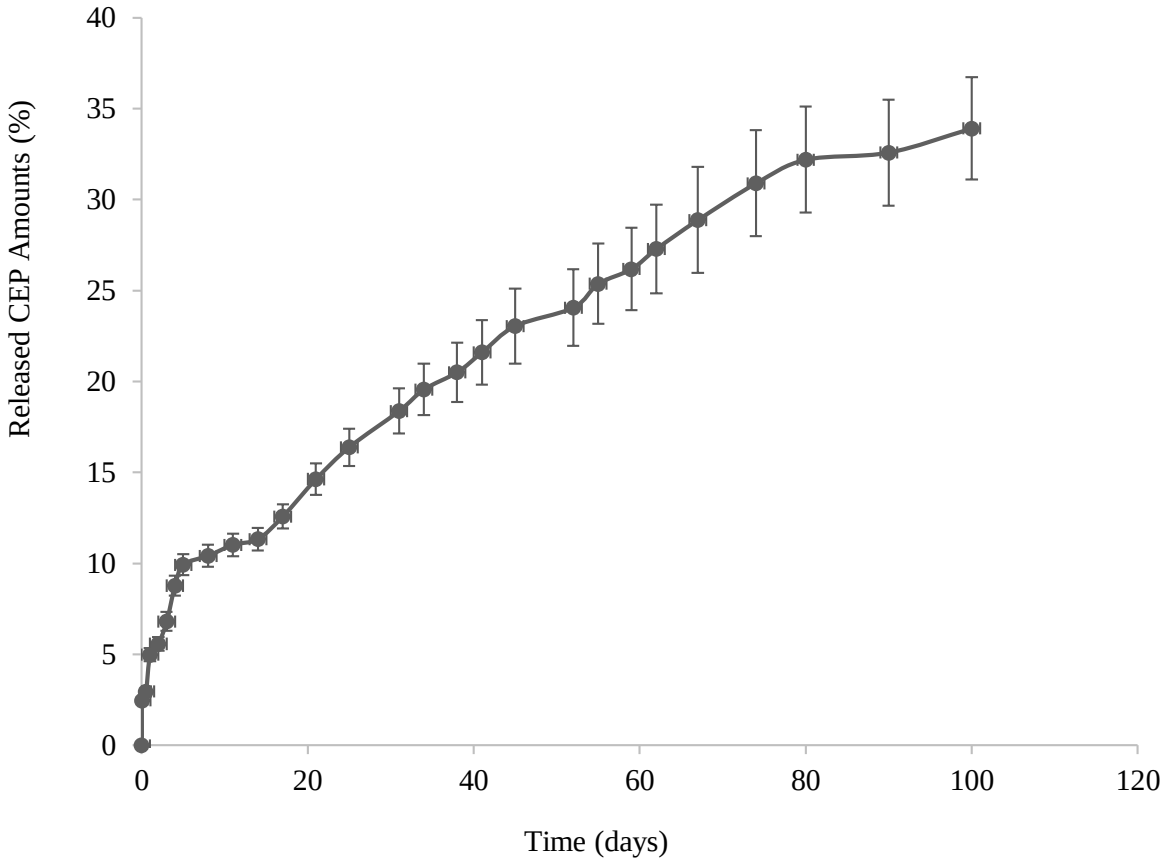

Figure 3.18: Long-term release profile of freeze-dried CEP loaded NPs.

3.5.2 CEP release from NP-loaded matrices

When NPs are incorporated in to matrix, an additional diffusion layer was formed, which can affect the release behavior. In order to understand this effect, CEP release profile was analyzed in two parallel experiments. CEP was loaded to PEG20-PEVA NPs (23% encapsulation efficiency) and half of total NPs (as volume) were freeze dried for CEP release from free NPs study while the remaining half was integrated to the matrices made by 2:1 PU/PEG-PUSe-PEG block copolymer. The release profiles of two groups were observed for 66 days and while ~ 23% of CEP (193.63 μg) was released from free NPs, ~ 21.5% of CEP (180.35 μg) was released from matrix-loaded NPs (Figure 3.19).

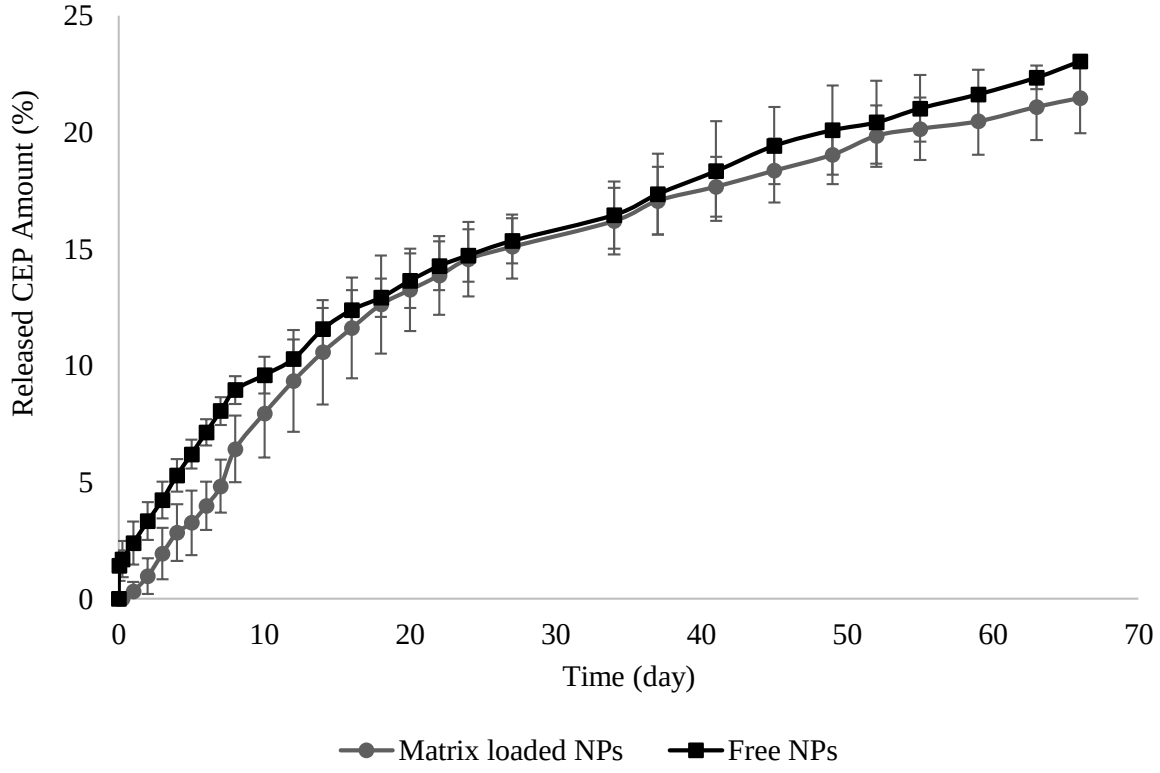

Figure 3.19: CEP release from free and matrix-loaded NPs.

As seen in Figure 3.19, two groups have similar release rates probably because of large pore size of matrices. CEP is not used as a conventional drug in hypothyroidism therapy but Li et al showed that low concentrations such as 0.001 mM CEP could block T cell activation *in vivo* conditions. According to the results in Figure 3.19, the first 10% of encapsulated CEP (83.5 μg, 0.022 mM) was released in 11 days and 13 days from free NPs and matrix-loaded NPs, respectively. Next 10% of CEP was released within 38-40 days because CEP relase rate was slowed down in both groups and this release trends continued up to Day 66. Although, current release values are not far from the literature (Li et al, 2016), there should be more research to optimize the dosage and control the release.

3.5.3 Se release from matrices

Se release from matrices made by 1:1 and 2:1 PU/PEG-PUSe-PEG block copolymer was followed for 7 days in both water including H_2O_2 (0.1% v/v) and ultra pure water. Samples were taken on Day 1, Day 3, and Day 7 and analysed by using ICP-MS.

In the literature, it has been stated that hydrophobic selenite groups tend to turn into hydrophilic selenoxide and selenone groups in the oxidative environment (Ma et al, 2010) and hydrophilic media is also preferred to increase the release of Se. For this reason, 0.1% H_2O_2 (v/v) was added to the reservoir including matrices made by 1:1 and 2:1 PU/PEG-PUSe-PEG (w/w) block copolymer and with this, an increase in the amount of released Se was aimed by enhancing the oxidation sensitivity of the selenide block copolymers. Since the oxygen in the media reacts with the matrices, their light yellow color has turned orange over time (Figure 2.2). At the same time, the presence of low concentration of H_2O_2 in the release media is preferred since it mimics the stress condition in the body; reactive oxygen species (ROS) amount increases under stressed conditions.

Cumulative release of Se from 1:1 and 2:1 PU/PEG-PUSe-PEG matrices after 7 days were 0.88 and 11.96 µg, respectively in ultra pure water (Figure 3.20).

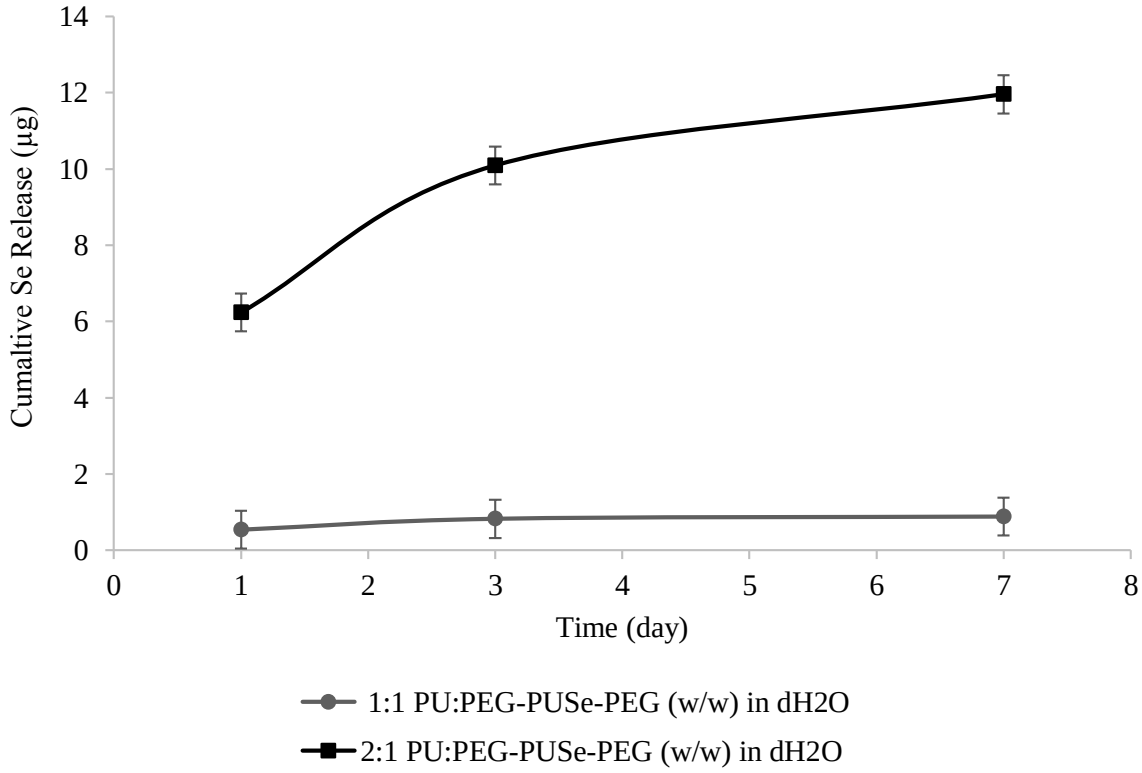

Figure 3.20 : Se release from matrices in ultra pure water.

As expected, in the presence of H_2O_2, the release of Se was much faster than the system prepared with ultrapure water and 2525.90 µg and 2097.76 µg Se were released from 1:1 and 2:1 PU/PEG-PUSe-PEG matrices, respectively (Figure 3.21). When the amounts were calculated as percentage, while 56% of total Se was released from 1:1

PU/PEG-PUSe-PEG matrix, 69% of total Se was released from 2:1 PU/PEG-PUSe-PEG matrix. As shown in figure 3.21, initial burst release which is between 1000-1500 µg/day for both matrices could be toxic for patient so initial Se concentration and the dimensions of matrix should be optimised before animal experiments.

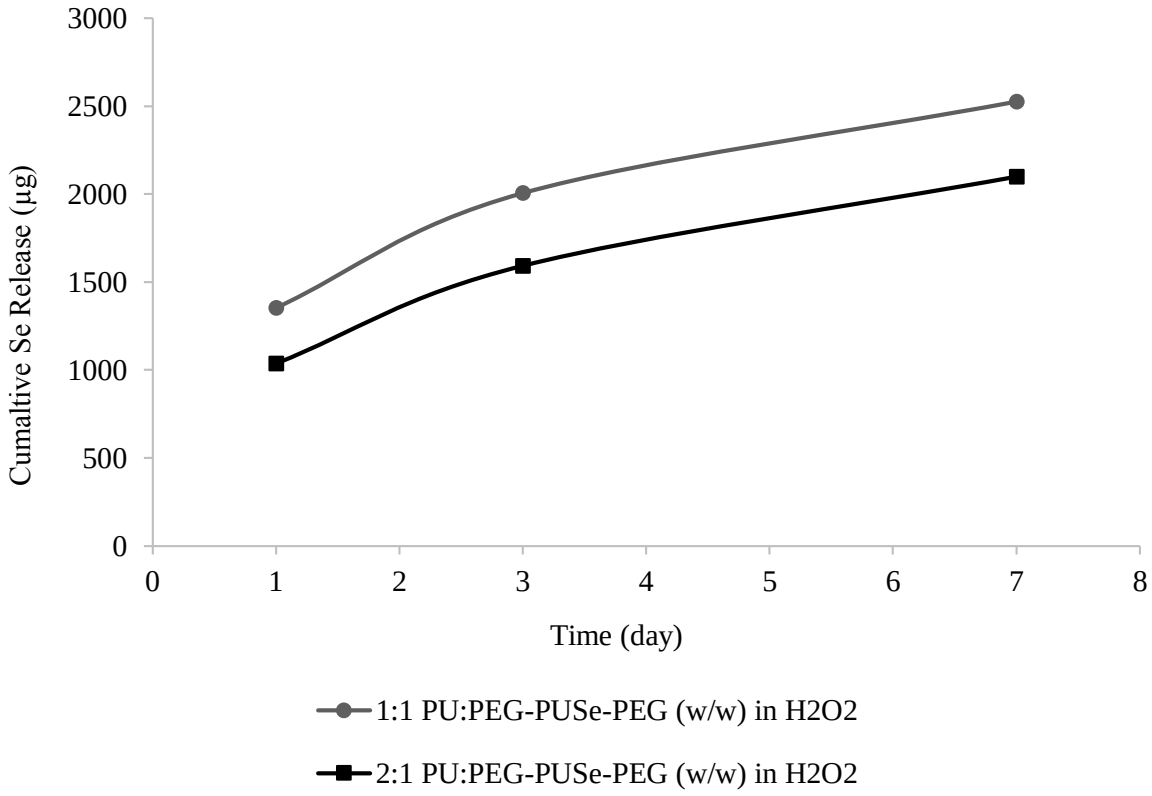

Figure 3.21 : Se release from matrices in water including H_2O_2.

In hypothyroidism patients, thyroid-hormone-induced oxidative stress was observed in target tissues (Venditti and Di Meo, 2006) therefore, this condition will probably enhance Se release from matrices. It was mentioned that taking 200 µg/day Se intake in addition to the daily diet causes decrease of TPOAb level in the serum (Turker et al, 2006). The matrices fabricated in this thesis could provide additional Se requirement for hypothyroidism patients by adjusting the release dosage of Se.

3.6 Cell Culture Studies

NIH 3T3 cells were used in all cell culture studies in this thesis. Cytotoxicity tests were carried out for observe cell viabilities in various conditions and different microscopy analyses were performed to observe cell morphologies.

3.6.1 Cytotoxicity tests of NPs (direct interaction)

3.6.1.1 Cell viability assay

In the first group, cells were seeded on NPs. The cytotoxicity test results showed that neither blank nor CEP loaded NPs have toxic effects on NIH 3T3 cells (Figure 3.22). According to the statistical analysis, on the 1st day a significant difference between positive control and cells on blank NPs, on the 4th day, there was a significant difference among all groups ($p < 0.05$), but on the 7th day, no significant difference was observed between groups. Increased cell proliferation in all groups was also consistent with statistical results.

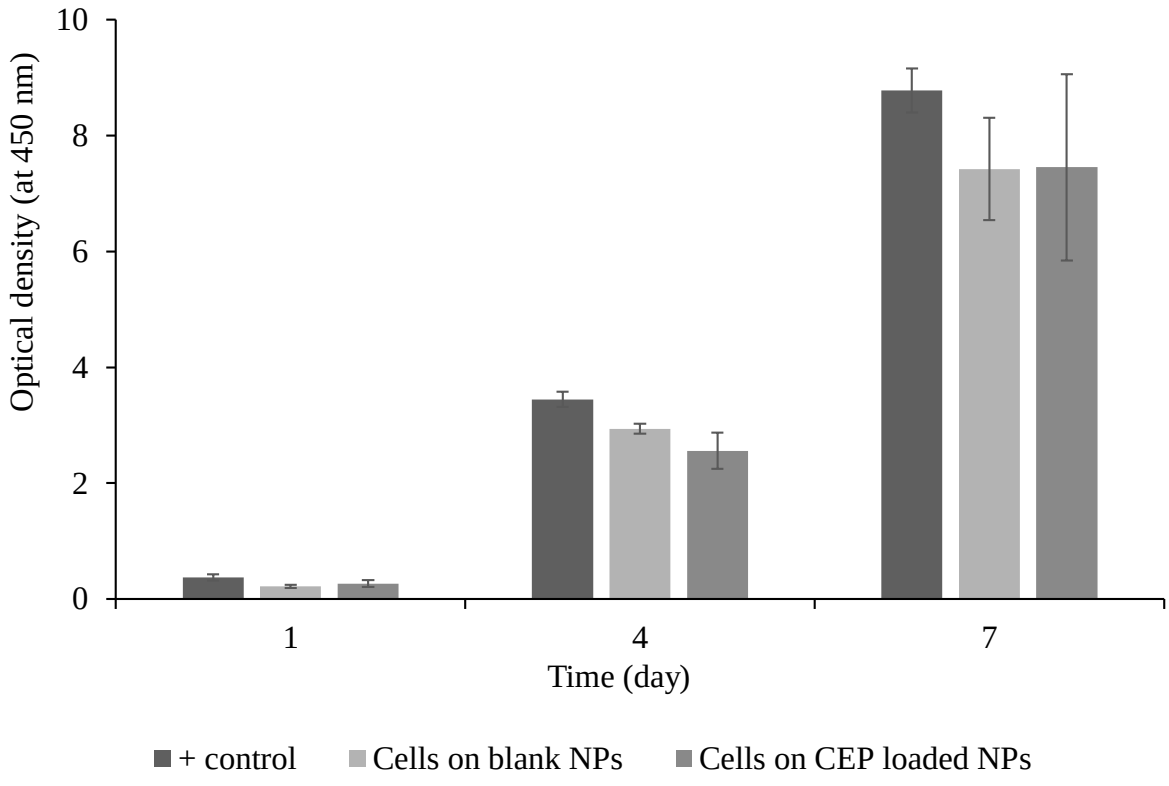

Figure 3.22 : Cytotoxicity analysis of NPs by direct interaction.

3.6.1.2 Microscopy analysis

The effects of blank and CEP loaded NPs on NIH 3T3 cells were captured by light microscopy and inverted fluorescence microscope. It was seen that, cells were proliferated and filled the cell culture plates in three days (Figure 3.23).

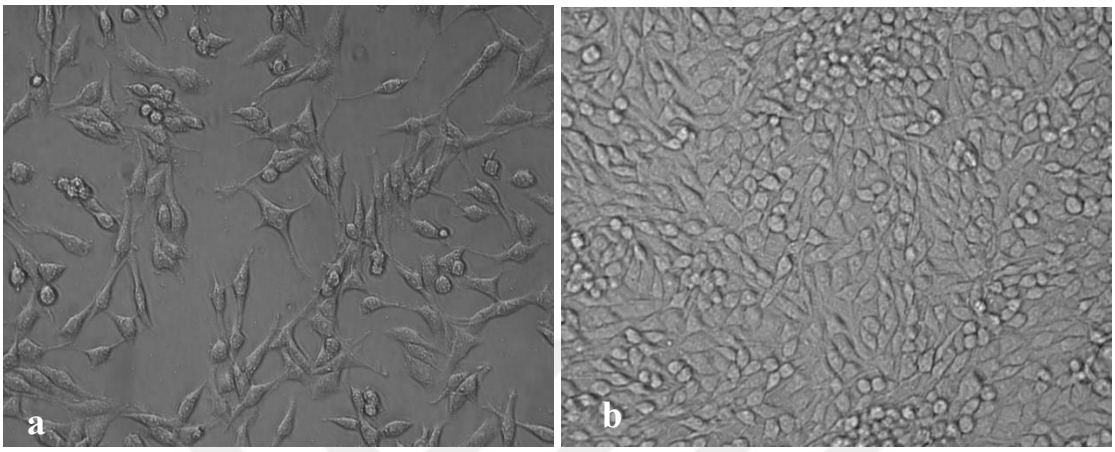

Figure 3.23 : Light microscopy images of 3T3 control group cells on a) the first, b) the third day (20X).

In accordance with light microscopy images, fluorescence microscopy images showed that 3T3 cells were spreaded well on cell culture plate surface on the fourth and seventh days (Figure 3.24).

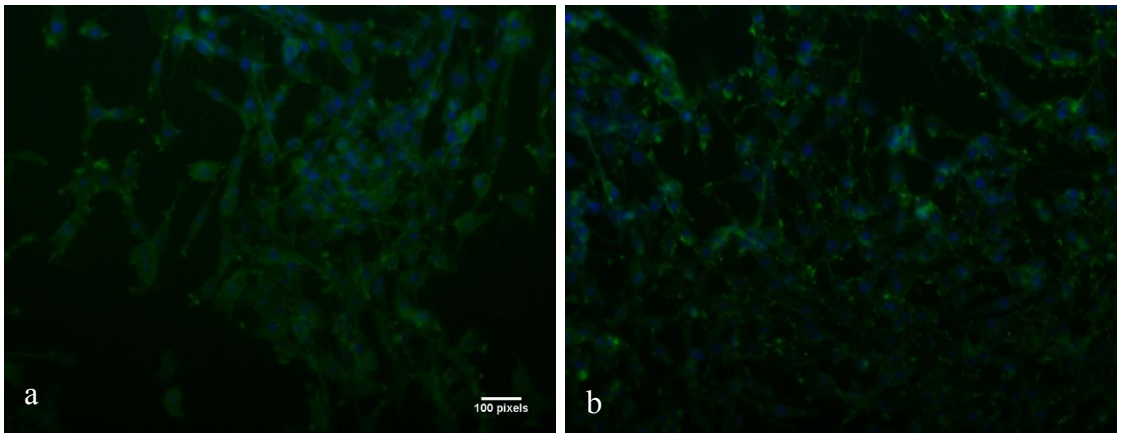

Figure 3.24 : Cells on blank (left) and CEP loaded NPs (right), a and b) on the 4th day, c and d) on the 7th day (20X) **(**Green: actin filaments, Blue: cell nuclei) (Scale bar; 100 pixel=37 μm).

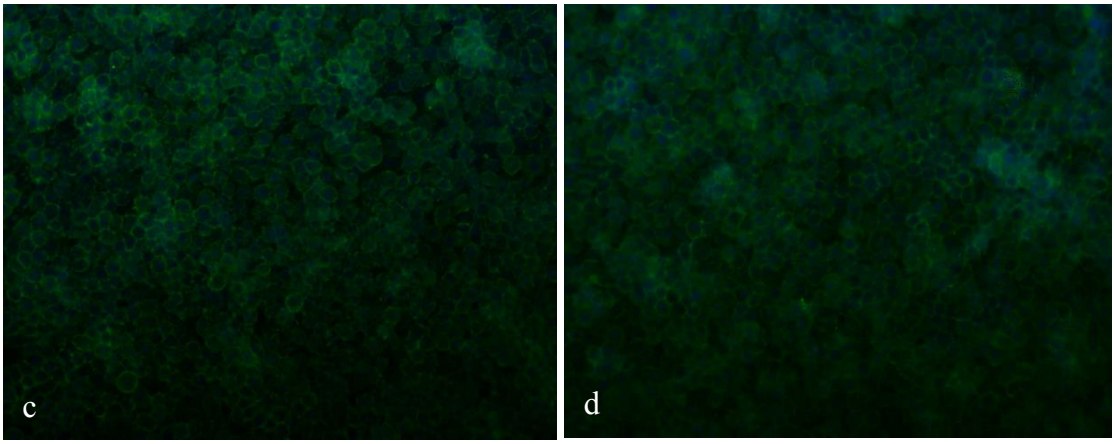

Figure 3.24 (continued): Cells on blank (left) and CEP loaded NPs (right), a and b) on the 4th day, c and d) on the 7th day (20X) (Scale bar; 100 pixel=37 μm).

3.6.2 Cytotoxicity tests of matrices (indirect interaction)

3.6.2.1 Cell viability assay

To evaluate the cytotoxicity of the matrices made by 100 % PU, 2:1 and 1:1 PU/PEG-PUSe-PEG block copolymer, eluents (soluble degradation products in DMEM) of these materials were tested on the growth and morphology of fibroblasts. Different amount of matrix eluents were applied to NIH 3T3 cells and according to MTS results, even at high concentration, the eluents did not have any negative effects on cells for both first and third day (Figure 3.25). According to statistical analysis, on the first day, there was no significant difference between any groups. On the third day, the groups which included 100 μl 100% PU and its positive control had a significant difference than other groups ($p < 0.05$). In general, when Figure 3.25 was analysed, it was observed that cell proliferations in all groups are not different from negative control group.

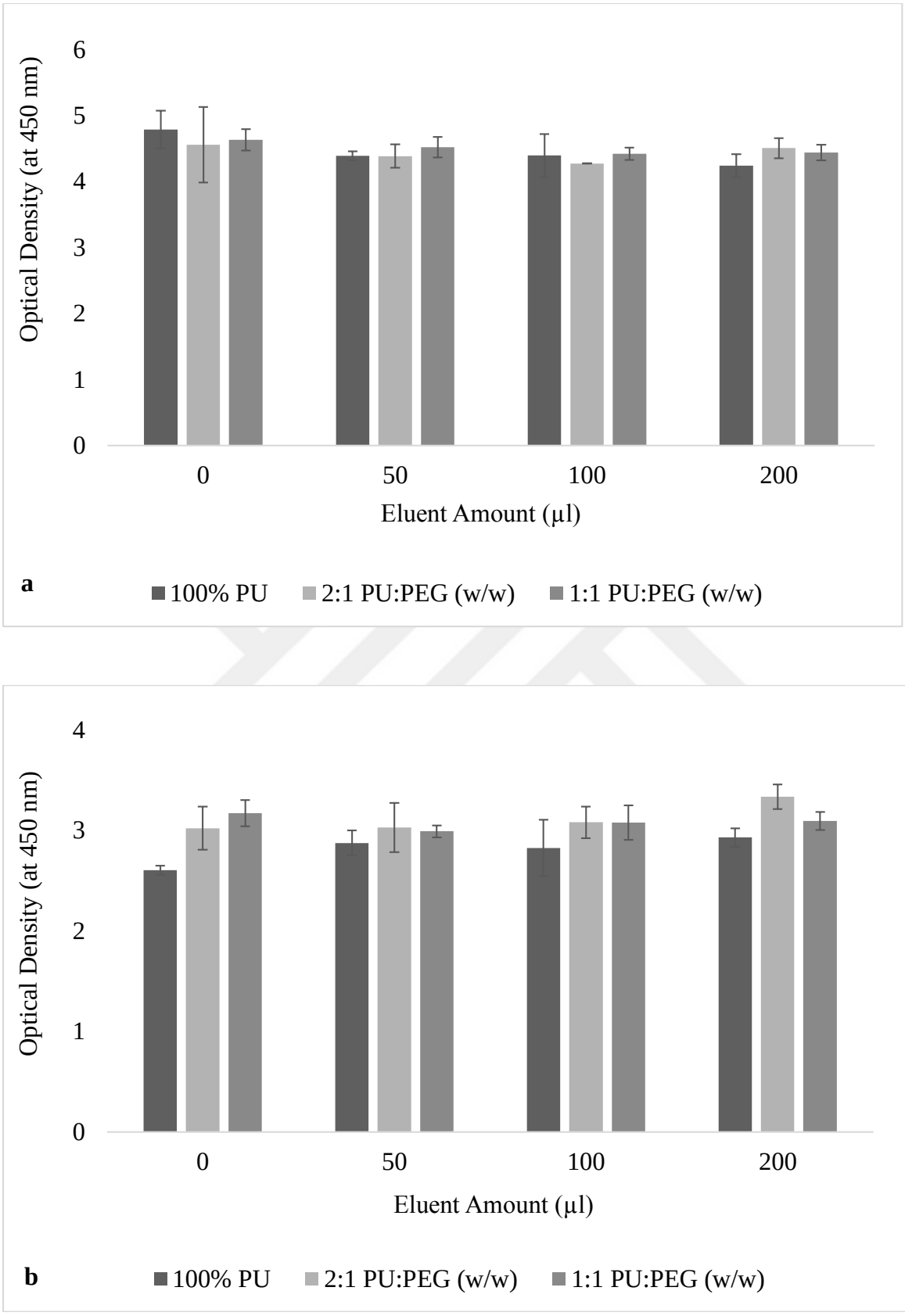

Figure 3.25 : Cytotoxicity analysis of matrix eluents collected on (a) Day 1 and (b) Day 3.

3.6.2.2 Microscopy analysis

Eluents of all matrices were implemented on cells via mixing cell culture media at various concentrations (Yeganegi, Kandel, & Santerre, 2010). It was seen that in the presence of eluents, 3T3 cells spreaded and covered TCPS surfaces for all samples, and no morphological changes were observed (Figure 3.26, Figure 3.27, Figure 3.28, and Figure 3.29).

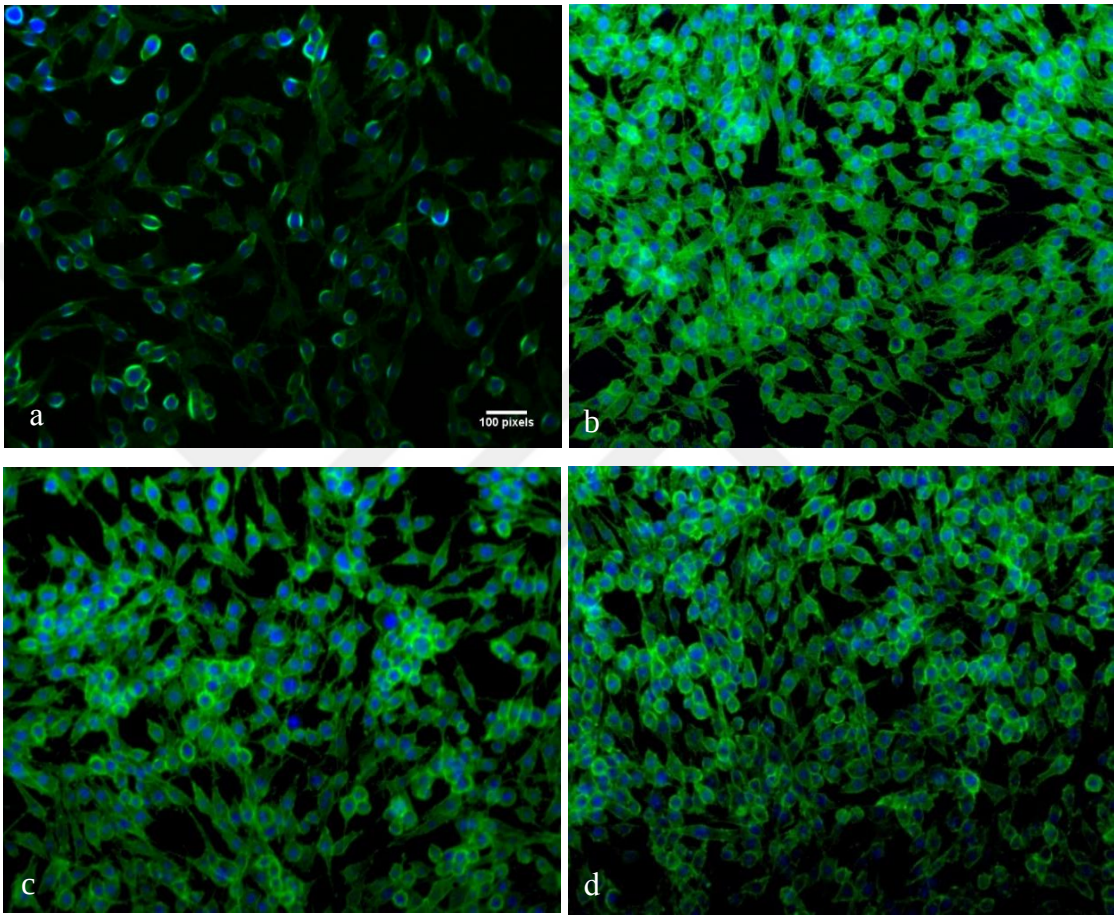

Figure 3.26 : Fluorescence microscope images (20X) of 3T3 cells on Day 1; a) negative control; 100% PU b) 50 µl, c) 100 µl, d) 200 µl eluent (Scale bar; 100 pixels = 37 µm).

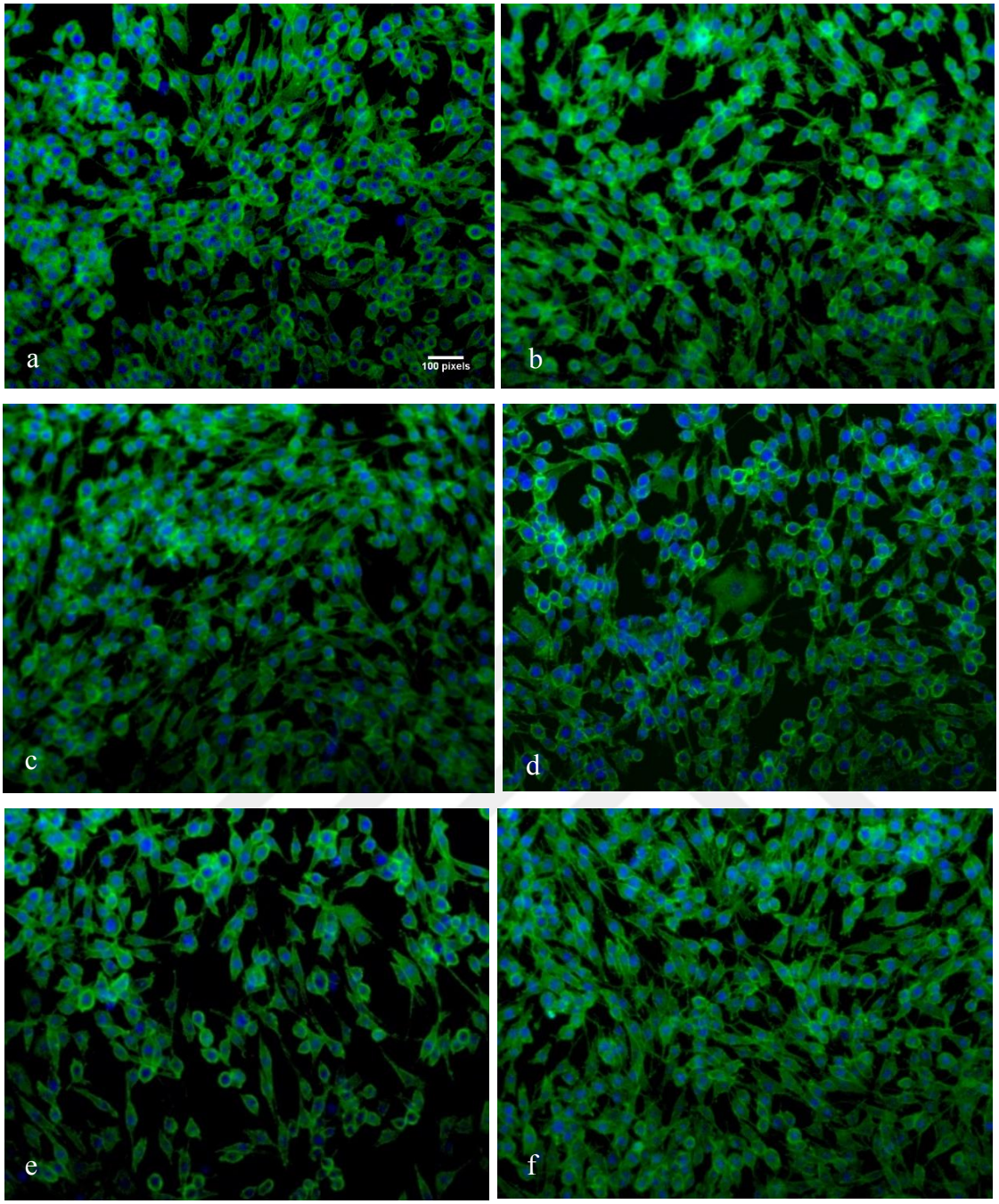

Figure 3.27 : Fluorescence microscope images (20X) of 3T3 cells on Day 1; 1:1 (w/w) copolymer a) 50 µl, c) 100 µl, e) 200 µl eluent; 2:1 (w/w) copolymer b) 50 µl, d) 100 µl, f) 200 µl eluent (Scale bar; 100 pixels = 37 µm).

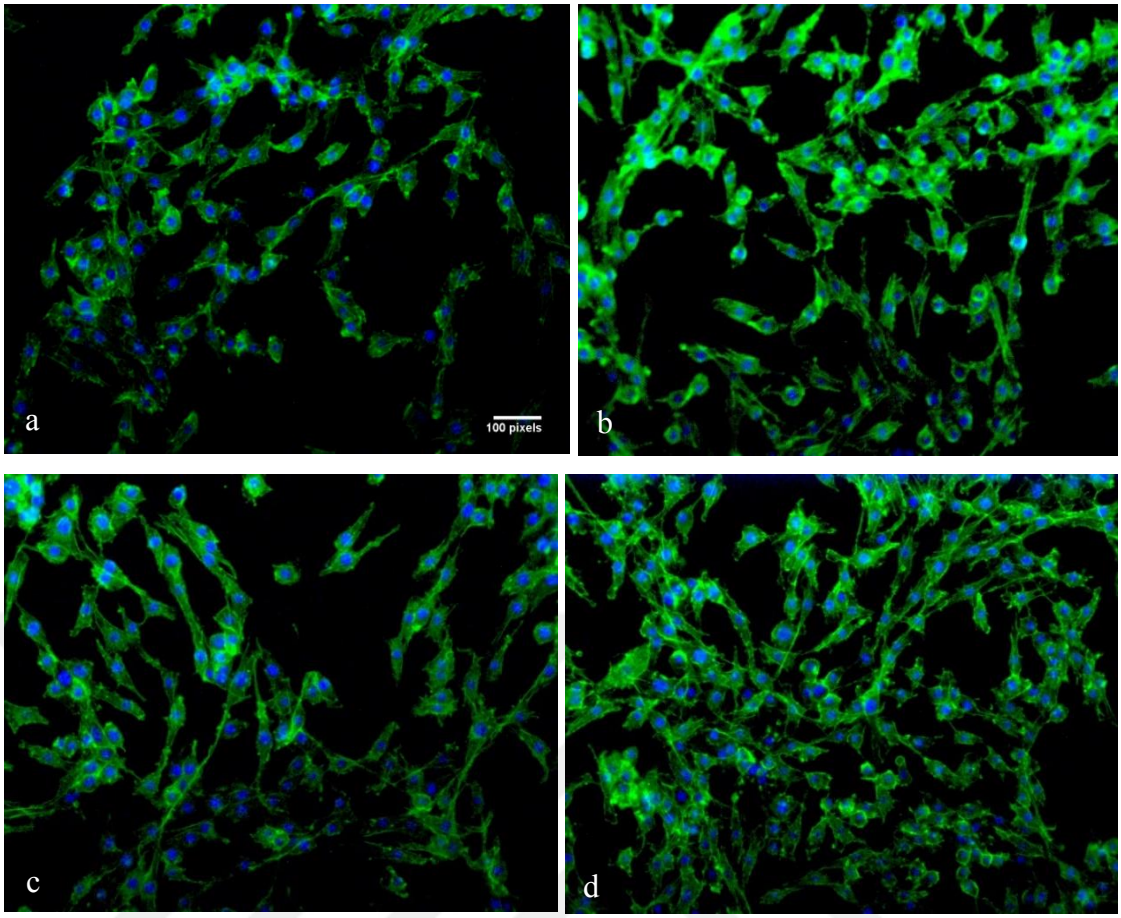

Figure 3.28 : Fluorescence microscope images (20X) of 3T3 cells on Day 3; a) negative control, and 100% PU b) 50 µl, c) 100 µl, d) 200 µl eluent (Scale bar; 100 pixels = 37 µm).

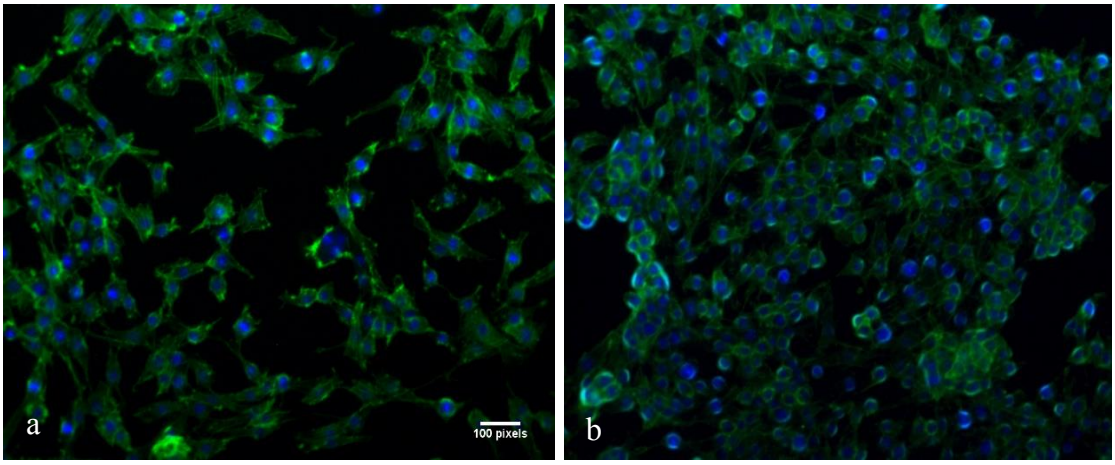

Figure 3.29 : Fluorescence microscope images (20X) of 3T3 cells on Day 3; 1:1 (w/w) copolymer a) 50 µl, c) 100 µl, e) 200 µl eluent; 2:1 (w/w) copolymer b) 50 µl, d) 100 µl, f) 200 µl eluent (Scale bar; 100 pixels = 37 µm).

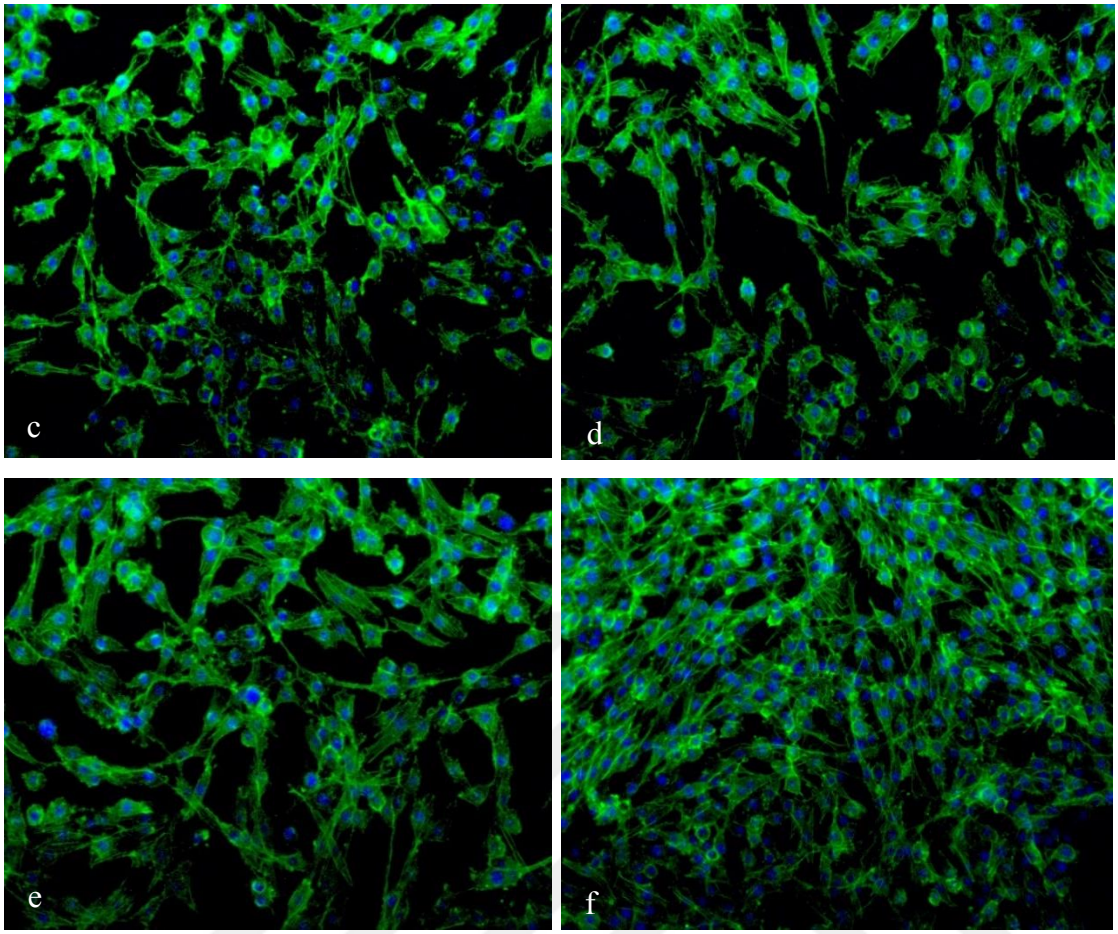

Figure 3.29 (continued) : Fluorescence microscope images (20X) of 3T3 cells on Day 3; 1:1 (w/w) copolymer a) 50 µl, c) 100 µl, e) 200 µl eluent; 2:1 (w/w) copolymer b) 50 µl, d) 100 µl, f) 200 µl eluent (Scale bar; 100 pixels = 37 µm).

3.6.3 Observation of cells on matrix (direct interaction)

In the third group, 3T3 cells were seeded on matrices with a volume of 0.5 cm^3 and tried to analyse with confocal laser scanning microscopy (CLSM) and scanning electron microscopy (SEM). DAPI which is used for staining cell nuclei, also stained polymer matrices, so no clear images can be obtained. Cell proliferation and interactions with matrices was therefore evaluated by using SEM. According to the images, NIH 3T3 cells were successfully attached and proliferated on all matrices. On Day 1, round shape cells were attached and located separately, and they had less cell-to-cell contact (Figure 3.30). On Day 3, fusiform cell structures and cell-cell interactions were observed (Figure 3.31). Cell numbers increased with time, and cells spreaded and contacted on porous matrices with the help of their filaments. It was seen that cellular morphology and cytoskeleton organization of cells on all types of matrices were similar to control gorups.

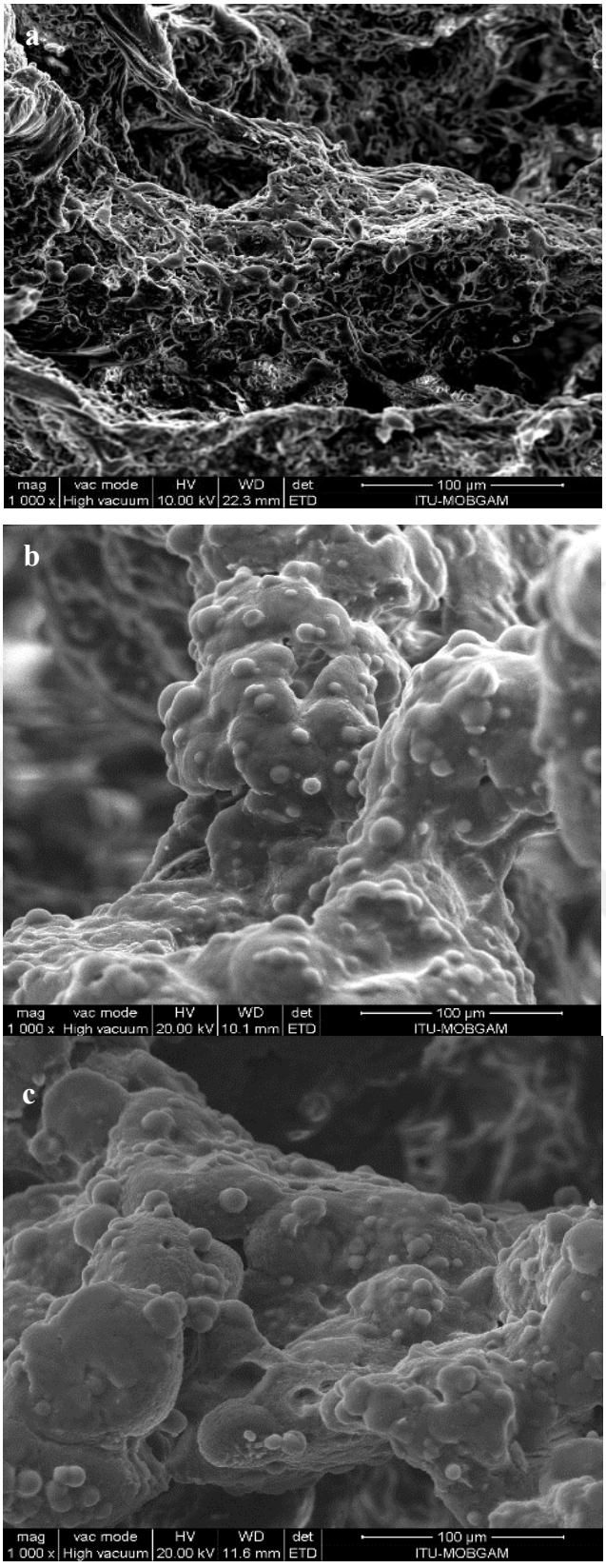

Figure 3. 30 : SEM micrographs of NIH 3T3 cells in (a) 100% PU, (b) 2:1 matrix, and (c) 1:1 matrix on Day 1.

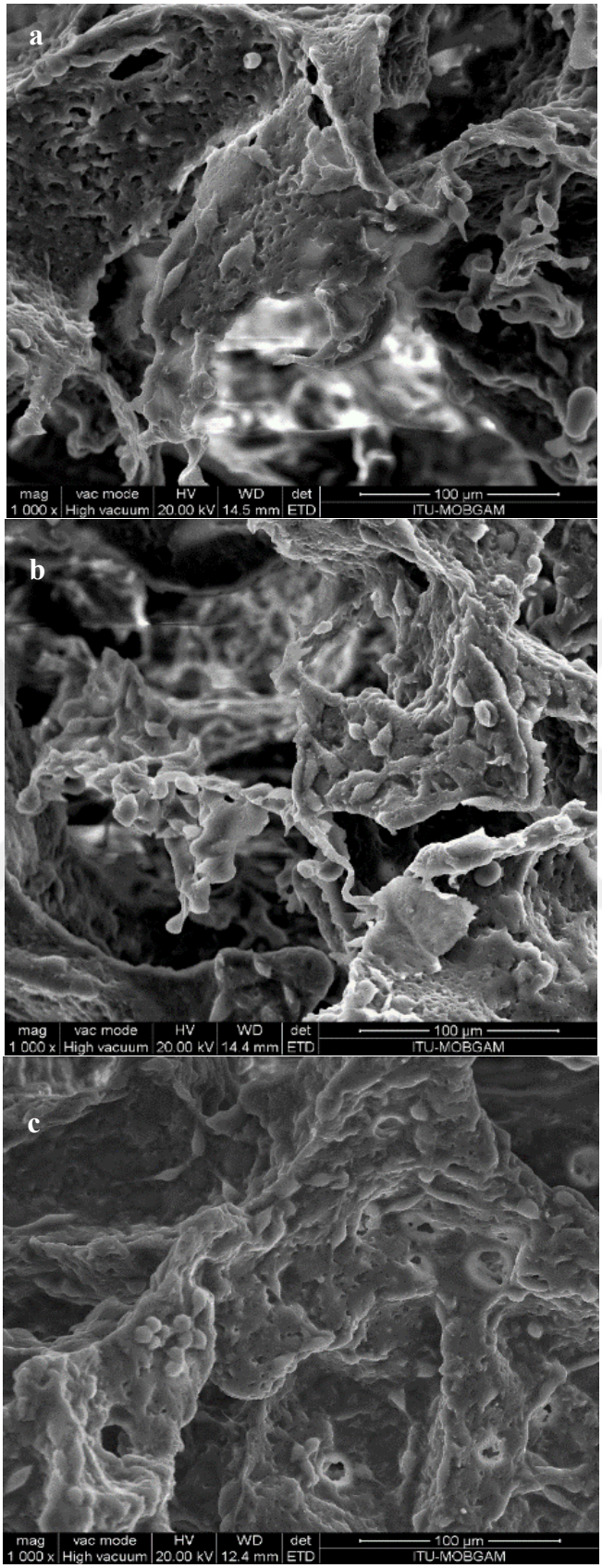

Figure 3. 31 : SEM micrographs of NIH 3T3 cells in (a) 100% PU, (b) 2:1 matrix, and (c) 1:1 matrix on Day 3.

4. CONCLUSIONS

Hypothyroidism is a common disease that is widely observed among the public and can not be treated permanently, instead its symptoms are alleviated with synthetic thyroid hormone supplementation. The main purpose of this thesis is to fabricate a multifunctional long-term release system to treat hypothyroidism by addressing both auto-immune response and hormone regulation. For this purpose, CEP which is a natural alkaloid was used to inhibit T cell activation and Se which is an essential nutrient for humans was used for reducing anti-TPO concentration. In order to use these agents efficienctly, Se containing polymeric matrix and NPs including CEP were synthesized and these NPs were loaded to matrices to obtain a dual effect controlled release system. Release profiles of these agents were examined and cytotoxicity of whole system was evaluated by cell culture studies.

At first, PEVA based NPs including PEG at different ratios (w/w) were synthesized and it was seen that 20% PEG (w/w of PEVA) resulted low average particle size (ca. 166 nm) and fairly monodisperse sample as desired. It was seen that adding more than 25% PEG (w/w of PEVA) increased particle size enormously and reducing the PEG ratio under 20% (w/w of PEVA) caused polydisperse sample. Similarly, increasing sonication time during synthesis decreased particle size but sonication more than 5 min increased polydispersity of particles so not preferred for further studies. PEG incorporation to particle structure was proved by Raman spectra.

Encapsulation efficiency and encapsulated drug amounts can be affected by initial drug concentrations but it was seen that the highest encapsulation efficiency was obtained with the lowest CEP ratio (10% of PEVA, w/w) because of the solubility limits of CEP in DCM.

Drying method was also found to affect CEP release from NPs and it was seen that lyophilization is more effective than drying in oven where NPs were agglomerated causing decrease on effective surface area of NPs. In a 14-day comparative study, while freeze dried NPs released ~ 11.3 % of encapsulated CEP, oven dried NPs released ~ 7.7 % of total encapsulated CEP. In long-term release study carried out with lyophilized NPs for 100 days, zero-order release profile was observed and ~ 35% of encapsulated CEP (~60 μg) was released.

In the second part, PEG-PUSe-PEG block copolymer was synthesized in two-step procedure including di-(1-hydroxylundecyl) selenide as by product and final copolymer synthesis. It was observed that increasing initial volumes and amounts of raw materials of block copolymer to scale-up the production affected the purity of both by-product and final copolymer negatively, so original concentrations, which resulted a very small amount of copolymer, were used during synthesis. PU at different ratios (w/w) was blended with PEG-PUSe-PEG block copolymer to fabricate matrices. The matrices made by both 2:1 PU and PEG-PUSe-PEG block copolymer (w/w) and 1:1 PU and PEG-PUSe-PEG block copolymer (w/w) had sponge like porous structure and their pores had a wide size distribution. When PEG20-PEVA NPs including CEP were loaded to matrix, they were distributed homogeneously and CEP release profile from incorporated NPs showed similar release profile compared to that of free NPs. It was seen that CEP release amounts in 66 days both from free NPs (~105 μg) and matrix loaded NPs (~98 μg) are not far from the effective amount (3.6 μg/day) used for mice models *in vivo* conditions.

Se release experiments were carried out in both ultra-pure water and water including H_2O_2 (0.1% v/v) to mimic stress conditions in hypothyroid patients who have higher reactive oxygen species in thyroid gland than healthy people. As expected, Se release rate in the presence of H_2O_2 (2525.90 μg and 2097.76 μg for 1:1 and 2:1 PU/PEG-PUSe-PEG matrices, respectively) was much faster than ultra-pure water (0.88 μg and 11.96 μg for 1:1 and 2:1 PU/PEG-PUSe-PEG matrices, respectively) and initial burst release which could be toxic for patients was observed. Since the release rates in water including H_2O_2 were not much different from the value specified in the literature (200 μg/day), the matrices should be optimized by adjusting initial Se concentration and the dimensions of matrix.

In the last part, cytotoxicity studies of both blank and CEP loaded NPs and matrices were carried out with NIH 3T3 fibroblastic cells at three different formats: Cell viability after direct and indirect (at different concentration of matrix eluents) interaction with NPs, and cell viability on matrix surfaces. According to cell viability assays (MTS), neither NPs nor matrices has toxic effect on cells. It was seen that, cytoskeleton organizations and cellular morphologies of cells were similar to control groups for all samples therefore cells could proliferate on NPs and attach on matrices.

In sum, a multifunctional long-term release system was fabricated using PEG20-PEVA NPs for CEP release and PEG-PUSe-PEG block copolymer for matrix-

mediated Se release. Long term CEP release was followed and it was seen that integrated NPs to matrices did not affect release profile of CEP, significantly. The release results showed that if concentration of both CEP and Se could be adjusted and controlled, the dual effect system, which has the capacity to prevent T-cell activation and decrease anti-TPO concentration, produced in this thesis has potential to be used as long-term local release system to increase patient compliance. In addition, oxidative stress-mediated Se release can be achieved to address the high oxidative stress seen in hypothyroid patients.

As future prospect, scaling CEP dose by using allometric approaches such as body surface area, body weight (mg/kg), pharmacokinetics, and physiological time from animals to humans should be investigated and more precise dose adjustment should be examined for prolonged release. Taking Se as supplement in addition to the daily diet, decreases TPOAb level in the serum of hypothyroidism patients so results showed that matrices fabricated by PU and PEG-PUSe-PEG block copolymer have potential to provide the amount of Se needed in patients. However, in order to determine the therapeutic dosage of Se, *in vivo* release studies in animal models under mild oxidative environment should be carried out.

REFERENCES

Akçakaya, A., Koç, B., & Ferhatoğlu, F. (2012). Tiroid anatomisi ve cerrahi yaklaşım. *Okmeydanı Tıp Dergis*i, *28* (1), 1-9.

Afsharzadeh, M., Hashemi, M., Mokhtarzadeh, A.,Abnous, K., & Ramezani, M. (2018). Recent advances in co-delivery systems based on polymeric nanoparticle for cancer treatment. *Artificial Cells, Nanomedicine, and Biotechnology*, *46* (6), 1095–1110.

Ahire, E., Thakkar, S., Darshanwad, M., & Misra, M. (2018). Parenteral nanosuspensions: a brief review fromsolubility enhancement to more novel and specificapplications. *Acta Pharmaceutica Sinica B*, *8* (5), 733–755.

Akindoyo, J. O., Beg, M. D. H., Ghazali, S., Islam, M. R., Jeyaratnam, N. & Yuvaraj, A.R. (2016). Polyurethane types, synthesis and applications – a review. *RSC Adv*., *6*, 114453–114482.

Amreddy, N., Babu, A., Muralidharan, R., Munshi, A., & Ramesh, R. (2017). Polymeric Nanoparticle-Mediated Gene Delivery for Lung Cancer Treatment. *Top Curr Chem (Z)*, *375* (35).

Benardot, D. (2011). *Advanced Sports Nutrition*, USA: Human.

Bhatia, S. (2016). *Nanoparticles Types, Classification, Characterization, Fabrication Methods and Drug Delivery Applications*, Switzerland:Springer, Cham.

Bhattacharjee, S. (2016). DLS and zeta potential – What they are and what they are not? *Journal of Controlled Release*, *235*, 337–351.

Bhusal, P., Sharma, M., Harrison, J., Procter, G., Andrews, G., Jones, D. S., Hill, A. G., & Svirskis, D. (2017). Development, Validation and Application of a Stability Indicating HPLC Method to Quantify Lidocaine from Polyethylene-co-Vinyl Acetate (EVA) Matrices and Biological Fluids. *Journal of Chromatographic Science*, *55* (8), 832–838.

Calonne, J., Isacco, L., Miles-Chan, J., Arsenijevic, D., Montani, J. P., Guillet, C., Boirie Y., & Dulloo, A. G. (2019). Reduced skeletal muscle protein turnover and thyroid hormone metabolism in adaptive thermogenesis that facilitates body fat recovery during weight regain. *Frontiers in Endocrinology*, *10*, 119.

Chaker, L., Bianco, A.C., Jonklaas, J., & Peeters, R.P. (2017). Hypothyroidism. *Lancet*, *390*, 1550–1562.

Chan, J. M., Zhang, L., Yuet, K. P., Liao, G., Rhee, J.W., Langer, R., & Farokhzad, O. C. (2009). PLGA-lecithin-PEG core-shell

nanoparticles for controlled drug delivery. *Biomaterials*, *30*, 1627–1634.

Chu, S. F., Kong, L. L., & Chen, N. H. (2018). Natural Small Molecule Drugs from Plants, Singapore: Springer.

Conti, B., Genta, I., Modena, T., & Pavanetto, F. (1995). Investigation on process parameters involved in polylactide-co-glycolide microspheres preparation. *Drug Dev Ind Pharm*, *21* (5), 615–622.

Cooper, D. S., & Ladenson, P. W. (2011). The thyroid gland. In D.G. Gardner, D. Shoback (Eds), *Basic and Clinical Endocrinology* (9th ed., pp.163-226). USA: The Mc- Graw Hill Companies.

D'souza, A. A., & Shegokar, R. (2016). Polyethylene glycol (PEG): a versatile polymer for pharmaceutical applications. *Expert Opinion On Drug Delivery*. *13* (9), 1257–1275.

Demirci, T, & Deliaşı, T. (2014). Tiroid hastalıklarında tanısal algoritmalar. *Turkiye Klinikleri J Endocrin-Special Topics, 7* (3).

Ersoy, C. O. (2014). Treatment of hypothyroidism. *Turkiye Klinikleri Journal of Endocrinology Special Topics, 7* (3), 37–40.

Feroz, S., Muhammad, N., Ranayake, J., & Dias, G. (2020). Keratin - Based materials for biomedical applications. *Bioactive Materials, 5*, 496–509.

Fujita, H. (1975). International Review of Cytology, G. H. Bourne, J. F. Danielli, K. W. Jeon (Eds), *Fine Structure of the thyroid gland. International Review of Cytology* (Vol: 40, pp.197–280). New York: Academic Press.

Gao, S., Li, X., Ding, X., Qi, W., & Yang, Q. (2017). Cepharanthine Induces Autophagy, Apoptosis and Cell Cycle Arrest in Breast Cancer Cells. *Cell Physiol Biochem*, *41*, 1633-1648.

Garla, V.V., Cardozo, L.L.Y., & Lien, L.F. (2019). Thyroid disease and reproduction. J.L. Eaton (Eds), *A clinical guide to diagnosis and management* (pp.19-43). Switzerland: Springer International Publishing.

Gartner, R., Barbara, C. H., & Gasnier, B. C. H. (2003). Selenium in the treatment of autoimmune thyroiditis. *BioFactors*, *19*, 165–170.

Gartner, R., Gasnier, B. C. H., Dietrich, J.W., Krebs, B., & Angstwurm, M.W. (2002). Selenium supplementation in patients with autoimmune thyroiditis decreases thyroid peroxidase antibodies concentrations. *J Clin Endocrinol and Metab*, *87*, 1687-91.

Gregory, A. B. (2012) Mechanisms of thyroid hormone action. *J Clin Invest*., *122* (9), 3035–3043.

Harris, J. M, & Chess, R. B. (2003). Effect of pegylation on pharmaceuticals. *Nat Rev Drug Discovery*., *2*, 214–221.

ISO (2016). Biological evaluation of medical devices - Part 1: Evaluation and testing within a risk management process, Guidance for Industry and Food and Drug Administration Staff. Silver Spring, MD: Food and Drug Administration (ISO 10993-1) Retrieved from: https://www.fda.gov/regulatory-information/search-fda-guidance-

documents/useinternational-standard-iso-10993-1-biological-evaluation-medicaldevices- part-1-evaluation-and.

Ivanova, E. P., Bazaka, K., & Crawford, R.J. (2014). *New Functional Biomaterials for Medicine and Healthcare*, Cambridge: Woodhead Publishing.

Jäger, E., Venturini, C. G., Poletto, F.S., Colomé, L.M., Pohlmann, J.P., Bernardi, A., Battastini, A. M., Guterres, S. S., & Pohlmann, A.R. (2009). Sustained release from lipid-core nanocapsules by varying the core viscosity and the particle surface area. *J Biomed Nanotechnol*, *5*, 130–140.

Karrina McNamara, K., & Tofail, S. A. M. (2017). Nanoparticles in biomedical applications. *Advances in Physics: X*, *2* (1), 54–88.

Kashirina, A., Yao, Y., Liua, Y., & Leng, J. (2019). Biopolymers as bone substitutes: a review. *Biomater. Sci*., *7*, 3961–3983.

Kline, G., & Sadrzadeh, H. (2017). Endocrine Biomarkers: Clinical Aspects and Laboratory Determination, *Thyroid disorders* (pp.41-93). Canada: Elsevier.

Kramer, C. K., von Mühlen. D., Kritz-Silverstein, D., & Barrett-Connor, E. (2009). Treated hypothyroidism, cognitive function, and depressed mood in old age: the Rancho Bernardo Study. *Eur J Endocrinol*, *161* (6), 917-921.

Kutlu, C., Çakmak, A. S., & Gümüşderelioğlu, M. (2014). Double-effective chitosan scaffold-PLGA nanoparticle system for brain tumour therapy: in vitro study. *Journal of Microencapsulation*, *31* (7), 700–707.

Kutlu Kaya, C., Gümrükçü, S., Saraç, A. S., & Kök, F. N. (2020). A multifunctional long-term release system for treatment of hypothyroidism. *J Biomed Mater Res*., *108A*, 760–769.

Lee, W., Park, J., Yang, E. H., Suh, H., Kim, S. H., Chung, D. S., Choi, K., Yang, C. W., & Park, J. (2002). Investigation of the factors influencing the release rates of cyclosporin A-loaded micro- and nanoparticles prepared by high-pressure homogenizer. *J Control Release*, *84*, 115–123.

Li, C. W., Menconi, F., Osman, R., Mezei, M., Jacobson, E. M., Concepcion, E., Chella S., Kastrinsky D. B., Ohlmeyer M., & Tomer, Y. (2016). Identifying a small molecule blocking antigen presentation in autoimmune thyroiditis. *The Journal of Biological Chemistry*, *291* (8), 4079–4090.

Li, C. W., Osman, R., Menconi, F., Concepcion, E., & Tomer, Y. (2020). Cepharanthine blocks TSH receptor peptide presentation by HLA-DR3: Therapeutic implications to Graves' disease. *Journal of Autoimmunity*, 108.

Ma, N., Li, Y., Ren, H., Xu, H., Lib, Z., & Zhang, X. (2010). Seleniumcontaining block copolymers and their oxidation-responsive aggregates. *Polymer Chemistry*, *1*, 1609–1614.

Mariotti, G. & Vannozz, L. (2019). Fabrication, Characterization, and Properties of Poly (Ethylene-Co-Vinyl Acetate) Composite Thin Films Doped with Piezoelectric Nanofillers, *Nanomaterials*, *9*, 1182.

McLachlan, S. M., & Rapoport, B. (2007). Thyroid peroxidase as an autoantigen. *Thyroid*, *17* (10), 939–948.

Menconi, F., Huber, A., Osman, R., Concepcion, E., M.Jacobson, E., Stefan M., David C.S., & Tomer, Y. (2010). Tg.2098 is a major human thyroglobulin T-cell epitope. *Journal of Autoimmunity, 35* (1), 45-51.

Mora-Huertas, C. E., Fessi, H., & Elaissari, A. (2010). Polymer-based nanocapsules for drug delivery. *Int J Pharm, 385*, 113–142.

Mozafari M., & Chauhan, N. P. S. (2019). *Advanced Functional Polymers for Biomedical Applications*, Amsterdam: Elsevier.

Mura, S., Nicolas, J., & Couvreur, P. (2013) Stimuli-responsive nanocarriers for drug delivery. *Nat Mater, 12*, 991–1003.

Onlaora, K.,Thiwawonga, T., & Tunhoo, B. (2019). Flexible and fully transparent WORM memory devices based on Ag nanoparticles blended with poly(ethylene-co-vinyl acetate). *Synthetic Metals, 258*, 116-200.

Özyardımcı Ersoy, C. (2014) Hipotiroidizm Tedavisi. *Turkiye Klinikleri J Endocrin-Special Topics,* 7 (3):37-40.

Piacentini, E., Bazzarelli, F., Poerio, T., Albisa, A., Irusta, S., Mendoza, G., Sebastian, V., & Giorno, L. (2020). Encapsulation of water-soluble drugs in Poly (vinyl alcohol) (PVA)- microparticles via membrane emulsification: Influence of process and formulation parameters on structural and functional properties, *Materials Today Communications*, 24.

Persani, L., & Bonomi, M. (2017). The multiple genetic causes of central hypothyroidism. *Best Practice & Research Clinical Endocrinology & Metabolism*, *31* (2), 255-263.

Qian, C., & McClements, D., J. (2011). Formation of nanoemulsions stabilized by model food-grade emulsifiers using high-pressure homogenization: Factors affecting particle size. *Food Hydrocolloids*, *25*, 1000-1008.

Rafiee, Z. & Keshavarz, V. (2015). Synthesis and characterization of polyurethane/ microcrystalline cellulose bionanocomposites. *Prog. Org. Coat*., *86*, 190–193.

Ribeiro, T. G., Chavez-Fumagalli, M.A., Valadares, D. G., Franca, J. R., Rodrigues, L. B., Duarte, M. C., Lage, ... Faraco, A. A. (2014). Novel targeting using nanoparticles: an approach to the development of an effective anti-leishmanial drug-delivery system. *Int J Nanomedicine, 9*, 877–890.

Riveiro, A., Maçon, A. L. B., del Val1, J., Comesaña, R. & Pou, J. (2018). Laser Surface Texturing of Polymers for Biomedical Applications. *Front. Phys., 6* (16).

Roberts , M. J. , Bentley , M. D. & Harris , J. M. (2012) Chemistry for peptide and protein PEGylation. *Advanced Drug Delivery Reviews , 64*, 116 – 27 .

Samuel, A. Z., & Umapathy, S. (2014) Energy funneling and macromolecular conformational dynamics: a 2D Raman correlation study of PEG melting. *Polymer Journal*, *46*, 330–336.

Shumaila, Lakshmi, G.B.V.S., Alam, M., Siddiqui, A. M., Zulfequar, M., & Husain, M. (2011). Synthesis and characterization of Se doped polyaniline. *Current Applied Pyhsics, 11*, 217-222.

Sundararajan, S., Kumar, A., Chakraborty, B. C., Samui, A. B., & Kulkarni, P. S. (2018). Poly(ethylene glycol) (PEG)-modified epoxy phasechange polymer with dual properties of thermal storage and vibration damping. *Sustainable Energy & Fuels*, *2* (3), 688–697.

Takacs, E. S., & Vlachopoulos, J. (2008). Biobased, biodegradable polymers for biomedical applications: properties and process. *Plastics Enginee*ring, *64* (9), 28.

Tao, J., Chow, S. F., & Zheng, Y. (2019). Application of flash nanoprecipitation to fabricate poorly water-soluble drug nanoparticles. *Acta Pharmaceutica Sinica B, 9* (1), 4–18.

Tavukçu, E.F. (2005). *Demir eksikliği anemisinin tiroid hormonları üzerine etkisi. (*Tıpta Uzmanlık Tezi), T.C. Sağlık Bakanlığı Dr. Lütfi Kırdar Kartal Eğitim ve Araştırma Hastanesi II. Çocuk Sağlığı ve Hastalıkları Kliniği, İstanbul.

Taylor, P. N., Albrecht, D., Scholz, A., Gutierrez-Buey, G., Lazarus, J. H., Dayan, C. M., & Okosieme, O. E. (2018). Global epidemiology of hyperthyroidism and hypothyroidism. *Nature Reviews Endocrinology*, 14, 301–316.

Tetteh, G. A. J. (2016). *Polyurethane-based scaffolds for bone tissue engineering* (PhD thesis). University of Sheffield, United Kingdom.

Tomer, Y., & Huber, A. (2009). The etiology of autoimmune thyroid disease: A story of genes and environment. *Journal of Autoimmunity*, *32*, 231–239.

Turker, O., Kumanlioglu, K., Karapolat, I., & Dogan, I. (2006). Selenium treatment in autoimmune thyroiditis: 9-month follow-up with variable doses. *The Journal of Endocrinology, 190* (1), 151–156.

Türkiye Endokrinoloji ve Metabolizma Derneği. (2013). *Tiroid Hastalıkları Tanı Ve Tedavi Kılavuzu* (5. Basım). Ankara: BAYT Bilimsel Araştırmalar Basın Yayın ve Tanıtım Ltd. Şti.

Url-1 <https://www.ncbi.nlm.nih.gov/books/NBK279601> date retrieved 31.05.2020.

Url-2 < http://msk-anatomy.blogspot.com/2013/06/thyroid-gland-anatomy.html> date retrieved 31.05.2020

Url-3 <https://www.dojindo.com/TechnicalManual/Manual_CK04.pdf> date retrieved 31.05.2020.

Vahabia, H., Gholamib, F., Karasevac, V., Laoutidc, F., Mangina, R., Sonnierd, R., & Saeb, M. R. (2017). Novel nanocomposites based on poly(ethylene-co-vinyl acetate) for coating applications: The complementary actions of hydroxyapatite, MWCNTs and ammonium

polyphosphate on flame retardancy. *Progress in Organic Coatings*, *113*, 207–217.

Varshosaz, J., & Moazen, E. (2014). Novel lectin-modified poly(ethylene-co-vinyl acetate) mucoadhesive nanoparticles of carvedilol: preparation and in vitro optimization using a two level factorial design. *Pharm Dev Technol*., *19* (5), 605–17.

Varshosaz, J., Taymouri, S., & Hamishehkar, H. (2014). Fabrication of Polymeric Nanoparticles of Poly(ethylene-co-vinyl acetate) Coated with Chitosan for Pulmonary Delivery of Carvedilol. *J. Appl. Polym. Sci*., *131*, 1.

Vauthier, C., & Ponchel, G. (2016). *Polymer Nanoparticles for Nanomedicines A Guide for their Design, Preparation and Development*, Switzerland: Springer International Publishing.

Venditti, P., & Di Meo, S. (2006). Thyroid hormone-induced oxidative stress. *Cellular and Molecular Life Sciences, 63* (4), 414–434.

Vinceti, M., Filippini, T., Del Giovane, C., Dennert, G., Zwahlen, M., Brinkman, M., ... Crespi, C.M. (2018). *Selenium for preventing cancer (Review)*, Boston: John Wiley & Sons, Ltd.

Webster, R, Didier, E., Harris, P., Siegel, N., Stadler, J., Tilbury, L., & Smith, D. (2007). PEGylated proteins: evaluation of their safety in the absence of definitive metabolism studies. Drug Metab Dispos., *35*, 9–16.

Weekley, C. M., Aitken, J. B., Finney, L., Vogt, S., Witting, P. K., & Harris, H. H. (2013). Selenium Metabolism in Cancer Cells: The Combined Application of XAS and XFM Techniques to the Problem of Selenium Speciation in Biological Systems. *Nutrients*, *5*, 1734-1756.

Yılmaz, G. (2009). *Klinik ve Subklinik Hipotiroidili Hastlarda Solunum Fonksiyonları* (Tıpta Uzmanlık Tezi). T.C. Sağlık Bakanlığı Okmeydanı Eğitim ve Araştırma Hastanesi 2. İç Hastalıkları Kliniği, İstanbul.

Zhou, B., Hu, Y., Li, J., & Li, B. (2014). Chitosan/phosvitin Antibacterial films fabricated via layer-by-layer deposition. *Int. J. Biol. Macromol*., *64*, 402–408.

Zhoua, Y., Quana, G., Wu, Q., Zhang, X., Niu, B., Wu, B., Huang, ... Wu, C. (2018). Mesoporous silica nanoparticles for drug and gene delivery. *Acta Pharm Sin B, 8*,165–77.

CURRICULUM VITAE

Name Surname **:** Ceren KUTLU KAYA

Place and Date of Birth **:** Ankara, 01.06.1986

E-Mail **:** kutlu.ceren@gmail.com

EDUCATION **:**

- **B.Sc.** **:** 2008, Ege University, Engineering Faculty, Bioengineering Department
- **M.Sc.** **:** 2011, Hacettepe University, Biengineering Division

PROFESSIONAL EXPERIENCE AND REWARDS:

- 2009-2012, Research Assistant, Fırat University, Bioengineering Department
- 2012-2013; Project Specialist, 5G Consulting
- 2013-2014; Project Manager, Boyut Ar-Ge Consulting
- 2014-2018; Senior Project Specialist, İstanbul Şehir University TTO
- 2019- …; Grants Team Manager, Özyeğin University TTO

PUBLICATIONS, PRESENTATIONS AND PATENTS ON THE THESIS:

- **Kutlu Kaya C.,** Gümrükçü S., Saraç A. S., and Kök F. N. 2020. A Multifunctional Long-term Release System For Treatment Of Hypothyroidism, *J Biomed Mater Res*., 108A, 760–769.
- **Kutlu Kaya C.,** Gümrükçü S., Saraç A. S., and Kök F. N**.** 2019**:** A Dual Effect Release System for Hypothyroid Therapy, 24th International Biomedical Sicence & Technology Symposium, October 17-20, 2019 İzmir, Turkey.

- **Kutlu Kaya C.,** Gümrükçü S., Saraç A. S., and Kök F. N. 2019: A Multifunctional Long-Term Release System for Hypothyroid Therapy, European Biotechnology Congress, April 11-13, 2019, Valencia, Spain.
- **Kutlu Kaya C.,** Gümrükçü S., Saraç A. S., and Kök F. N. 2018: Hipotiroidi Tedavisine Yönelik Kontrollü Salım Sistemi Tasarımı, 23. Biyomedikal Bilim Ve Teknoloji Sempozyumu, Aralık 15-16, 2018, Istanbul, Turkey.
- **Kutlu Kaya C.,** Gümrükçü S., Saraç A. S., and Kök F. N. 2018: Controlled Release System For Hypothyroid Therapy And Effect Of Drying Method to Release Profile, 14th Nanoscience and Nanotechnology Conference, September 22-25, 2018, Izmir, Turkey.

OTHER PUBLICATIONS, PRESENTATIONS AND PATENTS:

- **Kutlu C.,** Çakmak A. S., and Gümüşderelioğlu M. 2014. Double-effective Chitosan Scaffold-PLGA Nanoparticle System For Brain Tumour Therapy: *In Vitro* Study, *J Microencapsul,* 31(7): 700–707.
- Öngen G., Sargın S., Üstün Ö., **Kutlu C.,** Yücel M. 2012. Dipeptidyl Peptidase IV Production By Solid State Fermentation Using Alternative Fungal Sources, *Turkish Journal of Biology*, 36: 665-671.